UNIVERSITAT DE
BARCELONA

Asociación de Sistemas Nanoestructurados con Fluorometolona para el Tratamiento de Enfermedades Inflamatorias

Roberto Carlos González Pizarro

UNIVERSITAT DE
BARCELONA

Facultad de Farmacia y Ciencias de la Alimentación

Asociación de Sistemas Nanoestructurados con Fluorometolona para el Tratamiento de Enfermedades Inflamatorias

Roberto Carlos González Pizarro
2019

UNIVERSITAT DE BARCELONA

Programa de Doctorado

Investigación, Desarrollo y Control de Medicamentos

Asociación de Sistemas Nanoestructurados con Fluorometolona para el Tratamiento de Enfermedades Inflamatorias

Memoria presentada por **Roberto Carlos González Pizarro** para optar al título de doctor por la Universidad de Barcelona

Directoras

Dra. María Luisa García López   Dra. Marta Espina García

Doctorando
Roberto Carlos González Pizarro

Tutora
Dra. María Luisa García López

Roberto Carlos González Pizarro, 2019

Dedicada a lo más preciado, intangible y hermoso

A la memoria de mi hermana Krishnna

"Lo único que uno aprende es lo que uno averigua solo"

Isabel Allende

AGRADECIMIENTOS

AGRADECIMIENTOS

Ya culminada esta etapa doctoral, donde hubo momentos de altibajos de diferentes índoles, propios de un estudiante, que me han hecho reflexionar y tomar conciencia de todas las ayudas, apoyos, alegrías y afectos creados a lo largo de mi estancia en Barcelona. Debido a esto me gustaría dar mis agradecimientos a todas aquellas personas que formaron parte, de una forma u otra, en el término de mi tesis doctoral y que actualmente siguen formando parte de mi vida.

En primera instancia, agradezco a mis directoras de tesis la Dra. María Luisa García y la Dra. Marta Espina por recibirme en su grupo de investigación, darme su apoyo, su confianza y su cariño durante el transcurso de esta etapa. A la Dra. María Luisa García por su gran vocación en la dirección de mi tesis doctoral y su arduo compromiso en la revisión de mis trabajos. Especialmente, a la Dra. Marta Espina, por estar siempre a disposición en platicar tanto temas científicos como cotidianos, eres una persona que hace sentir a los demás de tu alrededor seguras y tranquilas.

A la Dra. María Antonia Egea por su gran capacidad pedagógica, voluntad y apoyo en los trabajos realizados. A la Dra. Ana Calpena, que ha estado desde mi tesis de máster compartiendo sus conocimientos y su energía para seguir adelante, muchas gracias por tus consejos y soporte. A la Dra. Lyda Halbaut, por su gran ayuda y voluntad en enseñarme todo respecto a los estudios reológicos.

A la Dra. Josefa Badia y la Dra. Laura Baldoma, por darme la oportunidad y permitirme trabajar en su laboratorio del Departamento de Bioquímica y Fisiología de la Facultad de Farmacia y Ciencias de

AGRADECIMIENTOS

Alimentación (UB). Gracias por su apoyo y ánimos para finalizar mis últimos meses.

A la Dra. Isabel Haro y la Dra. María José Gómara, por entregarme sus conocimientos durante mi tesis de máster, los cuales fueron mi base para emprender mi carrera doctoral.

I acknowledge to the University of Southern Denmark for allowing me to conduct my doctoral internship in the Department of Biochemistry and Molecular Biology of the Faculty of Sciences. I am especially grateful to PhD. Frank Kjeldsen for his confidence and support in carrying out the studies.

En el Departamento de Farmacia, Tecnología Farmacéutica y Fisicoquímica, particularmente a la sección de Fisicoquímica, me gustaría agradecer a los profesores y personal que me recibieron y que han sido cordiales durante todo este tiempo. A los compañeros del Lab 4 y 5, a Abie y Adrià, por su muy buena onda y amabilidad tanto dentro como fuera de la Universidad de Barcelona. A las compañeras del SDM y las que se han ido a sus respectivos países, Faviola, Ana, Marisol y Mónica, por todos esos buenos momentos vividos. A los compañeros que ya emprendieron su carrera como doctores fuera de la Universidad de Barcelona, Alexander, Gladys y Mireia, gracias por ayudarme sobre todo al principio. A mis compañeros del Lab, más bien compañeras, ustedes son geniales, simplemente cada vez que iba al Lab estaba a gusto y riéndome por supuesto. A Elena, eres un referente de cómo hacer un buen trabajo y claro, aunque seas un poco histérica acerca de tus pegatinas de "No tocar o Prohibido abrir" repartidas por todo Lab, se te quiere un montón. A Amanda, tu

perseverancia y tu fuerza de voluntad es una cualidad para seguir, ¡ah! discúlpame las veces que me reí de tus monólogos, ahora me doy cuenta de que escribir la tesis provoca tal efecto. A Marcelle, por tu ayuda en los trabajos con los cerditos (aún recuerdo tu miedo al manipularlos) y obviamente, por nuestra gran travesía por Japón, gracias por todo. A Martha Ariza, desde mis inicios dl máster en el CSIC, has sido una compañera dispuesta a compartir tus conocimientos sin ningún problema. A Pau, desde el laboratorio de Farmacognosia en la Universidad de Valparaíso hasta ahora has sido una gran compañera que trabaja eficientemente y con una alegría que contagia a los de su alrededor. A Anita, eres una amiga con un gran carisma y sedienta de encontrar más conocimiento, gracias por las múltiples discusiones científicas que siempre llegaron a buen puerto, continua así. A Camilla, tu extrovertida felicidad y tu energía siempre ha sido una motivación para despejarse del trabajo del Lab. A María, tu gran capacidad multitarea da esperanza de que es posible finalizar el doctorado, a pesar de estar trabajando, hacer la tesis y tener vida. A Ruth, acabas de llegar con una gran motivación, espero que se fortalezca aún más al estar en contacto con tan grandes compañeras en el Lab.

A los grandes personajes que encontré este último año perteneciente al Departamento de Bioquímica y Fisiología, particularmente al grupo de Colis. A Rodrigo y Naty, por su inmensa paciencia en enseñarme todo lo referente a cultivos celulares y como también toda la buena onda que se respiraba en el Lab, pues claro, estando tres chilenos juntos es imposible no pasarlo bien. Gracias por darme tranquilidad y motivarme estos últimos meses.

AGRADECIMIENTOS

A los amigos que he conocido en Barcelona. A mis compañeros del piso Carles III, Óscar, Gabo, Carlitos y Rodri, por darme tantos buenos momentos que hasta ahora me parecen casi inimaginables. A mis mexicanos, Rubén y Laurita, son demasiado buena gente y divertidos, gracias por todos esos desayunos de domingo y la bonita amistad que me han brindado. A Sussy, por estar siempre con una sonrisa en la cara y atenta cuando hacemos la próxima junta. A Daniel, ¡se nota que eres del sur de Chile!, sigue así de motivado y espero que todas tus proyecciones te resulten, gracias por todos esos consejos y conversaciones sobre esta etapa. Infine, ai miei amici italiani, Gemmina, Vale e Mimma, che mi hanno sempre incoraggiato e augurato il meglio, la stima e l'affetto che nutro per voi è sincero e duraturo.

A mis amigos de Chile, Patiño, Camilo, Javiera, Ale, Pía, Rudy, Claudio Badilla, Cristian Pino, Diego, Raulito, Michael, Catherine, Margaret y Naty. A pesar de que nos separa el charco se han mantenido en contacto deseándome siempre lo mejor y preguntándome cuando regreso a casa para juntarnos, ¡tranqui ya voy! A Mauri y Lucia, por su amistad durante todos estos años y su preocupación acerca de todo lo que me rodea. Mauri, gracias por mantener siempre la comunicación y cultivar esta amistad, eres un gran amigo.

Alla famiglia Parrotta e Benevento, che mi hanno accolto come un membro della famiglia fin dall'inizio, nonostante le difficoltà della lingua, trovano sempre un modo per comunicare nonostante questo limite, grazie per la comprensione e l'affetto. A tutti i cugini acquisiti, per i momenti di cazzeggio e per le mangiate ovviamente (anche se in questo nessuno scappa), grazie per avermi fatto sentire come se fossi a casa.

AGRADECIMIENTOS

A Grá, por ser parte de mi vida de una forma multifacética, como amiga, como compañera de Lab, como revisora de mis artículos y especialmente, ser la persona que me entrega tranquilidad y entusiasmo cada día. Te agradezco todo tu apoyo y ayuda, ya que sin ella esto no sería posible. Ahora si debes estar tranquila Grá, "sé lo que hago, sono un dottore".

A mi familia, que siempre han estado preocupados por mi bienestar y apoyándome para seguir adelante con mis metas. Particularmente, a mi mamá que cada día me mandaba fuerzas y cariños, los cuales fueron fundamentales para la culminación del doctorado. A mis primos, tíos y abuelos que siempre están preguntando en que estoy, aunque pocos entienden que es lo que hago, están ahí para recibirme y darme su cariño.

ÍNDICE

ÍNDICE

ACRÓNIMOS & ABREVIATURAS

AA	Ácido araquidónico
AINE	Fármaco antiinflamatorio no esteroideo
AMP	Péptido antimicrobiano
COX	Ciclooxigenasa
CPP	Péptido de penetración celular
CYP	Citocromo
DIEA	N-diisopropiletilamina
DLS	Dispersión dinámica de la luz
DoE	Diseño de experimentos
DSC	Calorimetría diferencial de barrido
EDC	Hidrocloruro (3-dimetilaminopropil)-3-etilcarbodimida
EE	Eficiencia de encapsulación
EMA	Agencia europea del medicamento
FDA	Food and drug admnistration
FMT	Fluorometolona
FTIR	Espectroscopia de infrarrojo con transformada de Fourier
G2	Péptido G2
HG	Hidrogel
HPMC	Hidroxipropilmetilcelulosa
LOX	Lipoxigenasa
LPS	Lipopolisacárido
LT	Leucotrieno
MC	Metilcelulosa
MR	Porcentaje de masa relativa
MRP	Proteína asociada a la resistencia a múltiples fármacos

ACRÓNIMOS & ABREVIATURAS

MTT	Bromuro de tetrazolio
MW	Peso molecular
NHS	N-hidroxisuccinimida
NP	Nanopartícula
P188	Poloxámero 188
P407	Poloxámero 407
$pAntp_{43-58}$	Secuencia de homeoproteína antenapedia de Drosophila
PEG	Polietilenglicol
PEO-PPO	Polioxietileno-polioxipropileno
P-gp	Glicoproteína-P
PG	Prostaglandina
PI	Índice de polidispersión
PIO	Presión intraocular
PLA_2	Enzima fosfolipasa A2
PLGA	Ácido poliláctico-co-glicólico
PVA	Alcohol polivinílico
Rho	Rodamina
SA	Araquidonato de sodio
S-MLS	Dispersión múltiple de la luz estática
TAT_{49-57}	Secuencia de la proteína activadora de transcripción
TEM	Microscopia electrónica de trasmisión
TX	Tromboxano
XRD	Espectroscopia de difracción de rayos X
Zav	Tamaño promedio de partícula
ZP	Potencial zeta

RESUMEN/ABSTRACT

Resumen

En el abordaje terapéutico de las enfermedades inflamatorias oculares se han utilizado tanto fármacos antiinflamatorios no esteroideos como corticoides en diferentes formas de dosificación, con la finalidad de devolver la homeostasis ocular. En el tratamiento de aquellos estados inflamatorios oculares que afectan estructuras del segmento anterior, generalmente los fármacos se administran en forma gotas oftálmicas, las cuales presentan un limitado efecto farmacológico, debido a las rutas de eliminación precorneales como la renovación lagrimal, que permite el acceso a los tejidos intraoculares de un 5% de la formulación instilada. Cuando el segmento posterior del ojo se ve afectado, la utilización de formas invasivas de administración como los implantes y las inyecciones intraoculares, conllevan a la incomodidad para el paciente y dificultan la adherencia al tratamiento. Particularmente, la utilización de corticoides en inflamaciones de la úvea (uveítis) causadas por enfermedades sistémicas como el Lupus, manifiestan un aumento de la presión intraocular como efecto secundario. Sin embargo, la Fluorometolona (FMT) es un corticoide de potencia moderada utilizado para el tratamiento de alergias e inflamaciones del segmento anterior del ojo sin inducir modificaciones apreciables de la presión intraocular (uno de los principales efectos adversos de estos fármacos). De acuerdo a lo anterior, el objetivo principal de este trabajo fue el desarrollo y caracterización de sistemas poliméricos nanoestructurados que contienen FMT para el tratamiento de afecciones inflamatorias del segmento anterior y posterior del ojo. Se desarrollaron tres sistemas con FMT: nanopartículas (NPs) de PLGA, gel de formación *in-situ*

RESUMEN/ABSTRACT

con NPs y NPs funcionalizadas con péptidos de penetración celular (TAT$_{49-57}$, pAntp$_{43-58}$ y G2). Las NPs de PLGA, el gel y las NPs funcionalizadas, demostraron características fisicoquímicas adecuadas para la administración ocular. Las NPs de PLGA y el gel termosensible mostraron un perfil biofarmaceútico de liberación sostenida de la FMT. Los tres sistemas desarrollados presentaron una óptima tolerancia ocular, demostrada por pruebas *in vitro* (MTT y HET-CAM®) e *in vivo* (test de Draize). Los ensayos de eficacia antiinflamatoria ocular evidenciaron que las NPs de PLGA y el gel de formación *in-situ* tienen un efecto significativamente mayor en la disminución de la inflamación comparado con el fármaco comercial. Por otro lado, las NPs funcionalizadas con TAT$_{49-57}$ y G2, fueron las que exhibieron un efecto mayor en la disminución de la expresión de citoquinas proinflamatorias, evidenciándose, además, una internalización *in vitro* e *in vivo* mayor que con el péptido pAntp$_{43-58}$. En conclusión, según los resultados obtenidos, los sistemas nanoestructurados con FMT desarrollados podrían constituir una nueva estrategia para el tratamiento de la inflamación ocular. Particularmente, las NPs serían útiles en el tratamiento diurno y el gel termosensible en el mantenimiento de una terapia nocturna.

Abstract

In the therapeutic approach to ocular inflammatory diseases, both non-steroidal anti-inflammatory drugs and corticosteroids have been used in different dosage forms with the aim of restoring ocular homeostasis. In the treatment, those ocular inflammatory states that affect structures of the anterior segment are generally administered as eye drops dosage form, which present a limited pharmacological effect, due to the precorneal elimination routes such as tear turnover, which allows access to intraocular tissues of 5% of the instilled formulation. When the posterior segment of the eye is affected, invasive forms of administration, such as implants and intraocular injections, lead to discomfort for the patient and make adherence to treatment difficult. In particular, the use of corticoids in inflammations of the uvea (uveitis) caused by systemic diseases such as Lupus, show an increase in intraocular pressure as a side effect. However, Fluorometholone (FMT) is a moderately potent corticosteroid used to treat allergies and inflammations of the anterior segment of the eye without inducing appreciable changes in intraocular pressure (main adverse effects of these drugs). According to the above, the main objective of this work was the development and characterization of polymeric nanostructured systems containing FMT for the treatment of inflammatory conditions of the anterior and posterior segment of the eye. Three systems were developed with FMT: PLGA nanoparticles (NPs), *in-situ* forming gel with NPs and functionalized NPs with cell-penetrating peptides (TAT$_{49-57}$, pAntp$_{43-58}$ and G2). PLGA NPs, gel and functionalized NPs demonstrated physicochemical characteristics suitable for ocular administration. The PLGA NPs and the

RESUMEN/ABSTRACT

thermosensitive gel showed a biopharmaceutical profile of sustained release of FMT. The three developed systems presented an optimal ocular tolerance, demonstrated by *in vitro* (MTT and HET-CAM®) and *in vivo* (Draize) tests. Ocular anti-inflammatory efficacy trials showed that PLGA NPs and *in-situ* forming gel have a significantly greater effect in reducing inflammation than the commercial drug. On the other hand, the NPs functionalized with TAT_{49-57} and G2, exhibited a greater effect in the reduction of the expression of proinflammatory cytokines, evidencing, in addition, an internalization *in vitro* as *in vivo* greater than with the peptide $pAntp_{43-58}$. In conclusion, according to the results obtained, the nanostructured systems with FMT developed could constitute a new strategy for the treatment of ocular inflammation. In particular, NPs would be useful in daytime treatment and thermosensitive gel in the maintenance of nocturnal therapy.

1. INTRODUCCIÓN

1.1. Anatomofisiología ocular

De todos los órganos del cuerpo humano, el ojo es el sistema altamente delicado y complejo de la percepción visual, donde la luz recibida por la retina es convertida en señales eléctricas, que se transmiten a través del nervio óptico hacia la corteza visual del cerebro, donde son procesadas para obtener una representación visual. El globo ocular, llamado así por su forma esférica, junto a un conjunto de músculos, nervios y vasos sanguíneos, se encuentra alojado y protegido dentro de las órbitas craneales que aseguran su correcto funcionamiento. El ojo humano mide aproximadamente 25 mm de diámetro anteroposterior y 80 mm de perímetro y consta de tres capas concéntricas principales (**Figura 1**) (Kels and Grant-Kels 2015):

- La córneo-escleral, capa más externa que recubre, protege y otorga el soporte necesario para mantener una presión intraocular adecuada (entre 13 y 19 mm Hg) con el objeto de que el ojo conserve su forma correcta. Esta capa está constituida por la córnea y la esclera, la primera se caracteriza por tener múltiples capas (epitelio, membrana de Bowman, estroma, capa de Dua, membrana de Descemet y endotelio) y ser transparente. La esclera, en cambio, destaca por ser fibrosa, vascularizada y de color blanco y se une a la córnea a través de un anillo de células madres, denominado limbo córneo-escleral, responsable de la regeneración del epitelio.

- La úvea, capa intermedia vascular central del ojo y que está constituida por el iris, el cuerpo ciliar y la coroides. Su función principal es proporcionar nutrición a la retina.

3

INTRODUCCIÓN

- La retina, membrana de tejido nervioso altamente especializada en convertir la luz que recibe en señales visuales para que el cerebro las interprete como imágenes del objeto observado (Morrison and Khutoryanskiy 2014; Dua et al. 2013).
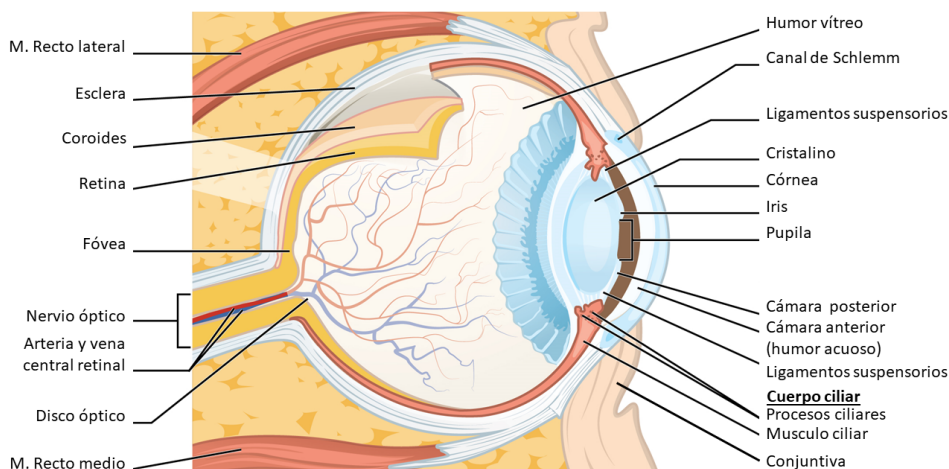

Figura 1. Estructuras del ojo humano.

Una molécula administrada tópicamente para el tratamiento de una afección ocular se enfrenta a diversos desafíos anatomofisiológicos, metabólicos, bioquímicos y farmacocinéticos, entre otros, limitando su efectividad en la recuperación de la homeostasis ocular (Hughes *et al.* 2005).

Desde el punto de vista anatomofisiológico, la primera barrera para el paso de los fármacos es la película lagrimal con un volumen promedio de 10 µL y una secreción basal de 1,2 µL·min^{-1} y cuya función principal es la protección del ojo frente a agentes externos y evitar la desecación. A su vez, el fluido lagrimal provee de lubricación a los parpados, de sistema antimicrobiano, de nutrientes para el epitelio corneal, de medio para el

desplazamiento del sistema inmunitario y permite la eliminación de sustancias irritantes o tóxicas (Agrahari *et al.* 2016).

La película lagrimal está constituida por varias capas, la primera es una capa lipídica apolar de 0,1 µm de espesor, compuesta por ésteres de colesterol, triglicéridos, ácidos grasos y fosfolípidos. La segunda es una capa acuosa, con un espesor de 7 µm, que contiene sales inorgánicas solubles en agua, urea, glucosa, proteínas, inmunoglobulinas y enzimas. Por último, una capa mucosa, que siempre había sido descrita como una capa independiente, pero actualmente nuevas investigaciones concluyen que ésta se integra con la capa acuosa, donde existe una concentración creciente de mucina libre que llega a formar un gel que se encuentra ligeramente unido al glicocálix de las células epiteliales de la córnea y de la conjuntiva (Gulati and Jain 2016). Las moléculas que logran atravesar la película lagrimal se enfrentan a dos rutas de absorción (**Figura 2**): la corneal y la no-corneal (conjuntiva/esclera).

A nivel corneal, está constituida por seis capas diferentes, aunque solo tres de ellas tienen importancia farmacológica: el epitelio, el estroma y el endotelio. El epitelio corneal es una membrana pavimentosa estratificada no queratinizante, formada por 4 o 5 capas de células de un espesor aproximado de 50 µm y con un ciclo de renovación de 7 días (Macwan, Hirani and Pathak 2016). Al ser la primera barrera celular ocular, esta capa posee la función de proteger y limitar la entrada de cualquier objeto extraño hacia el interior. Para esto las células se disponen ordenadamente y en forma compacta a través de uniones gap y uniones estrechas. Lo anterior conlleva a que esta capa sea altamente lipofílica, limitando la entrada a moléculas

hidrofílicas y favoreciendo el paso de moléculas hidrofóbicas que la atravesarían por permeación transcelular. Aquellas moléculas hidrofílicas, con tamaño inferior a 350 KDa que no logran permear el epitelio, lo atravesarían utilizando la ruta paracelular (Hämäläinen *et al.* 1997; Ghate and Edelhauser 2006). El estroma es una capa hidrofílica que se encuentra posterior al epitelio y representa el 90% del espesor de la córnea, está constituida por un gel de fibras de colágeno, mucopolisacáridos y proteínas. Posteriormente al estroma se encuentra la monocapa celular, llamada endotelio, que tiene la función de mantener la nutrición e hidratación del estroma a través de la bomba Na^+/K^+-ATPasa que asegura la transparencia de la córnea y evita la acumulación de líquido (Reim, Schrage and Becker 2001). A su vez, las uniones intercelulares amplias de esta capa presentan una baja resistencia a los compuestos hidrofílicos.

La molécula instilada que logra atravesar la córnea es distribuida por el humor acuoso, que ocupa la cámara anterior del ojo con la función de controlar la presión intraocular (Duan and Li 2013). Para lograr esta función, el cuerpo ciliar secreta humor acuoso con una tasa de renovación de 2 a 3 $\mu L \cdot min^{-1}$, fluido que provee de nutrientes a los tejidos vasculares circundantes y drena los desechos a través del canal de Schlemm (Malavade 2016). Desde el humor acuoso, una molécula podría alcanzar los tejidos del segmento anterior como el iris, el cristalino y el cuerpo ciliar utilizando la barrera hemato-acuosa o por permeación a través de los tejidos.
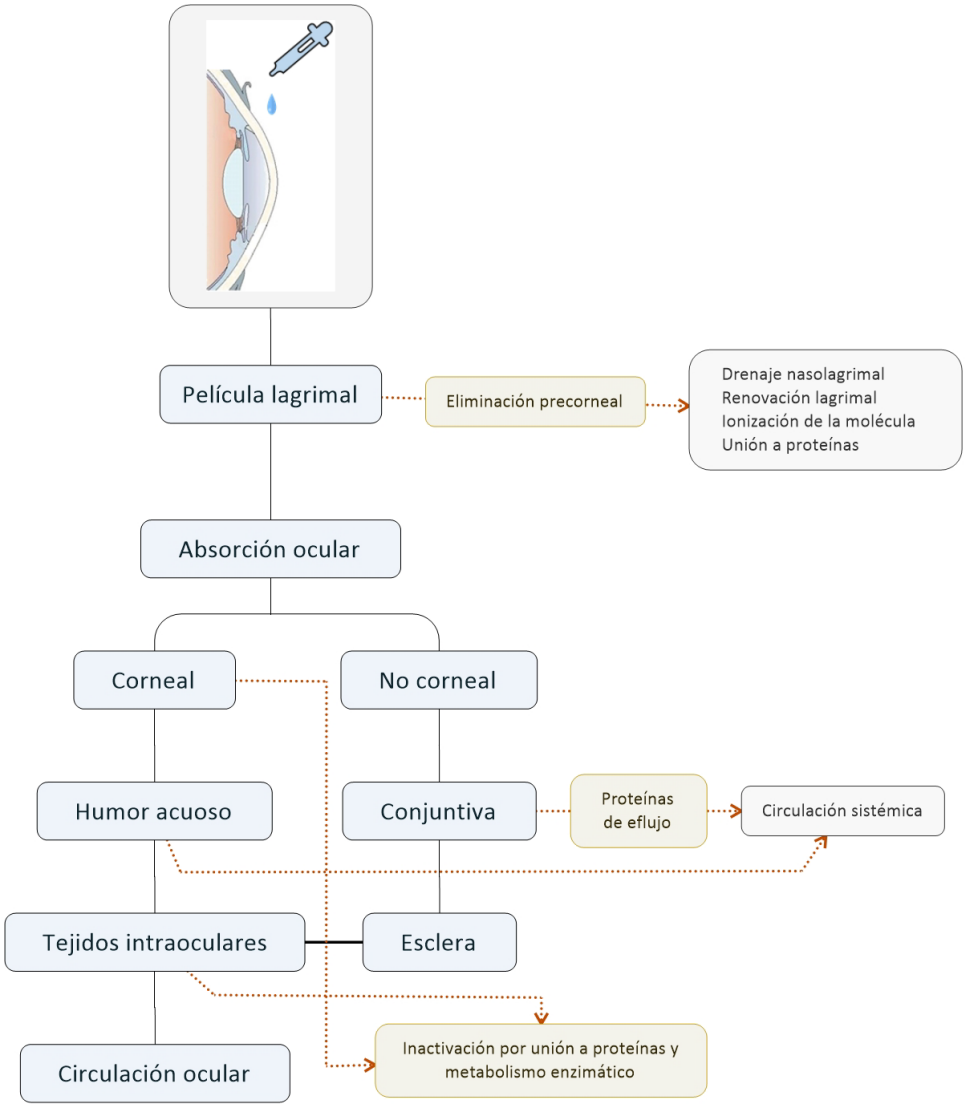
Figura 2. Rutas oculares de absorción y eliminación.

A nivel no-corneal, la primera barrera que se encuentra es la conjuntiva, específicamente la bulbar, membrana mucosa que recubre la parte frontal de la esclera. Está constituida por un epitelio estratificado columnar no queratinizado de cuatro o cinco capas y por una lámina propia

altamente vascularizada. Esta barrera posee uniones menos estrechas y espacios intracelulares más amplios que el epitelio corneal. A su vez, esta membrana presenta una superficie de 17 cm^2 en contraste con la de la córnea (1 cm^2). A este nivel, las moléculas hidrofílicas y de alto peso molecular poseen una mayor permeabilidad, comparado con la ruta corneal (Hazare *et al.* 2016). En el caso de las moléculas lipofílicas, su absorción se ve limitada por la naturaleza hidrofílica de la barrera y por la presencia de una elevada densidad de glicoproteína-P (P-gp) que restringe la entrada de fármacos lipofílicos y xenobióticos (Barar *et al.* 2016).

En la parte posterior de la conjuntiva se encuentra la esclera con un característico color blanco constituida, principalmente por tejido fibroso de colágeno orientado al azar. Esta estructura presenta, en su parte más externa, una capa delgada y vascularizada denominada epiesclera, en la zona central la capa avascular del estroma escleral formada prácticamente de fibras de colágeno y en la capa más interna se encuentra la lámina fusca de color marrón, debido a la migración de los melanocitos desde la coroides. La esclera presenta una función de protección, mantiene la forma del globo ocular y en ella se acoplan los músculos oculares. A nivel biofarmacéutico, la esclera es permeable a las moléculas hidrofílicas en menor grado que la conjuntiva y en mayor grado que la córnea. Una vez superada la barrera de la esclera, las moléculas se encuentran en la capa de la coroides, tejido altamente vascularizado que permite alcanzar los tejidos circundantes (Ansari and Nadeem 2016).

Además de las barreras descritas que debe atravesar un medicamento para alcanzar diferentes tejidos del segmento anterior ocular, hay que

considerar que el ojo es un órgano dinámico que si se le incorpora alguna molécula xenobiótica la detecta como un cuerpo extraño e inicia los mecanismos de eliminación para evitar su incorporación en el globo ocular (**Figura 2**) (Lakhani, Patil and Majumdar 2018).

El primer mecanismo reflejo es la dilución mediante la producción activa de lágrimas, llegando a generar un volumen cercano de 400 µL y favoreciendo la eliminación del medicamento a través del drenaje nasolagrimal. A su vez, el fluido lagrimal con pH de 7,4 ionizaría aquellos fármacos que dependen de su pKa, limitando su permeabilidad en las membranas lipofílicas (Angayarkanni *et al.* 2016). La presencia de proteínas, inmunoglobulinas y mucina libre en la película lagrimal conllevaría que los fármacos se unieran a ellas reduciendo su actividad y facilitando su eliminación por el arrastre de lágrima refleja, por lo que solo un 5% de la formulación estaría disponible para realizar su acción farmacológica (Araújo *et al.* 2009). Otra vía inmediata de disminución de la concentración del fármaco administrado tiene lugar en la conjuntiva. En este tejido, al ser vascularizado e inervado linfáticamente, se eliminan las moléculas que pasarían a la circulación sistémica a través de proteínas de membranas de eflujo, como la P-gp y la proteína asociada a la resistencia a múltiples fármacos (MRP), con el consiguiente riesgo de desencadenar efectos secundarios sistémicos (Aukunuru *et al.* 2001). A nivel del estroma escleral y corneal, aquellas moléculas cargadas positivamente son inactivadas debido a la unión con los proteoglicanos cargados negativamente. En la cámara anterior, las moléculas pueden ser eliminadas por la renovación del humor acuoso. Aquella molécula que logra atravesar el estroma escleral y el humor acuoso se aloja en la úvea (coroides, iris y

cuerpo ciliar), donde las enzimas del citocromo P450 (CYP) reductasa, específicamente 3A1 y 2B2, en conjunto con la barrera hemato-acuosa, inactivan y barren las moléculas del globo ocular, respectivamente (Guengerich 2017).

En general, una molécula por si sola se enfrenta a diversas dificultades para lograr un objetivo farmacológico en un paciente, puesto que un sistema de administración de fármacos depende de su coeficiente de reparto, de su capacidad mucoadhesiva, de su viscosidad, de su pKa y de su resistencia al metabolismo, entre otros, para obtener concentraciones farmacológicas constantes y efectivas en el tejido diana.

1.2. Enfermedades oculares inflamatorias

1.2.1. Uveítis y escleritis

La uveítis es una de las enfermedades intraoculares inflamatorias más comunes que conlleva la inflamación de las estructuras de la úvea (iris, cuerpo ciliar y coroides). Clínicamente, este término incluye más estructuras intraoculares como los segmentos anterior y posterior del ojo, clasificando la uveítis de acuerdo con su ubicación anatómica ocular (**Tabla 1**) (The Standardization of Uveitis Nomenclature (SUN) Working Group 2005). La manifestación de esta enfermedad puede tener diversas etiologías que van desde infecciones, traumas, efectos adversos de ciertos medicamentos, manifestaciones autoinmunes y hasta enfermedades inflamatorias sistémicas (Guly and Forrester 2010; Dalal, Nida Sen and Nussenblatt 2014). Actualmente la uveítis representa el 10% de las causas de ceguera en el mundo, pudiendo afectar a pacientes de cualquier edad y etnia. A nivel mundial, la prevalencia en promedio es de 160 personas por cada 100.000 habitantes y una incidencia por año de 35 personas por cada 100.000 habitantes (Papaliodis 2017).

Por otro lado, cuando la esclera presenta un estado inflamatorio se le denomina escleritis o epiescleritis, siendo el primero más severo, doloroso y de mayor repercusión en el proceso de la visión. La epiescleritis suele ser de carácter agudo y en la mayoría de los casos idiopática. La etiología de estos desórdenes inflamatorios de la esclera, al igual que en la úvea, responde a múltiples causas, una de ellas es el grupo de las enfermedades inflamatorias

sistémicas, como la artritis reumatoide, la enfermedad de Crohn, el Lupus y la enfermedad de Behcet, entre otras (Akpek *et al.* 1999).

Tabla 1. Enfermedades de uveítis según su clasificación anatómica.

Tipo	Desórdenes asociados
Anterior	Iritis, iridociclitis y ciclitis anterior.
Intermedia	Pars planitis, ciclitis posterior y vitritis.
Posterior	Focal, multifocal, coroiditis difusa, corioretinitis, retinitis y neuroretinitis.
Panuveítis	Todos los segmentos oculares involucrados.

1.2.2. Proceso molecular inflamatorio

La inflamación ocular es el proceso vascular que se inicia en respuesta a una lesión en un tejido. Esta lesión puede ser de origen externo, como un trauma, una exposición a un xenobiótico tóxico o un patógeno, o bien una respuesta a una enfermedad sistémica inflamatoria autoinmune. El desencadenamiento de la producción de factores de crecimiento, citoquinas y el trauma, inicia el proceso de reparación y aislamiento del agente que provoca la lesión en el tejido y se estimula a la enzima fosfolipasa A_2 (PLA_2), iniciando la biosíntesis de eicosanoides a partir de un fosfolípido, el ácido araquidónico (AA) que se encuentra presente en las membranas celulares. Los eicosanoides tales como las prostaglandinas (PGs) y los tromboxanos (TXs), son sintetizados por la vía enzimática ciclooxigenasa (COX), mientras que los leucotrienos (LTs) por la lipoxigenasa (LOX). El AA también puede ser metabolizado por el CYP450 generando ácido epoxieicosatetraenoico (EETs). Paralelamente, el AA es un mediador celular que puede estimular la producción de citoquinas proinflamatorias e iniciar

procesos apoptóticos. En general, los eicosanoides poseen la capacidad de provocar distintas respuestas fisiológicas, homeostasis vascular y agregación plaquetaria que regulan procesos inmunopatológicos e inflamatorios (**Tabla 2**) (Dennis and Norris 2015).

Tabla 2. Respuestas fisiológicas de los eicosanoides.

Vía principal	Mediador	Respuesta fisiológica
COX	PGE_2	Vasodilatación (↑PIO) y permeabilidad vascular; hiperalgesia; ↑IL-10; ↓TNF.
	PGD_2	Vasodilatación; ↑reclutamiento de eosinófilos y respuesta alérgica.
	$PGF_{2\alpha}$	↓PIO.
	PGI_2	↓Agregación plaquetaria; hiperalgesia; vasodilatación; ↑IL-10; ↓TNF.
	TXA_2	↑Agregación plaquetaria; vasoconstricción.
LOX	LTB_4	Reclutamiento de neutrófilos; permeabilidad vascular.
	LTC_4, LTD_4 y LTE_4	Permeabilidad vascular; extravasación de neutrófilos.
	HPETEs, HETEs y diHETEs	Hiperalgesia.
	HXA_3 y HXB_3	Hiperalgesia.
	LXA_4, 15-epi-LXA_4, LXB_4 y15-epi-LXB_4	Reclutamiento de neutrófilos; eferocitosis.
CYP	EETs	Vasodilatación; antihiperalgesia; ↓expresión COX2.

PIO: Presión intraocular.

1.2.3. Corticoides en el tratamiento de la inflamación: Fluorometolona

Los corticoides son potentes antiinflamatorios que inhiben la respuesta inflamatoria a través de tres vías principales (**Figura 3**). La primera vía es la inducción y activación de la proteína anexina I, que interactúa con la PLA$_2$ inhibiéndola. El bloqueo de la PLA$_2$ inhibe la producción de eicosanoides y la liberación de AA como mediador celular. La segunda vía es la inducción de la proteína MAPK fosfatasa I que desfosforila e inhibe toda la cascada de las proteínas MAPK, teniendo como consecuencia la inhibición de la PLA$_2$. A su vez, MAPK fosfatasa I inhibe la vía de Jun-terminal quinasa que tiene la función de activar los factores de transcripción proinflamatorios (Jun; Fos). La tercera vía antiinflamatoria importante es el bloqueo de la actividad transcripcional de NF-κB, inhibiendo la transcripción de citoquinas proinflamatorias y la expresión de las COXs (Rhen and Cidlowski 2005).

La efectividad de los corticoides en el tratamiento de la inflamación, en comparación con los antiinflamatorios no esteroideos (AINEs), es más completa debido a que los AINEs solo bloquean la vía de la COX. No obstante, los corticoides poseen efectos secundarios asociados importantes que a nivel ocular exacerban enfermedades como el glaucoma o las cataratas, cuando los tratamientos son prolongados. Uno de los efectos secundarios que se debe monitorizar durante el tratamiento con corticoides clásicos (prednisolona, dexametasona y betametasona) es la PIO, que lleva a padecer o agravar el glaucoma. Los corticoides de administración tópica son utilizados solamente para aquellas afecciones que se ubican en el segmento anterior con las limitaciones propias de la formulación y de la

barrera ocular que impide un tratamiento eficiente para alcanzar los resultados farmacológicos requeridos. Para el segmento posterior se utilizan corticoides sistémicos, intravítreales y perioculares que poseen una alta recurrencia de aumento de la PIO (Tripathi *et al.* 1999).
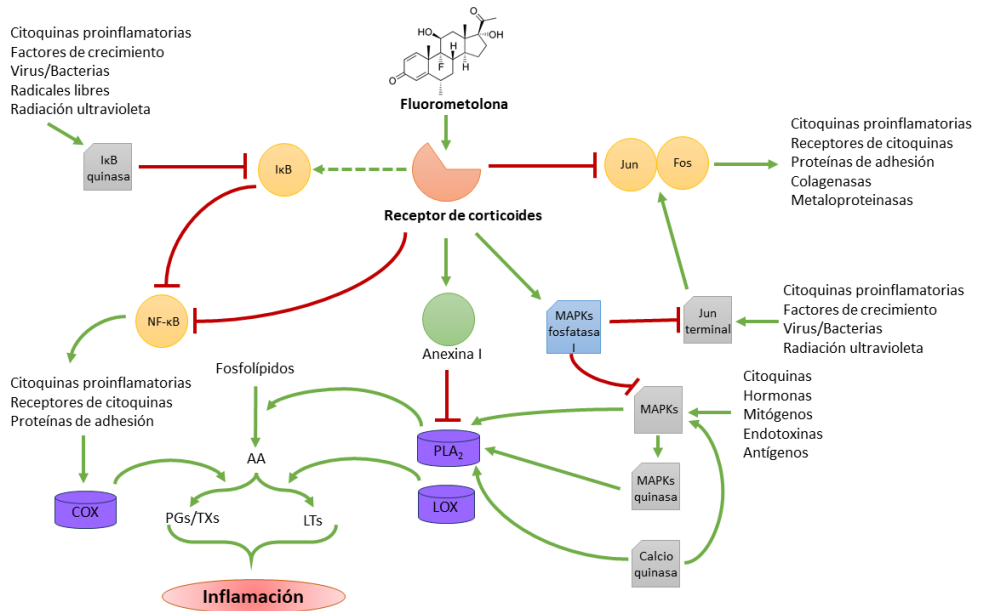

Figura 3. Mecanismo de inhibición de los corticoides.

La Fluorometolona (FMT) es un corticoide de nueva generación, de características lipofílicas con un LogP 2,34 y solubilidad en agua (a 25 °C) de 30 mg·L^{-1}. Su peso molecular es de 378,468 g·mol^{-1}, un punto de fusión entre 293-303 °C y prácticamente sin grupos ionizables (pKa: 12,65) (National center for Biotechnology Information 2019). Su forma farmacéutica comercial es en gotas oftálmicas de administración tópica y actualmente en el mercado existen dos especialidades: FML$^{®}$ e Isoptoflucon$^{®}$ con una concentración de 0.1% para el tratamiento de alergias

e inflamación ocular del segmento anterior. La FMT posee una potencia moderada y con menores efectos en el incremento de la PIO que los corticoides clásicos (incremento menor a 6 mm Hg) (Lin and Gong 2015; Chen *et al.* 2016; Pinto-Fraga *et al.* 2016; Shokoohi-Rad *et al.* 2018).

1.3. Sistemas nanoestructurados de uso oftálmico

Durante décadas para tratar enfermedades que afectan a los segmentos anterior y posterior del globo ocular, se han utilizado tanto tratamientos no invasivos, como invasivos para devolver la homeostasis a los tejidos oculares. Dentro de los tratamientos no invasivos, las soluciones, las suspensiones y los ungüentos son las formulaciones convencionales que se han utilizado con resultados terapéuticos poco eficaces, debido a las limitaciones anatómicas y a la dinámica de eliminación de xenobióticos en el ojo (Awan *et al.* 2009). Por otra parte, los tratamiento invasivos suelen ser poco prácticos, debido a su alta recurrencia de efectos adversos y la falta de adherencia al tratamiento (Morgan *et al.* 1988; Yasin *et al.* 2014). Por ello, la utilización de la nanotecnología como herramienta para sobrellevar estos desafíos ha sido la clave para el trasporte de fármacos, proteínas y genes hacia el interior del ojo. Los sistemas nanoestructurados tales como los hidrogeles (HGs), los liposomas, las nanopartículas (NPs) poliméricas y lipídicas han permitido obtener concentraciones efectivas en el lugar diana, con una disminución significativa de los efectos adversos (Silva *et al.* 2012; Vega *et al.* 2013; Abrego *et al.* 2015; Yu *et al.* 2018). Particularmente, la eficacia de un tratamiento farmacológico ocular no invasivo a través de nanosistemas se debe a las siguientes propiedades (Lalu *et al.* 2017):

- Aumento del tiempo de residencia precorneal.
- Liberación controlada y prolongada del fármaco.
- Evitan la eliminación del fármaco.
- Protección del fármaco de la ionización y del metabolismo.
- Direccionamiento del fármaco hacia el tejido diana.

Tabla 3. NPs poliméricas con corticoides para el tratamiento de la inflamación ocular.

Polímero	Fármaco	Método de preparación	Referencias
Quitosano	Dexametasona	Desplazamiento de solvente	(Kalam 2016)
Celulosa/Eudragit®	Dexametasona	Desplazamiento de solvente	(Balzus *et al.* 2017)
Eudragit RS 100	Prednisolona	Emulsificación espontanea	(Ibrahim *et al.* 2010)
Eudragit RS100	Metilprednisolona	Cuasi emulsión-difusión por solvente	(Adibkia *et al.* 2007)
Gelatina con ciclodextrina	Hidrocortisona	Desolvatación	(Vandervoort & Ludwig 2004)
Isopropilacrilamida	Dexametasona	Polimerización por radicales libres	(Rafie *et al.* 2010)
PLA-PEG	Betametasona	Emulsión-difusión por solvente	(Sakai *et al.* 2006)
PLGA	Triamcinolona	Emulsión-difusión por solvente	(Sabzevari *et al.* 2013)
PLGA	Hidrocortisona	Emulsión-difusión por solvente	(Yang *et al.* 2015)
PLGA	Dexametasona	Desplazamiento de solvente	(Pan *et al.* 2015)
PLGA	Fluocinolona	Hidratación de película	(Diebold & Calonge 2010)

De todos los sistemas nanoestructurados, las NPs poliméricas son los sistemas coloidales de características más biodegradables y más biocompatibles existentes, con tamaños entre 10 y 1.000 nm (Kumari, Yadav and Yadav 2010). A su vez, las NPs poliméricas cargadas con corticoides se han utilizados para el tratamiento de la inflamación ocular con una gran eficacia farmacológica (**Tabla 3**). Estas partículas pueden subdividirse en dos categorías según su conformación, en forma de vesícula (nanocápsulas) o como matriz polimérica (nanoesferas). Las nanocápsulas son sistemas constituidos por una membrana polimérica y en su interior se aloja el fármaco (núcleo). Por otra parte, las nanoesferas son sistemas formados por una matriz polimérica donde el fármaco se encuentra adsorbido en la superficie y disperso o disuelto en su interior (Rao and Geckeler 2011).

En general, las NPs que están constituidas por un polímero de características naturales o sintéticas se denominan de primera generación (**Figura 4**). Habitualmente el polímero sintético más utilizado es el ácido poliláctico-co-glicólico (PLGA), aprobado por las agencias de salud de la Unión Europea y de Estados Unidos (EMA y FDA) para el uso a nivel parenteral y tópico. Una de las características de interés del PLGA es la predicción de su cinética de degradación que depende de la proporción láctico/glicólico del polímero. A medida que la proporción de láctico aumenta (entre 50 y 100) y la de glicólico se reduce (entre 50 y 0), la tasa de degradación disminuye. Además, este polímero se considera no tóxico debido a su hidrolisis no enzimática generando como productos el ácido glicólico y el ácido láctico, los cuales son metabolizados por el ciclo de Krebs. Paralelamente, el PLGA es un polímero lipofílico que permite la encapsulación de sustancias de baja solubilidad en agua con una alta

reproducibilidad en su elaboración y una liberación del fármaco de forma controlada y prolongada. Comercialmente existen diferentes tipos de PLGA con diferentes pesos moleculares, viscosidad inherente, proporción de láctico/glicólico y grupo funcional terminal (Jain 2000; Makadia and Siegel 2011). Por ejemplo, el PLGA RG 503H es un polímero con una proporción 50/50 que posee un ácido carboxílico terminal que permite la conjugación con otros polímeros, tales como el polietilenglicol (PEG) o el copolímero polioxietileno (PEO)-polioxipropileno (PPO) (Kapoor *et al.* 2015). El recubrimiento de las NPs de PLGA con PEG se denomina pegilación y este tipo de sistema nanoestructurado es considerado de segunda generación (**Figura 4**). El PEO-PPO y el PEG forman en las NPs una capa hidrofílica en su superficie que les permite escapar del sistema retículo endotelial, aumentando su vida media en circulación y al mismo tiempo les otorgan la capacidad de interaccionar con la mucina de la película lagrimal aumentando la mucoadhesividad de las NPs. Por otra parte, los sistemas de tercera generación (**Figura 4**) tienen como objetivo el direccionamiento e internalización de las NPs a partir de receptores de membrana de las células blanco (Diebold and Calonge 2010). Para ello los anticuerpos o péptidos de penetración celular (CPPs) son conjugados en el grupo terminal de un espaciador hidrofílico como el PEG en las NPs. Este espaciador es necesario para que el agente esté expuesto en la superficie y de esta forma interaccione o se una a los receptores diana (Vasconcelos *et al.* 2015).

En resumen, las NPs de PLGA evitan la ionización del fármaco en la película lagrimal, otorgan un sistema de liberación controlado y retrasan el metabolismo enzimático. Con la incorporación del PEG en la superficie se proporciona un comportamiento anfipático, donde el núcleo de PLGA es

apolar y la superficie polar, lo que hace aumentar sus posibilidades de atravesar las capas oculares hidrofílicas y lipofílicas. También el PEG evita la eliminación rápida de las NPs, por lo que es posible realizar administraciones oculares menos recurrentes si se compara con los tratamientos convencionales oftálmicos, lo que facilitaría la adherencia del paciente al tratamiento. Finalmente, la conjugación con CPPs y anticuerpos permite específicamente la internalización celular e interacción con los receptores de membrana, otorgando un tratamiento específico con concentraciones efectivas del fármaco en el tejido diana y con menos efectos adversos (Diebold and Calonge 2010).
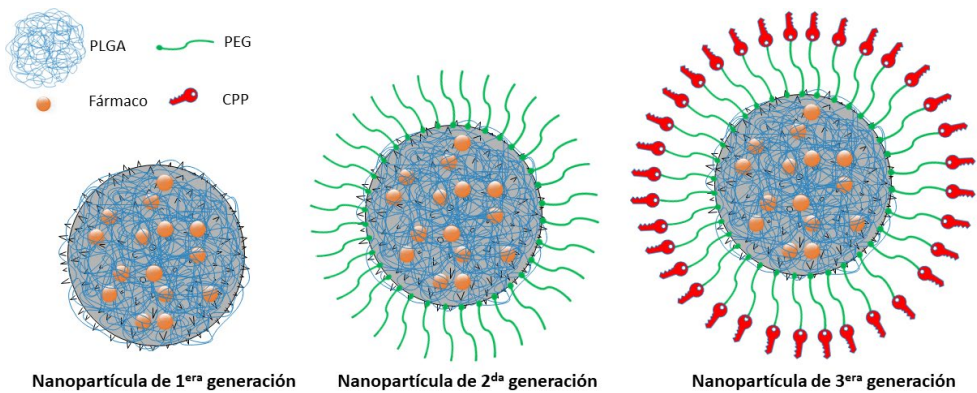

Figura 4. Generaciones de NPs.

Para conseguir aumentar el tiempo de residencia precorneal, los HGs son la respuesta para que una formulación permanezca más tiempo en contacto con el globo ocular, prologando la liberación del fármaco. Particularmente, los HGs son matrices tridimensionales de entrelazamiento polimérico con la capacidad de absorber grandes cantidades de agua para su formación. Los HGs se pueden clasificar en químicos y físicos según su tipo de entrecruzamiento. Los HGs químicos o también llamados permanentes,

su entrecruzamiento puede ser de características covalentes con distintos grupos funcionales (NH_2-, COOH- y OH-), por la acción enzimática o por una actividad radicalaria. Por otro lado, los HGs de activación física o reversibles se forman por diferentes tipos de interacciones no covalentes como puentes de hidrogeno, fuerzas de Van der Waals, iónicas, proteicas y de autoensamblaje entre polímeros (McKenzie *et al.* 2015; Parhi 2017). Algunas de las ventajas de los HGs son: su alta biocompatibilidad debido a su alta proporción de agua, su viscoelasticidad, su consistencia suave y su baja tensión superficial cuando entran en contacto con superficies acuosas, asemejándose a los tejidos vivos más que otros biomateriales sintéticos (Li and Mooney 2016). También presentan un entorno poroso capaz de alojar fármacos u otros sistemas, protegiéndolos del metabolismo o del efecto del pH. Además, este sistema facilita una liberación controlada dependiendo del hinchamiento, de la degradación y de la disolución del HG. Desde un punto de vista de la administración tópica ocular, se prefieren formulaciones de características newtonianas (líquidas) en vez de plásticas (cremas o ungüentos) para facilitar la instilación y de esta forma aumentar la adherencia al tratamiento. En el caso anterior, los HGs de formación *in-situ* aprobados para su comercialización utilizan como estímulo de activación el efecto del pH, sales inorgánicas, conjugación con grupos funcionales de proteínas como la mucina y/o la temperatura ocular (**Tabla 4**) (Kumar *et al.* 2013; Al-Kinani *et al.* 2018; Wu *et al.* 2018). Estos sistemas constituirían un comportamiento bimodal, newtoniano antes de la instilación y pseudoplástico o plástico cuando entra en contacto con el globo ocular. Uno de los métodos de formación de HGs *in-situ* de forma inmediata a nivel ocular es por el efecto de la temperatura. El resto de los sistemas de

activación requieren mayor tiempo para alcanzar el equilibrio termodinámico para la formación del HG, haciendo posible la eliminación de la formulación desde la zona precorneal como resultado de la renovación lagrimal (Cheng *et al.* 2016; Jain *et al.* 2016).

Tabla 4. HGs de gelificación *in-situ* comercializados.

Nombre del producto	Polímero	Sistema de activación	Compañía farmacéutica
Timoptic-XE® (Timolol)	Goma gellan	Ión	Merck Pharmaceuticals
Pilopine HS® (Pilocarpina)	Carbopol 940	pH	Alcon Laboratories
Azasite® (Azitromicina)	P407	Temperatura	InSite Vision
Timoptol-LA (Timolol)	Goma gellan	Ión	Laboratories Merck Sharp and Dohme
Virgan (Ganciclovir)	Carbopol 940	pH	Laboratories THEA-France

Un copolímero empleado de forma segura en las industrias farmacéutica y alimentaria son los poloxámeros. Este copolímero no iónico está constituido por dos unidades hidrofílicas de PEO localizadas al inicio y al final de la cadena polimérica, mientras que en la zona central se encuentra una unidad hidrófoba de PPO. Particularmente, el poloxámero 407 (P407) es un polímero que se autoensambla *in-situ* formando micelas hasta el punto de que el polímero gelifica completamente. El mecanismo de gelificación depende de la temperatura y de la concentración de P407. Sin embargo, las temperaturas de transición sol-gel se modifican cuando las formulaciones de P407 se cargan con sustancias viscosificantes, fármacos, tensoactivos u otros

sistemas de liberación (dos Santos *et al.* 2015; Almeida *et al.* 2017; Jung *et al.* 2017). Por lo tanto, una formulación adecuadamente optimizada para que gelifique a la temperatura corneal (32 °C cuando el ojo está abierto y 35 °C cuando está cerrado) es ideal para que ser instilada en forma de gotas oftálmicas.

Una de las estrategias terapéuticas actuales se basa en la incorporación de NPs poliméricas en sistemas gelificantes *in-situ* (**Figura 5**) que tienen por objetivo aumentar la biodisponibilidad del fármaco en el tejido ocular diana y disminuir periodicidad de administración. Esta estrategia permite una liberación más prolongada y controlada evitando el efecto de estallido que presentan las NPs en las primeras horas de la liberación e incrementando su tiempo de residencia precorneal (Huang and Brazel 2001; Gou *et al.* 2008).
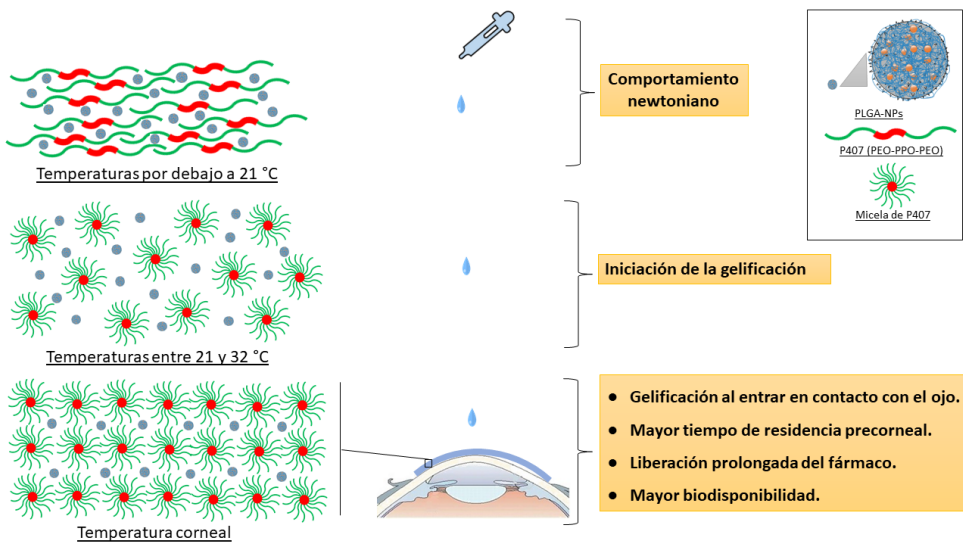

Figura 5. Sistema de gelificación *in-situ* cargado con NPs de PLGA.

1.4. Internalización de nanopartículas a través de péptidos de penetración celular (CPPs)

Uno de los desafíos farmacológicos más complejo de lograr a nivel ocular es la obtención de concentraciones efectivas de fármaco en el tejido a tratar, debido a las limitaciones de las barreras oculares y a la naturaleza de la misma formulación que no permite una adecuada permeación ocular. Dentro de las nuevas tecnologías moleculares para sobrellevar los inconvenientes que sufren los medicamentos convencionales, el empleo de CPPs es el enfoque más reciente y revolucionario para la internalización de macromoléculas y fármacos en las células oculares. Los CPPs son secuencias peptídicas entre 5 a 30 aminoácidos (aa) capaces de internalizarse en las células de forma no invasiva a través de diversos mecanismos tanto energéticos con receptores específicos como no energéticos y sin mediación de receptores. De acuerdo con sus propiedades fisicoquímicas pueden categorizarse en hidrófobas, anfipáticas y catiónicas, siendo esta última categoría donde se encuentra más CPPs de características positivas por sus secuencias ricas en residuos de arginina (Arg) (Guidotti, Brambilla and Rossi 2017).

La proteína activadora de transcripción (TAT) del virus de la inmunodeficiencia humana 1 (HIV-1) fue la primera proteína descubierta con propiedades catiónicas y capaz de internalizar macromoléculas hacia el interior de las células mediante formación de poros y penetración directa. A pesar de que han transcurrido más de 30 años desde su descubrimiento, en el año 1997, se identificó exactamente la secuencia que permite la internalización celular (TAT$_{49-57}$). Esta secuencia se ha utilizado

ampliamente en el transporte de proteínas terapéuticas y de otros sistemas de liberación como NPs (Shi *et al.* 2014). En un estudio preclínico el TAT$_{49-57}$ fue conjugado con un péptido inhibidor de Jun-terminal quinasa (XG-102) con el objeto de evitar la apoptosis celular en la isquemia cerebral, demostrándose su capacidad de atravesar la barrera hematoencefálica. Además, este nuevo fármaco XG-102 en el año 2016 completó su fase clínica III (NCT02235272) para el tratamiento de la inflamación intraocular, donde se evidenciaron mejoras significativas en comparación con la Dexametasona (Bolhassani, Jafarzade and Mardani 2017).

En el año 1991 se descubrió que el homeodominio de Antennapedia, una proteína de *Drosophila Melanogaster*, es capaz de internalizarse en células neuronales. En el año1994 se identificó específicamente la secuencia de 16 aa de los residuos 43-58 llamada pAntp$_{43-58}$ o Penetratin, responsable de la internalización celular. Esta secuencia, con propiedades básicas al igual que el TAT, ha sido utilizada tanto para la internalización de proteínas como para la transfección de ácidos nucleicos. Actualmente existen diversos estudios acerca de sus métodos de internalización, de los cuales los más aceptados son la formación invertida de micelas, la endocitosis y la translocación directa (Farkhani *et al.* 2014).

Desde el descubrimiento de los CPPs se ha relacionado la capacidad de internalizar moléculas con las cargas positivas y que éstas provengan de los residuos de Arg, por lo que queda demostrado que una secuencia sintética de 8 Arg (Poliarginina, R8) es suficiente para la traslocación celular. Particularmente, los grupos guanidinas de la cadena lateral de la Arg interaccionan a través de puentes de hidrógeno con los grupos cargados

negativamente, tales como los grupos carboxílicos, sulfatos y fosfatos de las proteínas de membrana, fosfolípidos y mucopolisacáridos, que llevan finalmente a la internalización celular por endocitosis o penetración directa (Pescina *et al.* 2018). En un estudio clínico, la secuencia R8 fue utilizada en conjugación con una ciclosporina (PsorBan®) para el tratamiento de la psoriasis, evidenciándose una alta eficacia en el tratamiento sin efectos sistémicos asociados al fármaco y comprobándose la capacidad de internalizar moléculas (Delcroix *et al.* 2010).

Una de las particularidades de los CPPs es su similitud con las características de los péptidos antimicrobianos (AMPs), principalmente por sus múltiples residuos de Arg y una carga neta positiva. Los AMPs son capaces de interaccionar fuertemente con la membrana plasmática al igual que CPPs translocándose al interior de las células, sin embargo, solo algunos AMPs son capaces de hacerlo sin permeabilizarla permanentemente. Los AMPs que permeabilizan la membrana permanentemente son los que conducen directamente a la muerte bacteriana y se consideran de los más tóxicos. También, existen otros AMPs con capacidad de translocarse sin efectos tóxicos directos, siendo considerados bacteriostáticos debido a la inhibición de las vías de síntesis de ADN y de proteínas, sin afectar las células humanas (Splith and Neundorf 2011). Dentro de los CPPs con actividad contra Gram (+), Gram (-) y antimicótica se encuentra el pAntp, Transportan, pVec, Pep-1, TAT, entre otros. Por otro lado, en el grupo de los AMPs citados con capacidad de translocar moléculas, sin causar daños en las células eucariotas, se encuentra la Lactoferricina, la Bac7$_{1-24}$, la Buforina II y la Pirrocoricina. También en el grupo de péptidos con actividad antimicrobiana se puede encontrar actividad CPP, como el mismo TAT

contra HIV-1 y péptidos antivírico contra el herpes simple, tales como el G2 y el gH625 (Pärn, Eriste and Langel 2015). Específicamente, el péptido G2 es una secuencia de 12 aa cargada positivamente con múltiples residuos de Arg. En un estudio donde se trató una infección ocular con herpes simple, el G2 fue conjugado covalentemente con Aciclovir, incrementando la eficacia antivírico (Ali *et al.* 2012). En otro estudio el G2 se utilizó para el tratamiento del herpes simple vaginal y se confirmó que el péptido forma poros de transmembrana (Tiwari *et al.* 2011). De acuerdo con los antecedentes, el G2 podría constituir un potencial CPP para el transporte de macromoléculas como proteínas o NPs al interior de células eucariotas.

2. OBJETIVOS

The main objective of this research is the development and characterization of controlled release polymeric nanostructured systems containing FMT for the treatment of inflammatory conditions of the anterior and posterior segment of the eye. In addition, biopharmaceutical behaviour, safety evaluation and therapeutic efficacy in the treatment of ocular inflammatory diseases are part of this PhD thesis.

Specific objectives:

- Develop, optimize and characterize polymeric nanostructured systems such as PLGA NPs and *in-situ* forming gels containing FMT.
- Synthesize and characterize the polymers Rhodamine-PLGA and maleimide-PEG-PLGA.
- Synthesize and conjugate the CPPs (TAT_{49-57}, $pAntp_{43-58}$ and G2) to FMT-loaded maleimide-PEG-PLGA NPs.
- Obtain a biopharmaceutical profile of sustained FMT release from PLGA NPs and *in-situ* forming gels.
- Evaluate the ocular tolerance of nanostructured systems developed by *in vitro* (HET-CAM® and MTT test) and/or *in vivo* (Draize test) studies.
- Demonstrate *in vivo* that PLGA NPs and *in-situ* forming gels are suitable for the treatment of inflammatory conditions of the anterior and posterior segments of the eye.
- Study and analyze the effects on proinflammatory cytokines and the uptake in both human corneal cells and in the mouse eye with conjugated NPs.

3. RESULTADOS

Los resultados obtenidos en los distintos estudios de la presente investigación han permitido generar tres publicaciones científicas en forma de artículos (dos de ellos ya publicados y el tercero enviado).

3.1. Development of fluorometholone-loaded PLGA nanoparticles for treatment of inflammatory disorders of anterior and posterior segments of the eye, *International Journal of Pharmaceutics*, 547 (2018) 338–346.

3.2. *In-situ* forming gels containing fluorometholone-loaded polymeric nanoparticles for ocular inflammatory conditions, *Colloids and Surfaces B: Biointerfaces*. 175 (2019) 365–374.

3.3. Ocular penetration of fluorometholone-loaded PEG-PLGA nanoparticles functionalized with cell-penetrating peptides. *Nanomedicine*, article submitted.

3.1. Development of fluorometholone-loaded PLGA nanoparticles for treatment of inflammatory disorders of anterior and posterior segments of the eye

Roberto González-Pizarro[a,b], Marcelle Silva-Abreu[a,b], Ana Cristina Calpena[a,b], María Antonia Egea[a,b], Marta Espina[a,b], María Luisa García[a,b].

[a]Department of Pharmacy, Pharmaceutical Technology and Physical Chemistry, Faculty of Pharmacy and Food Sciences, University of Barcelona, 08028 Barcelona, Spain.
[b]Institute of Nanoscience and Nanotechnology (IN2UB), University of Barcelona, Barcelona, Spain.

Development of fluorometholone-loaded PLGA nanoparticles for treatment of inflammatory disorders of anterior and posterior segments of the eye

Roberto Gonzalez-Pizarro[a], Marcelle Silva-Abreu[a,b], Ana Cristina Calpena[a,b], María Antonia Egea[b], Marta Espina[a,b], María Luisa García[a,b,*]

[a] Department of Pharmacy, Pharmaceutical Technology and Physical Chemistry, Faculty of Pharmacy and Food Sciences, University of Barcelona, 08028 Barcelona, Spain
[b] Institute of Nanoscience and Nanotechnology (IN2UB), University of Barcelona, 08028 Barcelona, Spain

ARTICLE INFO

ABSTRACT

The main objective of this study was the development and optimization of fluorometholone-loaded PLGA nanoparticles for the treatment of inflammatory conditions of the eye. Design of experiments was used to obtain nanoparticles with the best physicochemical characteristics. The optimized nanoparticles containing $1.5\,mg \cdot mL^{-1}$ of fluorometholone showed a negative surface charge ($-30\,mV$) and an average size below 200 nm being suitable for ocular administration. Drug-polymer interaction studies confirmed no new bonds were formed during the synthesis. Nanoparticles performance was assessed with biopharmaceutical behavior studies, ocular tolerance, anti-inflammatory efficacy and bioavailability. The biopharmaceutical behavior of the drug from nanoparticles was adjusted to hyperbola order showing a significantly greater permeation in the cornea than in the sclera. The optimized formulation had significantly greater anti-inflammatory effects than the commercial formulation. In addition, nanoparticles increased drug penetration toward the vitreous. Polymeric nanoparticles of fluorometholone could provide a suitable alternative for the treatment of inflammatory disorders of the anterior and posterior segments of the eye against of conventional topical formulations.

1. Introduction

The treatment of inflammatory eye diseases such as severe allergic conjunctivitis and uveitis is focused on the use of corticosteroids as anti-inflammatory drugs (Bielory et al., 2010). These ophthalmic drugs used topically have certain disadvantages ranging from the low amount of drug penetrating through the cornea to the limited residence time in the precorneal area. This causes that the suspensions need to be administered a greater many times per day to obtain a significant therapeutic effect (Gause et al., 2016). In other cases, in which the posterior segment is affected, as in posterior uveitis, intravitreal injections are used so that the drug can reach the target (Yasin et al., 2014). Moreover, the main ocular side effect after topical administration of corticosteroids include cataracts and increased intraocular pressure, which could induce visual disorders. Among all the corticosteroids, fluorometholone (FMT) is characterized by a highest pharmacological potency for inflammations of the anterior segment of the eye with a significantly lower risk of increasing intraocular pressure (Chen et al., 2016; Shokoohi-Rad et al., 2017).

Currently, the encapsulation of drugs in polymer matrices has been one of the solutions for overcoming the disadvantages presented by ophthalmic suspensions (Danhier et al., 2012). Particularly, PLGA nanoparticles (NPs) have proven to be one of the most suitable topical ocular administration systems, due to their sustained and prolonged release of the drug, mainly produced by diffusion (Kapoor et al., 2015). Once the NPs have been administered, the PLGA hydrolyzes in monomers (lactic acid and glycolic acid) with subsequent metabolism in the Krebs cycle, which makes this polymer highly biodegradable and biocompatible (Anderson and Shive, 2012; Diebold and Calonge, 2010; Makadia and Siegel, 2011).

In other studies, it has been shown that PLGA NPs are able to cross the tear film and the cornea, with the possibility of reaching deeper tissues such as the vitreous and the retina (Silva-Abreu et al., 2018; Tahara et al., 2017). In different reports, PLGA has been shown to protect the drug from deactivation by the enzyme cytochrome P450 present in the tear film, corneal epithelium and ciliary, increasing the half-life of the drug (Guengerich, 2017). According to the above, these systems would allow to reduce the side effects associated with the drug with a sustained and safe release without the need for repeated administrations (Siddique et al., 2015).

RESULTADOS

R. Gonzalez-Pizarro et al.

The main objective of this study was the development of FMT loaded-PLGA NPs (FMT-PLGA-NPs) able to reach tissues of the anterior and posterior segment of the eye with the aim to be administered less often than medications currently marketed. The physicochemical properties, drug-polymer interaction, short-term stability and *in vitro/ex vivo* biopharmaceutical behavior were also assayed. Ocular tolerance, *in vivo* anti-inflammatory efficacy and ocular bioavailability of FMT-PLGA-NPs were carried out as evidence of effectivity and usefulness of NPs as a novel treatment for ocular inflammatory disorders.

2. Material and methods

2.1. Materials

FMT was purchased from Capot Chemical (Hangzhou, China). PLGA RG 503H was obtained from Evonik Corporation (Birmingham, USA). Poloxamer 188 (P188) and Transcutol P® were given from BASF (Barcelona, Spain) and Gattefossé (Madrid, Spain), respectively. Acetone was purchased from Fisher Scientific (Pittsburgh, USA). Water through Millipore® MilliQ system was used for all the experiments and all the other reagents were of analytical grade.

2.2. Preparation and optimization of NPs

FMT-loaded PLGA NPs were prepared by solvent displacement method described elsewhere (Cañadas et al., 2016; Fessi et al., 1989). Briefly, PLGA (5.6–12.4 $mg \cdot mL^{-1}$) and the FMT (0.16–1.84 $mg \cdot mL^{-1}$) were dissolved in 5 mL of acetone. This organic phase was added slowly dropwise, under moderate stirring, into 10 mL of an aqueous solution of P188 (1.6–18.4 $mg \cdot mL^{-1}$) adjusted to pH 7.4. The NPs resulting were stirred for 10 min. After that, acetone was evaporated under reduced pressure.

Design of experiments (DoE) was employed using central composite design matrix generated by StatGraphics Centurion XV. The central composite design was developed to analyze the effects of the independents variables on the dependents (Nekkanti et al., 2015). Three factors (concentration of surfactant [cP188], drug [cFMT] and polymer [cPLGA]), 3-level central composite design on the measured response (average particle size (Zav), polydispersity index (PI), zeta potential (ZP) and entrapment efficiency (EE)) were established for this optimization procedure. Each factor was studied at five different levels coded (see Table 1) and the responses were modelled through the full second-order polynomial equation:

$$Y = \beta_0 + \beta_1 X_1 + \beta_2 X_2 + \beta_3 X_3 + \beta_{11} X_1^2 + \beta_{22} X_2^2 + \beta_{33} X_3^2 + \beta_{12} X_1 X_2 + \beta_{13} X_1 X_3 + \beta_{23} X_2 X_3 \quad (1)$$

where Y is the measured response, β_0 to β_{23} are the regression coefficients and X_1, X_2 and X_3 are the studied factors (Cano et al., 2018).

2.3. Analysis of NPs

Zav, PI, and ZP of NPs were determined by dynamic light scattering (DLS) and electrophoretic mobility, respectively, in a Zetasizer NanoZS (Malvern Instruments, Malvern, UK). Samples were diluted (1:10) and the experiments were performed with disposable capillary cells DTS1070 (Malvern Instruments) at 25 °C. The reported values correspond to the mean ± SD of three different batches of each NPs formulation.

The morphological examination of the NPs formulations was carried out by Transmission Electron Microscopy (TEM) on a Jeol model 1010. To visualize the NPs, copper grids carbon-coated (carbon only) were activated with a glow discharge vacuum system. Samples (10 μL) were placed on grids and negative staining performed with 2% uranyl acetate.

The EE of FMT in the NPs was quantified indirectly by measuring the non-entrapped drug in the dispersion medium. The free FMT was separated by a filtration/centrifugation technique (1:10 dilution) by using an Amicon Ultracell-100 kDa (Amicon® Ultra; Millipore Corporation, Massachusetts, USA) centrifugal filter devices at 25 °C and 5000 rpm for 10 min (Heraeus, Multifuge 3 L-R, Centrifuge. Osterode, GER). The EE was calculated according to the following equation:

$$EE(\%) = \frac{cFMT_0 - cFMT_1}{cFMT_0} \cdot 100 \quad (2)$$

where $cFMT_0$ and $cFMT_1$ are the total amount of FMT and free FMT in the supernatant, respectively. The samples were evaluated by a modified pharmacopeia method of RP-HPLC and validated according to the guidelines of the International Conference on Harmonization (ICH, 2005; USP 29-NF 24, 2006). Briefly, samples were quantified using HPLC Waters 2695 separation module and a Kromasil® C18 column (5 μm, 150 × 4.6 mm) with a mobile phase of methanol/water (65:35) at a flow rate of 1.0 $mL \cdot min^{-1}$. A diode array detector Waters® 2996 at a wavelength of 239 nm was used to detect the FMT. A volume of 10 μL of sample was injected. Data were processed using Empower 3® Software.

2.4. Interaction studies

2.4.1. X-ray diffraction (XRD) analysis

The state amorphous or crystalline of the drug in the NPs were determined by X-ray spectral measurements using Siemens D500 system (Karlsruher, GER). X-ray powder diffractograms were recorded using a Cu K″ radiation (45 kV, 40 mA, λ = 1.544 Å) in the range (2θ) from 2° to 60° with a step size of 0.026° and measuring time of 195.8 s per step.

2.4.2. Fourier transform infrared (FTIR) analysis

FTIR spectra of NPs and compounds separately were obtained using a Thermo Scientific Nicolet iZ10 with an ATR diamond and DTGS detector. The scanning range was 525–4000 cm^{-1}.

2.4.3. Differential scanning calorimetry (DSC) analysis

Thermograms were obtained on a Mettler TA 4000 system (Greifensee, Switzerland) equipped with a DSC 25 cell. The temperature was calibrated by the melting transition point of indium prior to sample analysis. All samples were weighed (Mettler M3 Microbalance) directly in perforated aluminum pans (approximate weight of 2.5 mg), heated (under a nitrogen flow) at a rate of 2 $°C \cdot min^{-1}$ from 20° to 120 °C together to an empty pan used as a reference. Data were evaluated using the Mettler STARe V 9.01 DB software (Mettler-Toledo).

2.5. Biopharmaceutical behavior

2.5.1. In vitro release study

To identify the release profile of the FMT from the polymer matrix of NPs, a study was carried out in amber Franz cells (15 mm diameter). A dialysis membrane MW 12000–14000 Da (Iberoamerica, Spain) was hydrated with the receptor medium methanol/water (65:35) for 24 h before mounted. The FMT-PLGA-NPs were compared with a commercial eye drops (Isoptoflucon® of 1 $mg \cdot mL^{-1}$) and the free drug (1 $mg \cdot mL^{-1}$) dissolved in phosphate buffer solution at pH 7.4. The sink conditions were sustained throughout the experiment for 46 h (Klose

Table 1
Variables and codes used in the experimental design.

Factor ($mg \cdot mL^{-1}$)	Levels				
	-1.68	-1	0	$+1$	$+1.68$
cFMT	0.16	0.50	1.00	1.50	1.84
cPLGA	5.60	7.00	9.00	11.00	12.40
cP188	1.60	5.00	10.00	15.00	18.40

et al., 2011). A volume of 300 μL of the samples was placed in the donor compartment and the receptor compartment was filled with receptor medium thermoregulated at 37° ± 0.5 °C in continuous agitation. Samples of 300 μL were withdrawn from the receptor compartment at fixed times and replaced by an equal volume of fresh receptor medium at the same temperature. The concentration of FMT released was measured by RP-HPLC. Values are reported as the mean ± SD of the triplicates. Akaike's information criterion (AIC) and coefficient correlation (r^2) were determined for each model as an indicator of the model's suitability (Ramos Yacasi et al., 2016).

2.5.2. Ex vivo corneal and sclera permeation study

The *ex vivo* FMT permeation from FMT-PLGA-NPs was evaluated using isolated pig cornea and sclera using Franz cells (9 mm diameter). Pig eyes (Landrace and Large White hybrid weighing 45–60 kg) were supplied from the Faculty of Medicine at Barcelona University, Spain. All experiments were developed following the Association for Research in Vision and Ophthalmology on the Use of Animals in Ophthalmic and Vision Research guidelines. These were approved by the Ethical Committee of the University of Barcelona (number 7428) and the Committee of Animal Experimentation of the Regional Autonomous Government of Catalonia, Spain (Law 32/2007 of November 7, 2007, and "Real Decreto 1201/2005", October 10, 2005). The pigs were sedated by intramuscular administration of ketamine (3 mg·kg^{-1}), xylazine (2.5 mg·kg^{-1}) and midazolam (0.17 mg·kg^{-1}) and euthanized by an overdose of sodium thiopental (100 mg·kg^{-1}) under deep propofol anesthesia (1 mg·kg^{-1}). Eyes were removed and immediately excised. The cornea and sclera were fixed in Franz cells with a diffusion segment of 0.64 cm^2. In all, 200 μL of the test formulation (FMT-PLGA-NPs and Isoptoflucon® of 1 mg·mL^{-1}) were incubated in Franz cells and filled with Transcutol P®/water (65:35). In all experiments, a constant temperature, thermoregulated with a water jacket of 32° ± 0.5 °C and 37° ± 0.5 °C was used for the cornea and sclera, respectively, with agitation at 600 rpm. Samples of 300 μL were withdrawn from the receptor compartment at fixed times and replaced by an equal volume of fresh receptor medium at the same temperature. Sink conditions were maintained throughout the experiment.

To quantify the retained amount of drug (Q_R) in the tissues tested, at the end of the permeation study, tissues were removed from each Franz cell. The cornea and sclera were cleaned using a 0.05% solution of sodium lauryl sulfate and washed with water. Afterward, the permeation segment of the tissues was excised, weighed and treated with methanol/water (65:35) under sonication for 15 min. FMT concentration was quantified using Triple Quadrupole LC/MS/MS Mass Spectrometer (Perkin-Elmer AB Sciex Instruments) in MRM (multiple reaction monitoring). The separate module was HPLC Agilent 1200 series equipped with an atmospheric pressure electrospray ionization ion source. The separation of the drug was carried out on reverse phase column (Kromasil® C18 of 5 μm, 150 × 4.6 mm) using a mobile phase composed of methanol/0.1% formic acid in water (65:35) at a flow rate of 0.6 mL·min^{-1}. Mass variation was recorded at 321.4 and 279.2 Da. Values were reported as the mean ± SD. All the experiments were performed by triplicate.

Permeation parameters were calculated by plotting the cumulative FMT permeating versus time, determining x-intercept by linear regression analysis. The permeability coefficient (K_P) (cm·h^{-1}), steady-state flux (J) (ng·h^{-1}·cm^{-2}) and amount of permeated at 24 h (Q_{24}) (μg) were calculated (Carvajal-Vidal et al., 2017).

2.6. Stability analysis of NPs

The physical stability of the NPs at 4 °C and 25 °C were evaluated by Static Multiple Light Scattering technology (S-MLS) using Turbiscan® Lab. S-MLS identifies the different destabilization phenomena of the colloidal suspension such as creaming, sedimentation, flocculation, and coalescence. NPs were placed in a cylindrical glass measuring cell that

was scanned by a pulsed near-infrared light source (λ = 880 nm) with two synchronous optical detectors (transmission and backscattering). Due to the opacity of the NPs formulation, only the backscattering profiles were used to evaluate the physical stability. The backscattering data were recorded every 24 h at different times after preparation (1, 15 and 30 days).

2.7. Ocular tolerance

2.7.1. In vitro ocular tolerance

In vitro ocular tolerance was assessed using the HET-CAM® test in order to ensure that the formulation of FMT-PLGA-NPs are not irritating when they are administered as eye-drops. Irritation, coagulation and hemorrhage phenomena were measured by applying 300 μL of the formulation studied on chorioallantoic membrane of a fertilized chicken egg, monitoring it during the first 5 min after the application. This assay was conducted according to the guidelines of ICCVAM (The Interagency Coordinating Committee on the Validation of Alternative Methods). The development of the test was carried out with 6 eggs for each formulation (FMT-PLGA-NPs and Isoptoflucon®), 3 for controls positive (NaOH 0.1 M) and negative (0.9% NaCl). The ocular irritation index (OII) was calculated by the sum of the scores of each injury according to the following expression:

$$OII = \frac{(301-h)\cdot 5}{300} + \frac{(301-v)\cdot 7}{300} + \frac{(301-c)\cdot 9}{300} \qquad (3)$$

where h, v and c are times (s) until the start of hemorrhage, vasoconstriction and coagulation, respectively. The formulations were classified according to the following: OII ≤ 0.9 nonirritating; 0.9 < OII ≤ 4.9 weakly irritating; 4.9 < OII ≤ 8.9 moderately irritating; 8.9 < OII ≤ 21 irritating (ICCVAM, 2010).

2.7.2. In vivo ocular tolerance

To corroborate the results obtained from the HEM-CAM® test, the formulations (FMT-PLGA-NPs and Isoptoflucon®) were evaluated using primary eye irritation test of Draize (Sánchez-López et al., 2016). For this case, pig eyes (Landrace and Large White) were used, where 50 μL of each sample were instilled in the eye conjunctival sac (n = 6/group) and a gentle massage was applied to ensure circulation of the sample through the eyeball. Possible signs of irritation were observed at the time of instillation and after 1 h of exposure using the untreated contralateral eye as a negative control. Draize score was determined by direct observation of the anterior segment of the eye and changes in ocular structures involving the cornea (turbidity or opacity), iris and conjunctiva (congestion, chemosis, swelling, and discharge) using Table S.3b Supplementary Material.

2.8. Anti-inflammatory efficacy

The induction of inflammation with the objective of evaluating the anti-inflammatory effect of FMT-PLGA-NPs compared to the commercial drug (Isopotoflucon®) and 0.9% control group (NaCl), was carried out using pigs (n = 6/group). The study was conducted with the application of 50 μL of 0.5% sodium arachidonate (SA) dissolved in PBS in the right eye, the left eye was used as control. After 30 min of exposure, 50 μL of each formulation were instilled. Evaluation of inflammation was performed from the application of formulations up to 150 min according to Draize modified scoring system (Sánchez-López et al., 2016).

2.9. Ocular bioavailability

The amounts of drug that permeated from the formulation FMT-PLGA-NPs and Isopotoflucon® were evaluated 4 h after its application. To this end, 50 μL of each formulation were administered to the pig's left eye. The amount of FMT retained from the different parts of the eye
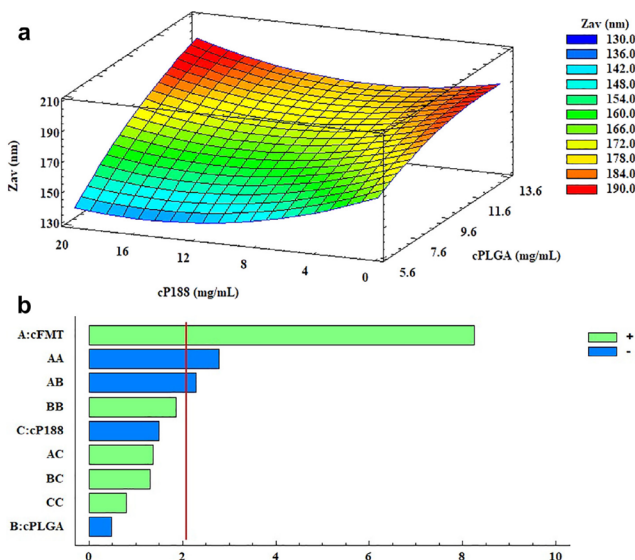
RESULTADOS

Fig. 1. Optimization of the FMT-PLGA-NPs. (a) Zav surface response at a fix 1.5 mg·mL^{-1} of FMT, (b) Pareto' diagram of the analyzed effect on EE.

(sclera, cornea, aqueous and vitreous humor) was quantified by RP-HPLC.

2.10. Statistical analysis

The multiple comparisons were developed using one-way ANOVA with Tukey post hoc test with a significance of $\alpha < 0.05$ after having confirmed the normality and equality of variances by Bartlett in the groups. All analyzed data were presented as mean ± SD. GraphPad Prism® 6.01 software for windows was used to analyze the data.

3. Results and discussions

3.1. Optimization of the FMT-PLGA-NPs

According to the results obtained from the matrix central composite design (Table S.1 Supplementary Material) it was possible to statistically correlate the effects of the independent variables on Zav and EE ($p < 0.05$). In the first case, Zav was highly influenced by cPLGA and cP188 (Fig. 1a). The study showed that as the amount of PLGA in the formulation increased, the NPs increased in size, the opposite happened when the concentration of cP188 increased. Zav's values (141.3–187.8 nm) were within the criteria of the ocular topical administration of nanostructured systems that would not cause irritation (Ali and Lehmussaari, 2006). In the second case, EE, mainly cFMT had a significantly positive effect (Fig. 1b), where the ratio of drug concentration and EE is proportional, reaching values close to 100% (Table S.1 Supplementary Material). The latter could be associated with the fact that cFMT did not have a significant effect ($p = 0.9818$) on Zav (Fig. S.1 Supplementary Material), which makes it clear that the load capacity of PLGA had not yet been reached. The other dependent variables (PI and ZP) were not correlated with any independent variable ($p > 0.05$), however, the PI and ZP values concluded that all the formulations were monodisperse systems (PI ≤ 0.1) and with a low

probability that sedimentation would occur (Patel and Agrawal, 2011). Finally, according to the results of the evaluated parameters and their significant effects it was possible to select an optimized nanoparticle formulation (FMT-PLGA-NPs) containing 7.0 mg·mL^{-1} of PLGA, 15 mg·mL^{-1} of P188 and 1.5 mg·mL^{-1} of FMT. Stability studies, physicochemical interactions, release, permeation, eye tolerance, and anti-inflammatory efficacy were carried out to this optimized formulation.

3.2. NPs physicochemical, morphological characterization and EE

The optimized formulation showed a Zav of 149.1 ± 3.5 nm and a PI of 0.079 ± 0.008, characteristic of monodisperse systems (PI < 0.1), suitable for ocular administration due the fact that there will not be NP populations that have a size greater than 10 μm that could cause ocular irritation associated with particle size (Ali and Lehmussaari, 2006). For the ZP, a negative value (−34.3 ± 1.6 mV) was obtained which was attributed to the PLGA polymer, specifically, to the terminal carboxylic groups of the polymer chain (Stolnik et al., 1995). The high PLGA entrapment capacity used in combination with high liposolubility of the FMT, explains the high value of EE (99.8 ± 0.2%) in the optimized formulation. Finally, to corroborate the Zav data coming from the DLS technique, the FMT-PLGA-NPs were visualized by TEM (Fig. 2). The TEM image showed that the NPs present similar values observed by DLS and without evidence of aggregation.

3.3. Interaction studies

To demonstrate the crystalline state of the components of the NPs and their interactions with each other, the XRD spectra of FMT-PLGA-NPs, PLGA, P188 and FMT were analyzed (Fig. 3a). PLGA shows XRD profiles without any crystalline state signal. The semicrystalline profile of P188 showed peaks at 19.15° and 23.43° (2θ), which were not seen in the FMT-PLGA-NPs. In relation to FMT, it showed a crystalline profile with sharp and intense peaks at 10.38°, 13.79°, 15.32°, 16.32°, 17.00°,

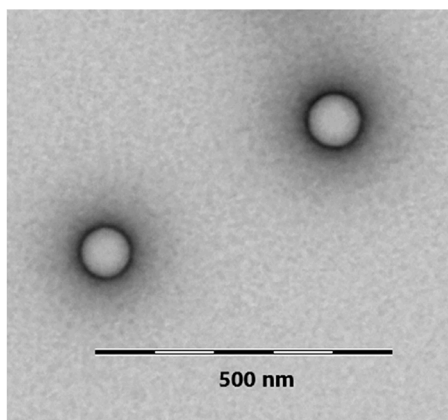**Fig. 2.** Transmission electron microscopy analysis of FMT-PLGA-NPs.

Fig. 3. Interactions studies of FMT-PLGA-NPs and NPs components (a) XRD patterns, (b) FTIR spectra, (c) DSC.

17.60° and 19.60° (2θ). The previous peaks were evidenced in a low intensity in the profile of FMT-PLGA-NPs, due to the fact that FMT was dispersed in the polymer matrix both in crystalline state and molecular dispersion (Panyam et al., 2004).

FTIR analysis was performed to identify the interactions between FMT, P188 and PLGA. According to the analysis of the spectra of each of the components (Fig. 3b), there was no evidence of the existence of a covalent bond between the elements that constituted the NPs. The IR spectrum of FMT showed several characteristic peaks, the first at a band of $3384\,cm^{-1}$ given by the signal of the stretching vibration of OH, some peaks from 2994 to $2876\,cm^{-1}$ corresponding to the stretching vibration of CH, some peaks at 1712 and $1654\,cm^{-1}$ due to the stretching vibration the C=O, and finally, stretching vibration product of C=C aromatic to the bands of 1612 and $1601\,cm^{-1}$ (Rodrigues et al., 2009). In the case of the PLGA, it had a characteristic intense band at $1750\,cm^{-1}$ corresponding to stretching vibration of the carbonyl group. Small peaks corresponding to stretching vibration of the alkanes were displayed between the bands 2997 and $2882\,cm^{-1}$. The stretching vibrations C–O and C–O–O were shown at the bands of 1166 and $1087\,cm^{-1}$, respectively (Li et al., 2001). In the P188 showed two intense peaks, the first at $2881\,cm^{-1}$ signal given by the stretching vibration of CH and the second at $1097\,cm^{-1}$ corresponding to the stretching vibration of C–O (Yan et al., 2010). The FMT-PLGA-NPs showed comparable profile to PLGA with additional peaks of low intensity corresponding to P188 (C–H) and to FMT (O–H, C–H and C=C).

The DSC thermograms of FMT, FMT-PLGA-NPs, P188 and PLGA are presented in the Fig. 3c, in which it is possible to observe an acute peak belonging to the melting transition of P188 with a $\Delta H = 132.69\,J{\cdot}g^{-1}$ and a $T_{max} = 54.24\,°C$ (Yan et al., 2010). The FMT showed a melting transition characterized by a $\Delta H = 105.09\,J{\cdot}g^{-1}$ and with a $T_{max} = 291.95\,°C$ that was not present in the profiles of the NPs developed (data not shown) because the P188 has a flash point near 260 °C. The PLGA showed the onset of the glass transition (T_g) at 51.87 °C and in the FMT-PLGA-NPs at 45.56 °C, this decrease T_g is attributed to the drug-polymer interaction (Abrego et al., 2014; Sánchez-López et al., 2017).

3.4. Biopharmaceutical behavior

3.4.1. In vitro release study
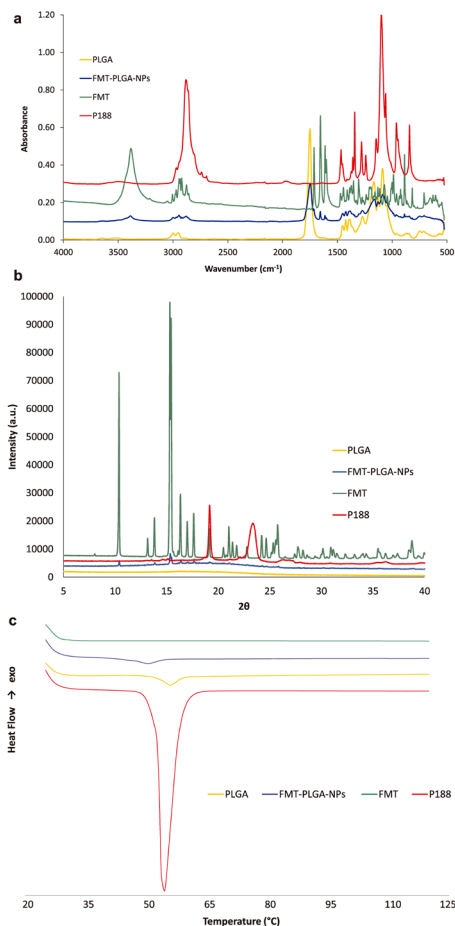
The *In vitro* release study of FMT from FMT-PLGA-NPs compared to Isoptoflucon® and Free-FMT was carried out through Franz diffusion cells. In Fig. 4, it is possible to observe that after 10 h the Free-FMT formulation released almost 100% of the FMT. In relation to the commercial solution (Isoptoflucon®), after 24 h amount released was close to 100%. All the above formulations were adjusted to a release profile of first order (Table 2), which is characterized by a rapid release followed by a constant release (Fangueiro et al., 2016). FMT-PLGA-NPs, had a release of 60% of the FMT, with continued increasing and sustained release of the drug, this system was adjusted to a profile of hyperbola order (Sánchez-López et al., 2017). The rapid release of the drug from NPs within the first 10 h was mainly due to the drug that is weakly bound to the most superficial areas of the polymeric matrix. In the sustained and increasing phase of the release of FMT, it could be due to a slow diffusion of the drug due to its affinity within the polymer matrix (Allahyari and Mohit, 2016; Anderson and Shive, 2012).
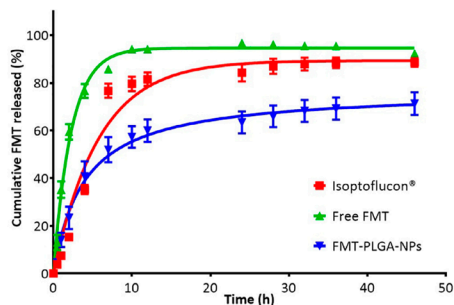
RESULTADOS

Fig. 4. *In vitro* profile release of FMT-PLGA-NPs (adjust to hyperbola equation) against free FMT and Isoptoflucon® (adjust to first order equation).

Table 2
Parameters for kinetic models of FMT-PLGA-NPs, free drug solution and Isoptoflucon®.

Models	Isoptoflucon®		Free FMT		FMT-PLGA-NPs	
	AIC	R^2	AIC	R^2	AIC	R^2
Zero Order	117.49	0.62	119.75	0.45	107.51	0.66
First Order	88.29	0.97	68.70	0.99	74.45	0.98
Higuchi	109.21	0.81	113.11	0.68	97.56	0.85
Hyperbola	94.73	0.94	80.54	0.98	74.38	0.99
Korsmeyer-Peppas	$n = 0.052$		$n = 0.030$		$n = 0.033$	
	106.73	0.85	103.98	0.85	91.85	0.91

3.4.2. Ex vivo corneal and sclera permeation study

Studies of corneal and scleral permeation were carried out for 6 h (Fig. 5). According to Table 3, the release of the FMT-PLGA-NP drug is faster and penetrates more at the corneal level than at the scleral level ($p < 0.001$). In the different parameters of scleral permeation (J, K_p and Q_{24}) there were no significant differences between the formulations tested, except for the Q_R, where FMT-PLGA-NPs retain more drug ($p < 0.01$) than the Isoptoflucon®. At corneal permeation level, it was observed that the formulation FMT-PLGA-NPs present significant differences in all parameters ($p < 0.01$) in contrast to the commercial formulation. Comparing the steady-state flux, the drug from the NPs permeated the cornea twice faster than Isoptoflucon®. The previous relation was maintained for the parameters Kp and Q_{24} at the corneal level. The Q_R of FMT-PLGA-NPs was significantly lower in the cornea than the other formulation analyzed. According to the corneal permeation parameters, the NPs formulation has a greater capacity to cross the drug per unit of time (Carvajal-Vidal et al., 2017).

3.5. Stability analysis of NPs

In accordance with the Fig. 6a, it is possible to observe that the designed NPs present high stability after one month a storage temperature at 4 °C. The previously described also happened with the NPs that were stored at 25 °C for 15 days (Fig. 6b). This stability is associated with the high ZP of the NPs (approximately -30 mV) that allow them to avoid flocculation and precipitation (Patel and Agrawal, 2011). After 30 days, the NPs stored at 25 °C begin to show signs of instability, due to the increase in temperature-dependent solubility of P188. This causes the release of P188 absorbed on the surface of the NP, gradually losing the ZP that causes the agglomeration and later, the flocculation of the nanostructured system (Fredenberg et al., 2011; Storm et al., 1995).
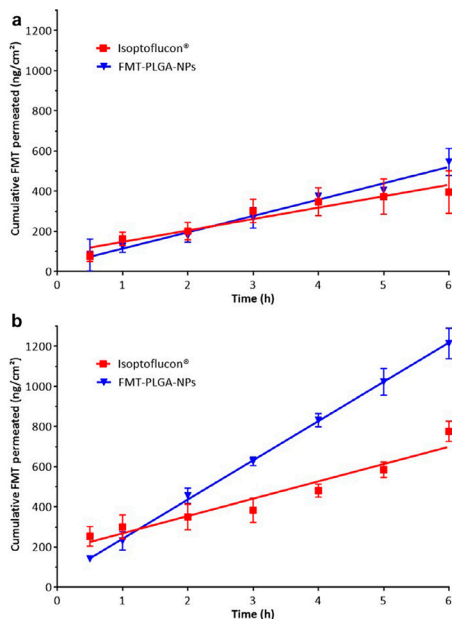

Fig. 5. *Ex vivo* permeation profile of FMT-PLGA-NPs compared with Isoptoflucon®. (a) Scleral permeation, (b) Corneal permeation.

3.6. Ocular tolerance

3.6.1. In vitro ocular tolerance

The HET-CAM® was tested on optimized NPs compared to the commercial drug (Table S.2 Supplementary Material). For this, the assay was validated by evaluating a positive and negative control. The positive control, 0.1 M NaOH, produced a severe hemorrhage (Fig. S.2a Supplementary Material), classifying this solution as irritating. In contrast, the negative control did not produce any type of injury, categorizing it as nonirritating (Fig. S.2b Supplementary Material). In relation to formulations of FMT-PLGA-NPs and Isoptoflucon®, both showed a high ocular tolerance with an OII ≤ 0.9 during the whole experiment, classifying it as nonirritating (Fig. S.2c and S.2d Supplementary Material).

3.6.2. In vivo ocular tolerance

The topical administration in the eyes of the pigs showed no signs of irritation in the different structures (cornea, iris and conjunctiva) evaluated (Fig. S.3 Supplementary Material). A value of OII = 0 was obtained both for the commercial formulation and for the optimized NPs, classifying them as nonirritating (Table S.3c Supplementary Material). These results agreed with the data obtained from the HET-CAM® assay and other studies (Abrego et al., 2015; Parra et al., 2016).

3.7. Anti-inflammatory efficacy assay

A study of anti-inflammatory efficacy was developed with the aim to determine the anti-inflammatory capacity in contrast with a commercial formulation (Isoptoflucon®) in an acute treatment. According to Fig. 7, both the formulation Isoptoflucon® and the FMT-PLGA-NPs

Table 3

FMT sclera and corneal permeation parameters from FMT-PLGA-NPs and Isoptoflucon[*].

Tissue	Formulation	J (ng·h^{-1}·cm^{-2})	K$_p$ (cm·h^{-1})·10	Q$_{24}$ (µg)	Q$_R$ (µg·g^{-1}·cm^{-2})
Sclera	Isoptoflucon[*]	88.87 ± 36.47	5.92 ± 2.43	1.36 ± 0.56	3.26 ± 0.27
	FMT-PLGA-NPs	126.94 ± 3.38	8.43 ± 0.23	1.95 ± 0.05	5.07 ± 0.06[i]
Cornea	Isoptoflucon[*]	134.66 ± 17.29	8.98 ± 1.15	2.07 ± 0.27	7.01 ± 0.16
	FMT-PLGA-NPs	305.16 ± 25.41[ii]	20.34 ± 1.69[ii]	4.69 ± 0.39[ii]	2.73 ± 0.30[i]

Letters represent statistical significance: [i]$p < 0.01$ and [ii]$p < 0.001$. J, steady-state flux; K$_p$, permeability coefficient; Q$_{24}$, permeated amount at 24 h; Q$_R$, retained amount.
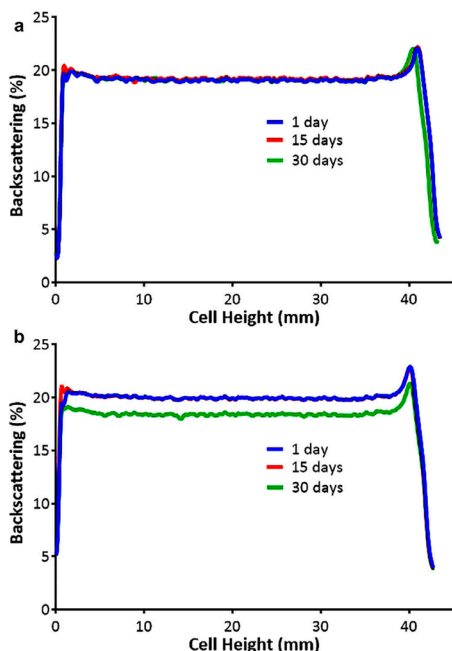

Fig. 6. FMT-PLGA-NPs backscattering profile. (a) Storage temperature at 4 °C, (b) Storage temperature at 25 °C.

showed a significant anti-inflammatory effect from the first 30 min of exposure when compared with the positive control (SA). When comparing the anti-inflammatory effect between the formulations, it is evident that there is a significant difference ($p < 0.01$) of a greater anti-inflammatory effect of FMT-PLGA-NPs throughout the treatment. The above difference is explained by the information from the corneal permeation studies performed. The FMT-PLGA-NPs had a greater and faster permeation of the drug, reflecting a faster and more effective anti-inflammatory effect in contrast to Isoptoflucon[*]. The nanostructured system gives the drug greater bioavailability at the corneal level and with the ability to reach deeper tissues such as vitreous and retina, making it useful for posterior uveitis (Bisht et al., 2017).

3.8. Ocular bioavailability

In order to determine the bioavailability of FMT in the different pig eye structures, the formulation of FMT-PLGA-NPs and Isoptoflucon[*]

were instilled for an exposure period of 4 h. The amount of FMT from FMT-PLGA-NPs in aqueous humor was 11.16 ± 1.31 µg·mL^{-1} significantly higher ($p < 0.0001$) to the other cavities. The amounts found in cornea, sclera and vitreous were 1.36 ± 0.12 µg·mL^{-1}, 0.82 ± 0.09 µg·mL^{-1} and 0.06 ± 0.03 µg·mL^{-1}, respectively. The amount of drug found in the aqueous humor correlates with the data on permeation and anti-inflammatory efficacy. The *ex vivo* permeation study showed that the formulation FMT-PLGA-NPs permeated greater amount of drug per unit of time with a lower retention than the other formulations tested, justifying that the NPs had a greater anti-inflammatory effect to the commercial formulation in the *in vivo* study. In this study, it was evidenced that the drug accumulates in the aqueous humor slowly releasing the drug to the deeper tissues such as the vitreous (Kalam and Alshamsan, 2017; Warsi et al., 2014). In the case of Isoptoflucon[*], no amounts of the drug were detected in any of the structures of the pig's eye with the quantification method used.

4. Conclusions

In the current study FMT-loaded PLGA NPs have been developed by solvent displacement technique, and in turn optimized using DoE, obtaining a formulation with physicochemical (Zav, ZP, PI and EE) and morphological characteristics suitable for ocular administration. Through the Zav information delivered by the DLS and TEM technique (Zav < 200 nm), the optimized formulation would not cause ocular irritation due to particle size. The formulation was submitted to the study of ocular tolerance *in vitro* and *in vivo* to argue the previously described, in which it was demonstrated that there is a high ocular tolerance of FMT-PLGA-NPs. The interaction studies showed that the drug is contained within the polymer matrix in the form of dispersion system and that the different components that make up the NPs do not have chemical interactions or strong covalent bonds that could affect pharmacology activity of FMT. The formulation FMT-PLGA-NPs shows a bimodal behavior in which the first 10 h presents a rapid release of the drug followed with increasing and sustained release of the drug. The permeation study allowed us to show that FMT-PLGA-NPs have a higher permeability at corneal level with a low corneal retention of the drug compared to the commercial formulation ($p < 0.01$). The low corneal permeation was corroborated by the bioavailability study, which showed that there is a greater amount of drug in the aqueous humor than in the other ocular structures, demonstrating that the system has the capacities to reach the vitreous. In the stability study of NPs, it is established that the system maintains its properties without signs of flocculation and/or sedimentation at a storage temperature of 4 °C, at higher temperatures they could solubilize the P188 causing the loss of ZP causing the flocculation of the NPs. In the *in vivo* study of anti-inflammatory efficacy, the permeation and dialysis data were corroborated, in which it was evidenced that the FMT-PLGA-NPs have a greater anti-inflammatory effect than the commercial formulation during the whole experiment. Considering all the aspects analyzed, the formulation developed would be useful for the acute and chronic treatment of ocular inflammatory conditions with the ability to reach the posterior segment.
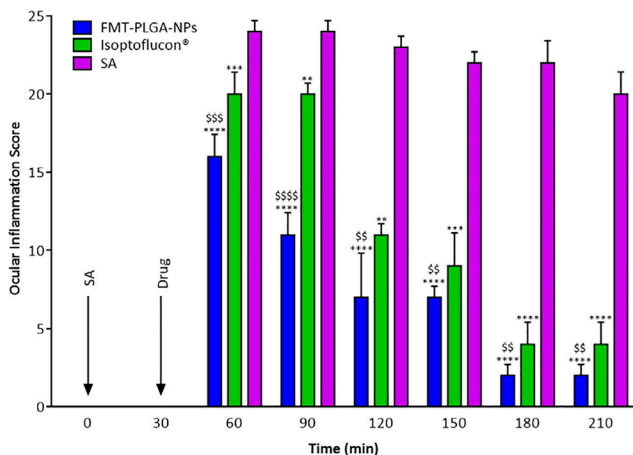
RESULTADOS

Fig. 7. Comparison of anti-inflammatory efficacy of FMT-PLGA-NPs and Isoptoflucon*. Values are expressed as mean ± SD; $^{**}p < 0.01$, $^{***}p < 0.001$, and $^{****}p < 0.0001$ significantly lower than the inflammatory effect induced by SA; $^{\$\$}p < 0.01$, $^{\$\$\$}p < 0.001$, and $^{\$\$\$\$}p < 0.0001$ significantly lower than the inflammatory effect induced by Isoptoflucon*.

References

Abrego, G., Alvarado, H., Souto, E.B., Guevara, B., Bellowa, L.H., Parra, A., Calpena, A., Garcia, M.L., 2015. Biopharmaceutical profile of pranoprofen-loaded PLGA nanoparticles containing hydrogels for ocular administration. Eur. J. Pharm. Biopharm. 95, 261–270. http://dx.doi.org/10.1016/j.ejpb.2015.01.026.

Abrego, G., Alvarado, H.L., Egea, M.A., Gonzalez-Mira, E., Calpena, A.C., Garcia, M.L., 2014. Design of nanosuspensions and freeze-dried PLGA nanoparticles as a novel approach for ophthalmic delivery of pranoprofen. J. Pharm. Sci. 103, 3153–3164. http://dx.doi.org/10.1002/jps.24101.

Ali, Y., Lehmussaari, K., 2006. Industrial perspective in ocular drug delivery. Adv. Drug Deliv. Rev. 58, 1258–1268. http://dx.doi.org/10.1016/J.ADDR.2006.07.022.

Allahyari, M., Mohit, E., 2016. Peptide/protein vaccine delivery system based on PLGA particles. Hum. Vacc. Immunother. 12, 806–828. http://dx.doi.org/10.1080/21645515.2015.1102804.

Anderson, J.M., Shive, M.S., 2012. Biodegradation and biocompatibility of PLA and PLGA microspheres. Adv. Drug Deliv. Rev. 64, 72–82. http://dx.doi.org/10.1016/j.addr.2012.09.004.

Bielory, B.P., Perez, V.L., Bielory, L., 2010. Treatment of seasonal allergic conjunctivitis with ophthalmic corticosteroids: in search of the perfect ocular corticosteroid in the treatment of allergic conjunctivitis. Curr. Opin. Allergy Clin. Immunol. 10, 469–477. http://dx.doi.org/10.1097/ACI.0b013e32833dfa28.

Bisht, R., Mandal, A., Jaiswal, J.K., Rupenthal, I.D., 2017. Nanocarrier mediated retinal drug delivery: overcoming ocular barriers to treat posterior eye diseases. Wiley Interdiscip. Rev. Nanomed. Nanobiotechnol. e1473. http://dx.doi.org/10.1002/wnan.1473.

Cañadas, C., Alvarado, H., Calpena, A.C., Silva, A.M., Souto, E.B., García, M.L., Abrego, G., 2016. In vitro, ex vivo and in vivo characterization of PLGA nanoparticles loading pranoprofen for ocular administration. Int. J. Pharm. 511, 719–727. http://dx.doi.org/10.1016/j.ijpharm.2016.07.055.

Cano, A., Ettcheto, M., Espina, M., Auladell, C., Calpena, A.C., Folch, J., Barenys, M., Sánchez-López, E., Camins, A., García, M.L., 2018. Epigallocatechin-3-gallate loaded PEGylated-PLGA nanoparticles: a new anti-seizure strategy for temporal lobe epilepsy. Nanomed. Nanotechnol. Biol. Med. 14, 1073–1085. http://dx.doi.org/10.1016/J.NANO.2018.01.019.

Carvajal-Vidal, P., Mallandrich, M., García, M., Calpena, A., 2017. Effect of different skin penetration promoters in halobetasol propionate permeation and retention in human skin. Int. J. Mol. Sci. 18, 2475. http://dx.doi.org/10.3390/ijms18112475.

Chen, P.-Q., Han, X.-M., Zhu, Y.-N., Xu, J., 2016. Comparison of the anti-inflammatory effects of fluorometholone 0.1% combined with levofloxacin 0.5% and tobramycin/dexamethasone eye drops after cataract surgery. Int. J. Ophthalmol. 9, 1619–1623. http://dx.doi.org/10.18240/ijo.2016.11.13.

Danhier, F., Ansorena, E., Silva, J.M., Coco, R., Le Breton, A., Préat, V., 2012. PLGA-based nanoparticles: an overview of biomedical applications. J. Control. Release 161, 505–522. http://dx.doi.org/10.1016/j.jconrel.2012.01.043.

Diebold, Y., Calonge, M., 2010. Applications of nanoparticles in ophthalmology. Prog. Retin. Eye Res. 29, 596–609. http://dx.doi.org/10.1016/j.preteyeres.2010.08.002.

Fangueiro, J.F., Calpena, A.C., Clares, B., Andreani, T., Egea, M.A., Veiga, F.J., Garcia, M.L., Silva, A.M., Souto, E.B., 2016. Biopharmaceutical evaluation of epigallocatechin gallate-loaded cationic lipid nanoparticles (EGCG-LNs): In vivo, in vitro and ex vivo studies. Int. J. Pharm. 502, 161–169. http://dx.doi.org/10.1016/j.ijpharm.2016.02.039.

Fessi, H., Puisieux, F., Devissaguet, J.P., Ammoury, N., Benita, S., 1989. Nanocapsule formation by interfacial polymer deposition following solvent displacement. Int. J. Pharm. 55, R1–R4. http://dx.doi.org/10.1016/0378-5173(89)90281-0.

Fredenberg, S., Wahlgren, M., Reslow, M., Axelsson, A., 2011. The mechanisms of drug release in poly(lactic-co-glycolic acid)-based drug delivery systems – a review. Int. J. Pharm. 415, 34–52. http://dx.doi.org/10.1016/J.IJPHARM.2011.05.049.

Gause, S., Hsu, K.-H., Shafor, C., Dixon, P., Powell, K.C., Chauhan, A., 2016. Mechanistic modeling of ophthalmic drug delivery to the anterior chamber by eye drops and contact lenses. Adv. Colloid Interface Sci. 233, 139–154. http://dx.doi.org/10.1016/J.CIS.2015.08.002.

Guengerich, F.P., 2017. Intersection of the roles of cytochrome P450 enzymes with xenobiotic and endogenous substrates: relevance to toxicity and drug interactions. Chem. Res. Toxicol. 30, 2–12. http://dx.doi.org/10.1021/acs.chemrestox.6b00226.

ICCVAM, 2010. In: ICCVAM-Recommended Test Method Protocol: Hen's Egg Test – Chorioallantoic Membrane (HET-CAM) Test Method. NIH Publ., pp. B29–B38 N° 10-7553.

ICH, 2005. International Conference on Harmonisation of Technical Requirements for Registration of Pharmaceuticals for Human Use (ICH), ICH Q2 (R1) Validation of Analytical Procedures: Text and Methodology.

Kalam, M.A., Alshamsan, A., 2017. Poly (D, L-lactide-co-glycolide) nanoparticles for sustained release of tacrolimus in rabbit eyes. Biomed. Pharmacother. 94, 402–411. http://dx.doi.org/10.1016/J.BIOPHA.2017.07.110.

Kapoor, D.N., Bhatia, A., Kaur, R., Sharma, R., Kaur, G., Dhawan, S., 2015. PLGA: a unique polymer for drug delivery. Ther. Deliv. 6, 41–58. http://dx.doi.org/10.4155/tde.14.91.

Klose, D., Delplace, C., Siepmann, J., 2011. Unintended potential impact of perfect sink conditions on PLGA degradation in microparticles. Int. J. Pharm. 404, 75–82. http://dx.doi.org/10.1016/J.IJPHARM.2010.10.054.

Li, Y.-P., Pei, Y.-Y., Zhang, X.-Y., Gu, Z.-H., Zhou, Z.-H., Yuan, W.-F., Zhou, J.-J., Zhu, J.-H., Gao, X.-J., 2001. PEGylated PLGA nanoparticles as protein carriers: synthesis, preparation and biodistribution in rats. J. Control. Release 71, 203–211. http://dx.doi.org/10.1016/S0168-3659(01)00218-8.

Makadia, H.K., Siegel, S.J., 2011. Poly lactic-co-glycolic acid (PLGA) as biodegradable controlled drug delivery carrier. Polymers (Basel) 3, 1377–1397. http://dx.doi.org/10.3390/polym3031377.

Nekkanti, V., Marwah, A., Pillai, R., 2015. Media milling process optimization for manufacture of drug nanoparticles using design of experiments (DOE). Drug Dev. Ind. Pharm. 41, 124–130. http://dx.doi.org/10.3109/03639045.2013.850709.

Panyam, J., William, D., Dash, A., Leslie-Pelecky, D., Labhasetwar, V., 2004. Solid-state solubility influences encapsulation and release of hydrophobic drugs from PLGA/PLA nanoparticles. J. Pharm. Sci. 93, 1804–1814. http://dx.doi.org/10.1002/jps.20094.

Parra, A., Clares, B., Rosselló, A., Garduño-Ramírez, M.L., Abrego, G., García, M.L., Calpena, A.C., 2016. Ex vivo permeation of carprofen from nanoparticles: a

comprehensive study through human, porcine and bovine skin as anti-inflammatory agent. Int. J. Pharm. 501, 10–17. http://dx.doi.org/10.1016/j.ijpharm.2016.01.056.

Patel, V.R., Agrawal, Y.K., 2011. Nanosuspension: an approach to enhance solubility of drugs. J. Adv. Pharm. Technol. Res. 2, 81–87. http://dx.doi.org/10.4103/2231-4040.82950.

Ramos Yacasi, G.R., García López, M.L., Espina García, M., Parra Coca, A., Calpena Campmany, A.C., 2016. Influence of freeze-drying and γ-irradiation in preclinical studies of flurbiprofen polymeric nanoparticles for ocular delivery using D-(+)-trehalose and polyethylene glycol. Int. J. Nanomed. 11, 4093–4106. http://dx.doi.org/10.2147/IJN.S105606.

Rodrigues, L.B., Leite, H.F., Yoshida, M.I., Saliba, J.B., Junior, A.S.C., Faraco, A.A.G., 2009. In vitro release and characterization of chitosan films as dexamethasone carrier. Int. J. Pharm. 368, 1–6. http://dx.doi.org/10.1016/J.IJPHARM.2008.09.047.

Sánchez-López, E., Egea, M.A., Cano, A., Espina, M., Calpena, A.C., Ettcheto, M., Camins, A., Souto, E.B., Silva, A.M., García, M.L., 2016. PEGylated PLGA nanospheres optimized by design of experiments for ocular administration of dexibuprofen – in vitro, ex vivo and in vivo characterization. Colloids Surf. B: Biointerfaces 145, 241–250. http://dx.doi.org/10.1016/j.colsurfb.2016.04.054.

Sánchez-López, E., Ettcheto, M., Egea, M.A., Espina, M., Calpena, A.C., Folch, J., Camins, A., García, M.L., 2017. New potential strategies for Alzheimer's disease prevention: pegylated biodegradable dexibuprofen nanospheres administration to APPswe/PS1dE9. Nanomedicine 13, 1171–1182. http://dx.doi.org/10.1016/j.nano.2016.12.003.

Shokoohi-Rad, S., Daneshvar, R., Jafarian-Shahri, M., Rajaee, P., 2017. Comparison between betamethasone, fluorometholone and loteprednol etabonate on intraocular pressure in patients after keratorefractive surgery. J. Curr. Ophthalmol. 1–6. http://dx.doi.org/10.1016/J.JOCO.2017.11.008.

Siddique, M.I., Katas, H., Iqbal Mohd Amin, M.C., Ng, S.-F., Zulfakar, M.H., Buang, F., Jamil, A., 2015. Minimization of local and systemic adverse effects of topical glucocorticoids by nanoencapsulation: in vivo safety of hydrocortisone-hydroxytyrosol loaded chitosan nanoparticles. J. Pharm. Sci. 104, 4276–4286. http://dx.doi.org/10.1002/jps.24666.

Silva-Abreu, M., Calpena, A.C., Espina, M., Silva, A.M., Gimeno, A., Egea, M.A., García, M.L., 2018. Optimization, biopharmaceutical profile and therapeutic efficacy of pioglitazone-loaded PLGA-PEG nanospheres as a novel strategy for ocular inflammatory disorders. Pharm. Res. 35, 11. http://dx.doi.org/10.1007/s11095-017-2319-8.

Stolnik, S., Garnett, M., Davies, M., Illum, L., Bousta, M., Vert, M., Davis, S., 1995. The colloidal properties of surfactant-free biodegradable nanospheres from poly(β-malic acid-co-benzyl malate)s and poly(lactic acid-co-glycolide). Colloids Surf. A: Physicochem. Eng. Asp. 97, 235–245. http://dx.doi.org/10.1016/0927-7757(95)03081-N.

Storm, G., Belliot, S.O., Daemen, T., Lasic, D.D., 1995. Surface modification of nanoparticles to oppose uptake by the mononuclear phagocyte system. Adv. Drug Deliv. Rev. 17, 31–48. http://dx.doi.org/10.1016/0169-409X(95)00039-A.

Tahara, K., Karasawa, K., Onodera, R., Takeuchi, H., 2017. Feasibility of drug delivery to the eye's posterior segment by topical instillation of PLGA nanoparticles. Asian J. Pharm. Sci. 12, 394–399. http://dx.doi.org/10.1016/J.AJPS.2017.03.002.

USP 29-NF 24, 2006. United States Pharmacopeia and National Formulary (USP 39-NF 34). United States Pharmacopeial Convention, Rockville, Md.

Warsi, M.H., Anwar, M., Garg, V., Jain, G.K., Talegaonkar, S., Ahmad, F.J., Khar, R.K., 2014. Dorzolamide-loaded PLGA/vitamin E TPGS nanoparticles for glaucoma therapy: pharmacoscintigraphy study and evaluation of extended ocular hypotensive effect in rabbits. Colloids Surf. B: Biointerfaces 122, 423–431. http://dx.doi.org/10.1016/j.colsurfb.2014.07.004.

Yan, F., Zhang, C., Zheng, Y., Mei, L., Tang, L., Song, C., Sun, H., Huang, L., 2010. The effect of poloxamer 188 on nanoparticle morphology, size, cancer cell uptake, and cytotoxicity. Nanomedicine 6, 170–178. http://dx.doi.org/10.1016/j.nano.2009.05.004.

Yasin, M.N., Svirskis, D., Seyfoddin, A., Rupenthal, I.D., 2014. Implants for drug delivery to the posterior segment of the eye: a focus on stimuli-responsive and tunable release systems. J. Control. Release 196, 208–221. http://dx.doi.org/10.1016/j.jconrel.2014.09.030.

Supplementary Material

Table S.1: Values of the three experimental factors according to the matrix designed by 3-level central composite and measured responses

| Factorial points	cFMT (mg·mL⁻¹)	cPLGA (mg·mL⁻¹)	cP188 (mg·mL⁻¹)	Zav (nm)	PI	ZP (mV)	EE (%)
F1	1.0	9.0	1.6	187.8 ± 1.6	0.09 ± 0.01	-38.7 ± 0.6	99.58 ± 0.02
F2	0.5	7.0	5.0	155.5 ± 6.2	0.08 ± 0.02	-29.3 ± 1.1	99.22 ± 0.01
F3	0.5	11.0	15.0	177.7 ± 5.7	0.07 ± 0.02	-30.9 ± 2.0	99.36 ± 0.21
F4	1.8	9.0	10.0	167.8 ± 5.1	0.08 ± 0.02	-30.8 ± 2.5	99.84 ± 0.02
F5	1.5	11.0	15.0	178.7 ± 0.1	0.09 ± 0.03	-30.7 ± 0.8	99.78 ± 0.03
F6	1.5	7.0	5.0	156.5 ± 3.7	0.07 ± 0.01	-28.4 ± 6.1	99.84 ± 0.08
F7	1.5	7.0	15.0	149.1 ± 3.5	0.08 ± 0.01	-34.2 ± 1.6	99.76 ± 0.07
F8	1.0	5.6	10.0	141.3 ± 1.1	0.08 ± 0.02	-28.3 ± 2.6	99.75 ± 0.01
F9	1.5	11.0	5.0	172.1 ± 3.7	0.06 ± 0.02	-29.5 ± 1.3	99.71 ± 0.01
F10	0.2	9.0	10.0	166.3 ± 0.8	0.08 ± 0.02	-30.3 ± 1.5	98.38 ± 1.08
F11	1.0	9.0	18.4	161.7 ± 5.6	0.06 ± 0.02	-31.1 ± 0.9	99.64 ± 0.04
F12	1.0	12.4	10.0	178.8 ± 2.3	0.10 ± 0.05	-33.8 ± 4.0	99.77 ± 0.08
F13	0.5	7.0	15.0	151.1 ± 1.4	0.08 ± 0.02	-34.5 ± 1.6	98.71 ± 0.03
F14	0.5	11.0	5.0	177.6 ± 1.6	0.07 ± 0.01	-33.7 ± 1.5	99.47 ± 0.36
F15ᶜᵖ	1.0	9.0	10.0	164.4 ± 9.3	0.10 ± 0.03	-32.9 ± 3.3	99.46 ± 0.11
F16ᶜᵖ	1.0	9.0	10.0	162.4 ± 2.3	0.07 ± 0.01	-33.5 ± 0.4	99.53 ± 0.03

ᶜᵖ Central points

RESULTADOS
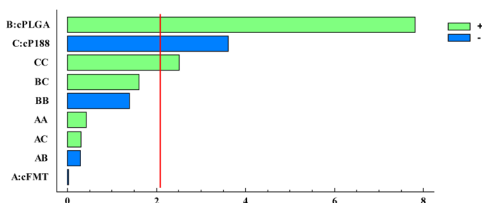
Figure S.1. Pareto diagram of the analyzed effect on Zav.

Table S.2: Ocular tolerance *in vitro* by HET-CAM® test.

Formulation	Medium Score	Classification
FMT-PLGA-NPs	0.37 ± 0.17	Nonirritating
Isoptoflucon®	0.81 ± 0.49	Nonirritating
NaCl	0.00 ± 0.00	Nonirritating
NaOH	13.72 ± 1.48	Irritating
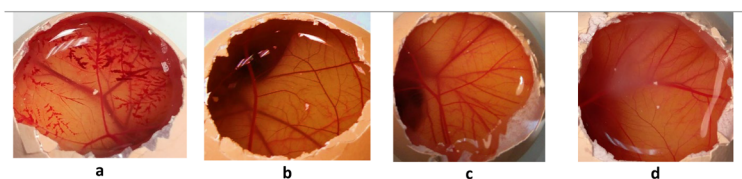
Figure S.2. HET-CAM® test after 5 min. (a) Positive control, (b) Negative control, (c) FMT-PLGA-NPs, (d) Isoptoflucon®.

Table S.3: Determination score Draize. (a) Ocular tolerance levels according to Draize, (b) Draize score system, (c) Ocular tolerance *in vivo.*

a)

Draize Test	
OII	Classification
0	Nonirritating
0 − 15	Weakly irritating
15 − 30	Moderately irritating
30 − 50	Irritating
50	Very irritating

b)

Tissue	Injury	Evaluation
Cornea	**A) Degree of cloudiness or opacity** - Absence of ulceration - Diffuse areas - Translucent areas - Opalescent areas - Full opacity **B) Affected area** - None - A quarter or less - More than a quarter but without means - More than half but less than three quarters - More than three quarters up a whole plane	0 1 2 3 4 0 1 2 3 4
Iris	**A) Iris injury score** - Normal - Deep folds, congestion, swelling, moderate circumcorneal injection - No reaction to light, hemorrhage, great destruction	0 1 2
Conjunctiva	**A) Redness** - Normal glasses - Some clearly injected vessels - Diffuse redness - Big diffuse redness **B) Chemosis or Inflammation** - None - Some - Marked with partial disorder of the eyelids - Eyelid more or less closed - Semi eyelids **C) Sweat** - None - Periocular wetting - Any amount anomalous - Wetting and eyelid hairs	0 1 2 3 0 1 2 3 4 0 1 2 3
	IIO = Corneal (A·B·5) + Iris (A·5) + Conjuctiva (A+B+C)·2	

c)

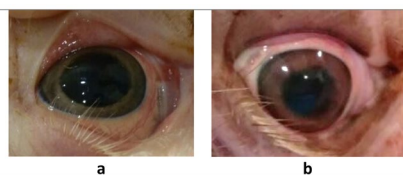| Formulation	Medium Score	Classification
FMT-PLGA-NPs	0.00 ± 0.00	Nonirritating
Isoptoflucon®	0.00 ± 0.00	Nonirritating

Figure S.3. Draize test at the endpoint. (a) FMT-PLGA-NPs, (b) Isoptoflucon®.

3.2. *In-situ* forming gels containing fluorometholone-loaded polymeric nanoparticles for ocular inflammatory conditions

Roberto González-Pizarro[a], Paulina Carvajal-Vidal[a], Lyda Halbaut Bellowa[a], Ana Cristina Calpena[a,b], Marta Espina[a,b], María Luisa García[a,b].

[a]Department of Pharmacy, Pharmaceutical Technology and Physical Chemistry, Faculty of Pharmacy and Food Sciences, University of Barcelona, 08028 Barcelona, Spain.
[b]Institute of Nanoscience and Nanotechnology (IN2UB), University of Barcelona, Barcelona, Spain.

In-situ forming gels containing fluorometholone-loaded polymeric nanoparticles for ocular inflammatory conditions

Roberto Gonzalez-Pizarro[a], Paulina Carvajal-Vidal[a], Lyda Halbault Bellowa[a], Ana Cristina Calpena[a,b], Marta Espina[a,b], María Luisa García[a,b,*]

[a] *Department of Pharmacy, Pharmaceutical Technology and Physical Chemistry, Faculty of Pharmacy and Food Sciences, University of Barcelona, 08028, Barcelona, Spain*
[b] *Institute of Nanoscience and Nanotechnology (IN2UB), University of Barcelona, Barcelona, Spain*

ARTICLE INFO

ABSTRACT

Thermosensitive gels have been developed and optimized in such a way that they become gels at corneal temperature and with a viscosity that allows the adequate release of the Fluorometholone (FMT)-loaded PLGA nanoparticles (NPs) in order to improve ocular anti-inflammatory efficacy against a commercial formulation. It has been shown that gels avoid burst release of the drug in the first hours with a slow and increasing profile after administration. NPs have maintained their average size and spherical shape within the gels as confirmed by transmission electron microscopy (TEM). In turn, the *in-situ* gelling of the formulations allows the administration in eye drops dosage form due to its state of sol at temperatures below 25 ˚C. Ocular tolerance studies have shown that no formulation causes eye irritation. The administration of the developed formulations has improved the precorneal residence time reflected in the ocular bioavailability, where deep tissues as aqueous humour and crystalline were reached. In conclusion, the use of thermosensitive gels for the topical application of NPs has demonstrated their effectiveness in the acute and preventive treatment of ocular inflammatory conditions.

1. Introduction

Fluorometholone (FMT) is one of the many corticosteroids used in ophthalmology for the treatment of allergic and inflammatory conditions of the anterior segment of the eye [1]. Since its incorporation to ocular treatment, this drug has shown certain advantages over other corticosteroids commonly used, such as high anti-inflammatory potency and low risk of increasing intraocular pressure that leads to a lower prevalence of corticoid-induced cataracts and glaucoma [2]. On the other hand, FMT has the disadvantage of having a low corneal penetration that results in ineffective therapeutic levels for treatment in the posterior area of the eye [3]. Furthermore, in the eye drops dosage form, the formulation is rapidly eliminated from the precorneal area as a consequence of tear turnover, having only a half-life of ocular residence around 1–2 min. To overcome these difficulties, various strategies have been developed to increase the half-life and therapeutic efficacy of ocular drugs ranging from increased viscosity with the use of ointments or gels to intravitreal injections for the treatment of diseases committed in the posterior area of the eye such as posterior uveitis [4].

One of the strategies currently used to increase the bioavailability of hydrophobic drugs such as corticosteroids is the development of nanoparticles (NPs) of poly (lactic-co-glycolic acid) (PLGA) [5]. Particularly, the incorporation of the drug into the polymer matrix creates a system that protects the drug from the enzymatic metabolism present in the tear film and allows a controlled and prolonged release of the drug [6–8]. The PLGA NPs, in turn, possess the ability to carry the drug to deep tissues, where conventional commercial formulations fail to reach [9].

The latest research to solve the problem of residence time in the precorneal area of eye drops focuses on the development of formulations that gelling *in-situ* when they come into contact with the eye due to the effect of pH, salts or temperature [10–12]. Poloxamer 407 (P407) is a triblock copolymer surfactant formed by polypropyleneglycol and two blocks of polyethyleneglycol at the ends, which has the characteristic of behaving as a newtonian or viscoelastic solution (gel) depending on the temperature and concentration used [13]. The development of PLGA NPs incorporated in a thermosensitive gel would be able to solve the disadvantages of commercialized eye drops, which would allow gelling at corneal temperature [14], avoiding the burst release of the drug from the NPs in the first hours administered, resulting in increased drug concentration in deep eye tissues such as aqueous humour and crystalline [15,16].

RESULTADOS

In the present study, a formulation of P407 with FMT-loaded PLGA NPs (FMT-PLGA-NPs), which gelling at corneal temperature, has been developed and optimized, with the aim of increasing its bioavailability in deep ocular tissues and treating inflammatory conditions of the anterior and posterior area of the eye. For this, morphometry and morphology of the NPs, rheological analysis, *in vitro* release profiles and short-term stability of the gels were also carried out. Eye tolerance, ocular bioavailability and anti-inflammatory efficacy studies were conducted with the aim to demonstrate the suitability of this system in the treatment of ocular inflammatory diseases.

2. Material and methods

2.1. Materials

FMT and PLGA RG 503H were purchased from Capot Chemical (Hangzhou, China) and Evonik Corporation (Birmingham, USA), respectively. Poloxamer 188 (P188) and P407 were given from BASF (Barcelona, Spain). Methylcellulose A4M (MC) and Benzalkonium chloride were purchased from Sigma-Aldrich (Madrid, Spain). Sodium alginate (65–75% guluronic and 25–35% mannuronic acid, ≈ 220 kDa) was provided by Fagron Iberica (Terrassa, Spain). Water through Millipore® MilliQ system was used for all the experiments and all the other reagents were of analytical grade.

2.2. Preparation and characterization of NPs

FMT-loaded NPs (FMT-PLGA-NPs) previously optimized in our group were prepared by the solvent displacement method [7]. Briefly, the PLGA ($9.0 \, mg \, mL^{-1}$) and FMT ($1.5 \, mg \, mL^{-1}$) were dissolved in 5 mL of acetone. The organic phase was added slowly dropwise, under stirring, into 10 mL of an aqueous solution of P188 ($15 \, mg \, mL^{-1}$) adjusted to pH 7.4. After that, the organic solvent was evaporated under reduced pressure.

Morphometry (average particle size (Zav), polydispersity index (PI)) and zeta potential (ZP) of NPs were determined in a Zetasizer NanoZS (Malvern Instruments, Malvern, UK) by dynamic light scattering (DLS) and electrophoretic mobility, respectively. Samples were diluted in MilliQ water (1:10) and experiments were performed with disposable capillary cells DTS1070 (Malvern Instruments) at 25 °C. The reported values correspond to the mean ± SD.

The entrapment efficiency (EE) of FMT in the NPs was quantified indirectly by measuring the non-entrapped drug in the dispersion medium. The free FMT was separated by a filtration/centrifugation technique (1:10 dilution) at 25 °C and 5000 rpm for 10 min using an Ultracell–100 kDa centrifugal filter devices (Amicon® Ultra; Millipore Corporation, Massachusetts). The EE was calculated according to the following equation:

$$EE \, (\%) = \frac{cFMT_0 - cFMT_1}{cFMT_0} \cdot 100 \qquad (1)$$

where $cFMT_0$ and $cFMT_1$ are the total amount of FMT and free FMT in the filtrated, respectively. The samples were evaluated by HPLC, according to the method described previously [7]. Data were processed using Empower 3® Software.

2.3. Elaboration and optimization of gels

An amount of 0.025 g of sodium alginate were dissolved in 10 mL of FMT-PLGA-NPs under agitation (800 rpm for 3 min) using the Unguator®. After one day of rest, MC (0–1% w/v) and benzalkonium chloride (0.01% w/v) were added and stirred at 1000 rpm for 5 min. The previous preparation was left to stand overnight to then add the P407 (15–25% w/v) under agitation of 1000 rpm for 5 min. The pH was adjusted to 7.4 with NaOH.

Design of Experiments (DoE) was employed using a multi-level factorial design 3^2 generated by StatGraphics Centurion XV. The matrix

Table 1
Coding for the gelling capacity test.

Coding	Observation
0	No gelling occurs.
1	Slow gelling and dissolves quickly.
2	Immediate gelling and remains for a few hours.
3	Immediate gelling and remains for an extended period.

was developed to analyze the effects the two independent variables (concentrations of P407 [cP407] and MC [cMC]) on the three dependents variables (gelling capacity (Gt), sol-gel temperature transition ($T_{sol-gel}$) and viscosity (Vc)) [17]. Each independent variable was studied at three different levels coded (-1), a (0) and (+1) sign (see Table S.1 Supplementary Material).

2.4. Analysis of gels

2.4.1. Gelling capacity test

The determination of the Gt was carried out by placing 100 μL of gel in 2 mL of simulated tear fluid (SFL) at 34 ± 0.5 °C (average temperature of the ocular surface) [14,18]. The SFL was composed of 6.7% w/v sodium chloride, 2.0% w/v sodium bicarbonate, 0.08% w/v calcium chloride dehydrate in purified water [19]. The gelation was carried out by visual examination according to Table 1.

2.4.2. Rheological properties of the gels

Rheological properties of gels were carried out using a rheometer HAAKE Rheostress 1 (Thermo Fisher Scientific, Karlsruhe, Germany) equipped with a cone-plate geometry set-up with a fixed lower plate and an upper cone (Haake C60/2Ti, 6 cm diameter). The temperature sweep test was performed to determine the $T_{sol-gel}$ *in-situ* of gels. For oscillatory testing, storage modulus (G') and loss modulus (G'') values were measured from 5 to 50 °C with a constant frequency of 1 Hz and a constant stress (0.5 Pa). The transition temperature was set when G' equals G'' (cross-over point). For rotational testing, viscosity curves and flow curves were recorded for 3 min during the ramp-up period from 0 to 100 s^{-1}, 1 min at 100 s^{-1} (constant share rate period) and finally 3 min during the ramp-down period from 100 to 0 s^{-1}. All determinations were performed in triplicate.

2.4.3. Flow ability test

The flow ability was tested using the inverted tube method. 3 mL of each formulation were added in a tube of 10 mL and incubated in a thermoregulated bath. Three test temperatures were used, storage temperature (5 ± 0.5 °C), room temperature (25 ± 0.5 °C) and pre-corneal temperature (34 ± 0.5 °C). The evaluation was carried out investing the tube after 30 s. The thermosensitive gel would be suitable when it does not flow after an incubation of 30 s at 34 °C [20].

2.4.4. Morphological characterization

The morphological examination of the gels was carried out by transmission electron microscopy (TEM) on a Jeol 1010 instrument. This study was used to evaluate if the morphology of the NPs remained in the gel. The NPs were visualized with copper grids carbon-coated (carbon only). Samples (10 μL) were placed on grids and negative staining performed with 2% uranyl acetate.

2.4.5. In vitro release profile

To identify the cumulative release profile of the FMT from the optimized gels and FMT-PLGA-NPs compared with a commercial eye drops, a study was carried out in amber Franz cells using a dialysis membrane MW 12,000–14,000 Da, under sink conditions [21]. Isoptoflucon® is a commercial ophthalmic suspension of FMT that has been used as a reference for *in vitro* and *in vivo* studies. A volume of 300 μL of

the samples was placed in the donor compartment and the receptor compartment was filled with receptor medium thermoregulated at $34 \pm 0.5\,°C$ in continuous agitation. Samples (300 µL) were withdrawn from the receptor compartment at fixed times and replaced by an equal volume of fresh receptor medium at the same temperature. The samples were quantified by HPLC using the same method as in EE. Data were processed using Empower 3® Software. Values were reported as the mean $\pm$ SD of the triplicates. Akaike's information criterion (AIC) and coefficient correlation (r^2) were determined for each model as an indicator of the model's suitability [22].

2.5. Stability analysis of gels

The physical stability of the optimized gels at 4 °C was evaluated by static multiple light scattering technology (S-MLS) using Turbiscan® Lab. Gels were placed in a cylindrical glass measuring cell that was scanned by a pulsed near-infrared light source ($\lambda = 880$ nm). Due to the opacity of the gels, only the backscattering profiles were used to evaluate the physical stability. The backscattering data were recorded every 24 h at different times after preparation (1, 20 and 60 days).

2.6. Ocular tolerance

2.6.1. In vitro ocular tolerance
In vitro ocular tolerance was assessed using the HET-CAM® test to ensure that the gels are not irritating at ocular level. Hemorrhage, vasoconstriction and coagulation phenomena were measured by applying 300 µL of the formulation on the chorioallantoic membrane of a fertilized chicken egg, monitoring it during the first 5 min after the application. The development of the test was carried out with 6 eggs for each optimized formulation, 3 as positive (NaOH 0.1 M) and negative (0.9% NaCl) controls [23]. The ocular irritation index (OII) was calculated by the sum of the scores of each injury according to the following expression:

$$OII = \frac{(301 - h) \cdot 5}{300} + \frac{(301 - v) \cdot 7}{300} + \frac{(301 - c) \cdot 9}{300} \qquad (2)$$

where h, v and c are times (s) until the start of hemorrhage, vasoconstriction and coagulation, respectively. The formulations were classified according to the following: $OII \leq 0.9$ nonirritating; $0.9 < OII \leq 4.9$ weakly irritating; $4.9 < OII \leq 8.9$ moderately irritating; $8.9 < OII \leq 21$ irritating [24,25].

2.6.2. In vivo ocular tolerance
To corroborate the results obtained from the HEM-CAM® test, the formulations (optimized gels, FMT-PLGA-NPs and Isoptoflucon®) were evaluated using primary eye irritation test of Draize [26]. For this case, New Zealand albino male rabbits of 2.5 kg average weight were used, where 50 µL of each sample were instilled in the eye conjunctival sac (n = 6/group) and a gentle massage was applied to ensure circulation of the sample through the eyeball. Possible signs of irritation were observed at the time of instillation and after 1 h of exposure using the untreated contralateral eye as a negative control. Draize score was determined by direct observation of the anterior segment of the eye and changes in ocular structures involving the cornea, iris and conjunctiva [7].

2.7. Therapeutic efficacy

The induction of inflammation with the objective of evaluating the anti-inflammatory effect of optimized gels and FMT-PLGA-NPs compared to the commercial drug (Isoptoflucon®) and 0.9% control group (NaCl), was carried out using New Zealand albino male rabbits (n = 6/group). The study was conducted with the application of 50 µL of 0.5% sodium arachidonate (SA) dissolved in PBS in the right eye, using the left eye as a control. After 30 min of exposure, 50 µL of each formulation were instilled. In order to evaluate the prevention of inflammation, both

the formulations were administered 30 min before the induction of ocular inflammation. The evaluation of inflammation was performed from the application of formulations up to 150 min according to Draize modified scoring system [26].

2.8. Ocular bioavailability

The amounts of drug that permeated from optimized gels, FMT-PLGA-NPs and Isoptoflucon® were evaluated 4 h after its application. To this end, 50 µL of each formulation were administered to the rabbit's left eye. The experiment was carried out according to the Ethics Committee of Animals Experimentation from the University of Barcelona (CEEA-UB). The rabbits were anesthetized with intramuscular administration of ketamine (35 mg/kg) and xylazine (5 mg/kg) and euthanized by an overdose of sodium pentobarbital (100 mg/kg) administered for cardiac injection under deep anesthesia. The amount of FMT retained in the different parts of the eye (sclera, cornea, crystalline, aqueous humour and vitreous humour) was quantified by RP-HPLC.

2.9. Statistical analysis

The multiple comparisons were developed using two-way ANOVA with Tukey post-hoc test with a significance of $\alpha < 0.05$ after having confirmed the normality and equality of variances by Bartlett in the groups. All analyzed data were presented as mean $\pm$ SD. GraphPad Prism® 6.01 software for windows was used to analyze the data.

3. Results and discussions

3.1. Characterization of NPs

FMT-PLGA-NPs, optimized by our research group previously [7], showed values Zav, PI, ZP and EE of 150.8 ± 0.7 nm, 0.082 ± 0.014, -27.9 ± 0.3 mV and $98.4 \pm 1.4\%$, respectively. These results ensure that the formulation FMT-PLGA-NPs meets the requirements for ocular administration, since the population of NPs are smaller than 10 µm, which avoid eye irritation and a its high ZP provide a colloidal stability between NPs [27,28].

3.2. Optimization of the gels

In Fig. 1a it is possible to visualize the significance and the type of effect in the Gt response. The Gt depends on several factors in its assessment, such as the ability to form a gel and the time that the gelled gel can remain in a SFL solution. In particular, cP407 and cMC have a significantly positive effect ($p < 0.01$) on the response of Gt. Analyzed each of the factors and their influence on the response of Gt, the cP407 has the ability to form the gel and cMC provides the system with longer gelled time, both proportional to the concentration used.

For the response of Vs, the same relation is fulfilled as in Gt, where both factors are statistically significant (Fig. 1b). The relationship is proportional to the concentration, the cP407 has a greater influence on Vs ($p < 0.0001$) while the cMC has a less influence ($p < 0.01$), but necessary to increase strength or keep the gel constituted longer.

From the Fig. 1c it is possible to show that cP407 has a significant negative effect ($p < 0.001$) in the response of $T_{sol-gel}$, which means that as the concentration of cP407 increases the $T_{sol-gel}$ decreases [29]. In Fig. S.1 Supplementary Material it is possible to observe the surface responses of each independent variable.

According to the analysis of the factorial design used (Table 2), three formulations were selected (PG2, PG5 and PG8), due to the *in-situ* gelation property with the ability to remain constituted at the corneal temperature. Therefore, morphological characterization, stability studies, drug release, ocular tolerance, cytotoxicity, ocular bioavailability, anti-inflammatory and prophylaxis efficacy of the optimized formulations were carried out.

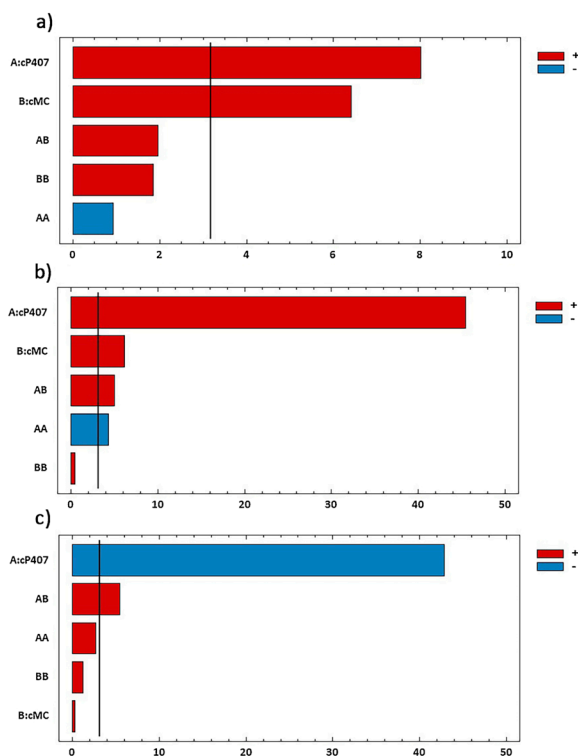**Fig. 1.** Optimization of the gels. Pareto diagram of the analyzed effect on a) Gt, b) Vs, c) $T_{sol-gel}$.

Table 2
Values of the two experimental factors according to the matrix designed by 3^2 multifactorial and the measured response.

Factorial points	cP407 (w/v)	cMC (w/v)	Gt	Vs (mPa·s) at 100 s^{-1}	$T_{sol-gel}$ (°C)
PG1	15	0.0	0	129.6 ± 5.2	33.11 ± 0.41
PG2	20	0.0	1	3133.0 ± 26.5	21.55 ± 0.36
PG3	25	0.0	1	4879.5 ± 110.5	12.17 ± 0.07
PG4	15	0.5	0	226.6 ± 10.2	31.06 ± 0.22
PG5	20	0.5	1	3347.0 ± 76.6	20.85 ± 0.01
PG6	25	0.5	2	5521.5 ± 108.2	13.77 ± 0.19
PG7	15	1.0	1	262.1 ± 5.7	30.19 ± 0.31
PG8	20	1.0	2	3611.0 ± 109.6	22.20 ± 0.38
PG9	25	1.0	3	6486.5 ± 117.3	14.84 ± 0.40

Table 3
Best adjustment model of optimized gels.

Parameter	PG2	PG5	PG8
Rheological model	Hershel-Bulkley[a] (r = 0.999) Cross[d] (r = 0.987)	Hershel-Bulkley[a] (r = 0.994) Cross[d] (r = 0.997)	Hershel-Bulkley[a] (r = 0.955) Cross[d] (r = 0.994)

[a] ascending section.
[d] descending section.

keep in this state for 2 h on average. These formulations, at a concentration of 20% of P407 have the characteristic of gelling *in-situ* at a temperature close to 34 °C and when the MC is added, the system acquires greater strength so that the gel stays longer.

3.3. Analysis of gels

3.3.1. Gelling capacity test

The gelling capacity of the formulations PG2, PG5 and PG8 are directly related to the increasing amount of MC (0–1%) used. In the case of PG2 and PG5 (Fig. S.2 Supplementary Material), a score of "slow gelling and dissolves quickly" was obtained (Table 2), in which the formulation gelled in SFL keeping for at least 30 min. PG8 (Fig. S.2c Supplementary Material) gelled when contacting SFL, being able to

3.3.2. Rheological properties

The gels PG2, PG5 and PG8 presented a non-newtonian behaviour (Table 3), adjusting in the ascending section to a plastic flow (Herschel-Bulkley equation) and in the descending section, to a pseudoplastic profile (Cross equation) [30]. This bimodal behaviour at corneal temperature allows characterizing the gels when they are administered. Particularly, the optimized gels will need an increasing force of the blinking to flow in the ocular cavity, so that later, the interactions
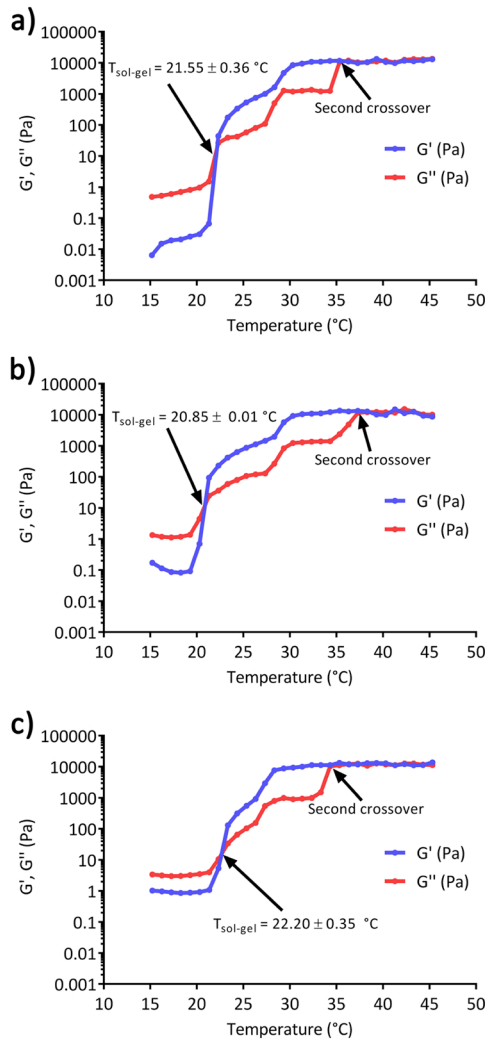
Fig. 2. Sol-gel temperature transition of gels. a) PG2, b) PG5, c) PG8.

between the polymeric chains of the P407 will be broken making it flow at an almost constant viscosity without reaching the value 0 of shear stress [31]. In the case of viscosity, these were proportional to the aggregate amount of MC in each formulation (Table 2). Overall, the rheological behaviour at a constant temperature makes the gel possess the slow release of the particles and a viscosity that allows it to be longer in contact with the eye [32]. The flow and viscosity curves of the gels can be observed in Fig. S.3 Supplementary Material.

3.3.3. $T_{sol\text{-}gel}$ and flow ability

The $T_{sol\text{-}gel}$ determination through the crossover between G' and G" of the optimized formulations are visualized in Fig. 2. The selected gels presented similar $T_{sol\text{-}gel}$ among them. According to the graphs it is possible to show that gelation starts around 21 °C increasing its viscosity (G") gradually as the temperature increases until it becomes equal with the elastic behaviour (G'). At corneal temperature, the gels reach the second crossover, where the viscosity remains constant [33]. The above is confirmed with the flow ability test, where the formulations do
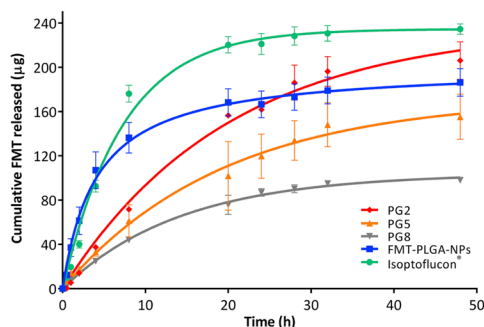
Fig. 3. *In vitro* release profiles of gels (adjust to first order equation), FMT-PLGA-NPs (adjust to hyperbola equation) and Isoptoflucon® (adjust to first order equation).

not flow at a temperature of 34 °C.

At the molecular level, at temperatures below 21 °C, the gel behaves like a newtonian fluid where the P407 molecules are in a disordered state. From the temperature of 21 °C approximately, the molecules begin to be ordered in micelles, initiating the sol-gel transition, completely gelling at the corneal temperature. The gels PG2 and PG5 have a regular flow between a temperature of 5 and 25 °C. In the case of PG8, it flows with difficulty, mainly caused by the amount of MC (1%) present in the formulation. This gelling behaviour of the optimized formulations allow their administration as eye drops dosage form and enabling the gelation when it comes in contact with the eyeball, which results in an increase in the residence time avoiding the rapid elimination by the lacrimal stimulation [32]. In Table S.2 Supplementary Material, the flow ability data of the rest of the gels of the design are visualized, which did not fulfill the condition of low flow at the corneal temperature and be gelled at 34 °C.

3.3.4. Morphological characterization

Through the analysis of TEM images (Fig. S.4 Supplementary Material), it was possible to visualize the NPs contained in the gels. According to these images, it was confirmed that the NPs maintained their spherical shape, average size and absence of aggregation, concordant with the data coming from the DLS and the TEM images of the optimized NPs made in the preliminary study [7].

3.3.5. In vitro release profile

In Fig. 3 it is possible to demonstrate the controlled release of FMT from the gels and FMT-PLGA-NPs. In the first instance, Isoptoflucon® presents a rapid release of FMT reaching 100% at 24 h, adjusting to a profile of first order ($r^2 = 0.999$, AIC = 69.523). The NPs presented a release close to 80%, characterized by an initial burst release in the first 4 h reaching 45% of drug released due to the drug weakly bound on the surface of the NPs [34]. The best model that adjusted the formulation FMT-PLGA-NPs was the hyperbola ($r^2 = 0.982$, AIC = 68.151), where the release in the last section of the profile (4–10 h), is slow and growing without reaching a plateau, by the affinity of the drug to the polymer matrix [35]. Finally, the formulations PG2, PG5 and PG8 presented a slow and increasing release of FMT of approximately 70%, 50% and 40%, respectively, at 24 h. As it is possible to observe in Fig. 3, at the time of 24 h PG2 reaches the released amount of FMT-PLGA-NPs, progressively increasing until the end of the experiment (48 h). PG2 does not present a burst release effect in the first 4 h, allowing the drug to be released slowly and sustainably, due to the increase in viscosity and the constant erosion rate attributed to the *in-situ* formation of the gel [36]. It should be noted that the formation of the gel containing the nanoparticles prevents the burst release creating a repository of the

drug within the gelling matrix, allowing a greater release of drug than FMT-PLGA-NPs [37,38]. In turn, although the three formulations of gels have similar $T_{sol-gel}$, they present a release at 24 h different from each other, probability due to the viscosity given by MC (0–1%). Finally, PG2 ($r^2 = 0.984$, AIC = 70.745), PG5 ($r^2 = 0.925$, AIC = 80.943) and PG8 ($r^2 = 0.992$, AIC = 42.868) adjusted a profile of first order, without reaching a plateau at the end of the study [39].

3.3.6. Stability analysis of gels

The gel formulations were evaluated for stability within a period of 60 days at storage conditions of 4 °C. According to Fig. 4 (a–c), it is evident that the PG5 and PG8 formulations have greater stability than PG2. This difference is mainly due to the viscosity that prevents the precipitation of the NPs inside the gelling system, at a temperature of 4 °C, since at this temperature the gels are in liquid state (suspension), which increases the instability of the gel [40,41]. Despite the above, the instability of PG2 is within the allowed margins (Backscattering ≤ 20%). Due to this behaviour of the gels at a temperature of 4 °C, they must be resuspended with gentle agitation before being administered.

3.3.7. Ocular tolerance

The *in vitro* eye tolerance study (HET-CAM® test) of the optimized gels, showed OII values lower than 0.9, categorizing the formulations as nonirritating (Table S.3 Supplementary Material). In the case of NPs and the commercial drug (Isoptoflucon®), these have been evaluated in a previous study in our group, concluding that they are nonirritating [7]. In order to corroborate these data, the *in vivo* evaluation was carried out through the Draize test of the formulations of gels, NPs and Isoptoflucon® in albino New Zealand rabbits. In this study, it was concluded that the evaluated formulations are not irritating (OII = 0) [41,42] (Table S.4 Supplementary Material).

3.3.8. Therapeutic efficacy

Through the realization of two *in vivo* studies, it was possible to confirm the anti-inflammatory capacity of the optimized gels, both in an acute treatment of ocular inflammation and in the prevention of it. The optimized gels (PG2, PG5 and PG8) present evident significant differences regarding positive control ($p < 0.01$) and the commercial drug ($p < 0.05$) at 60 min of the anti-inflammatory efficacy test (Fig. 5a). The formulations PG2 and PG5 maintained significant differences regarding Isoptoflucon® until the end of the study. FMT-PLGA-NPs also had a significant anti-inflammatory effect ($p < 0.05$) up to 150 min. This proves that optimized thermosensitive gels increase the effect of the drug more than when it is loaded into NPs or in commercial eye drops. This is mainly due to the *in-situ* formation of the gel at corneal temperature, which leads to an increase in viscosity (PG2 <
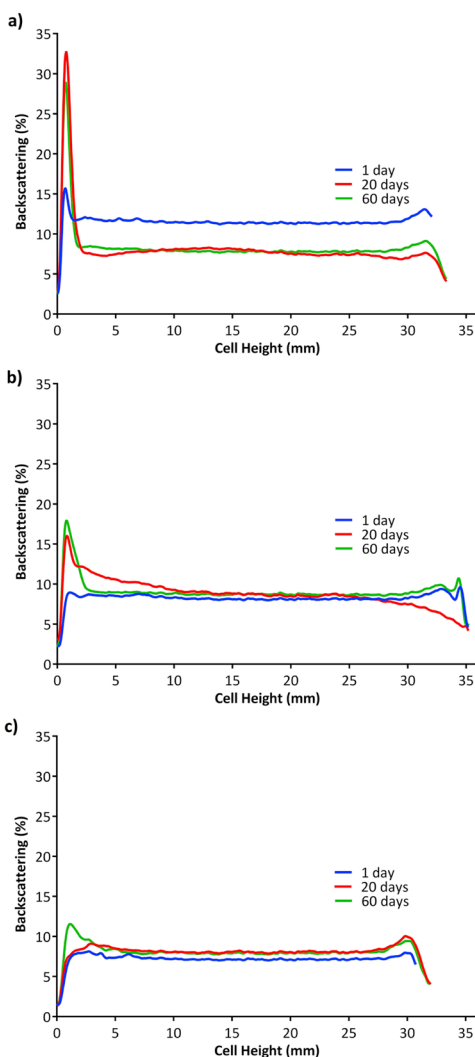
Fig. 4. Backscattering profile of optimized gels at 4 °C. a) PG2, b) PG5, c) PG8.

PG5 < PG8), resulting in prolongation of the residence time of the formulation in the precorneal area, increasing penetration ocular and in turn, avoiding the rapid elimination of the drug by tearing [16].

In order to observe the usefulness of the formulations in a prophylactic treatment of inflammation, these were applied at the beginning of the study and after 30 min inflammation was induced with SA (Fig. 5b). Gels and NPs reduced inflammation significantly ($p < 0.05$) regarding positive control at 60 min. Particularly, PG2 and PG5 were the

formulations that obtained significant differences evident when compared with the commercial drug ($p < 0.05$) from 60 min until the end of the study. In addition, Isoptoflucon® from 180 min up to 210 min, obtained a significant efficiency ($p < 0.05$) in decreasing inflammation regarding SA. At the end of the study, it was concluded that PG2 and PG5 decrease inflammation more effectively than other formulations when compared with SA ($p < 0.0001$) and Isoptoflucon® ($p < 0.01$). It is also possible to visualize that the anti-inflammatory degree of the
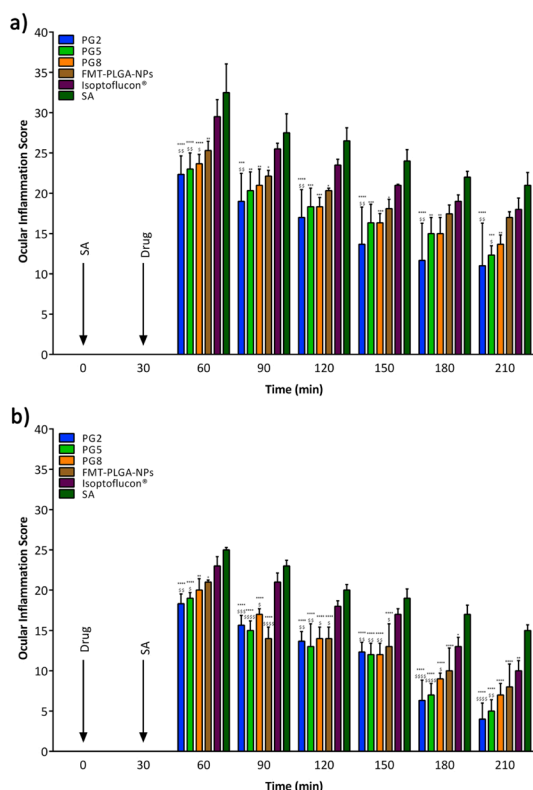
Fig. 5. Comparison of anti-inflammatory efficacy of PG2, PG5, PG8, FMT-PLGA-NPs and Isoptoflucon*. a) Inflammation treatment, b) inflammation prevention. Values are expressed as mean $\pm$ SD; ** $p < 0.01$, *** $p < 0.001$ and **** $p < 0.0001$ significantly lower than the inflammatory effect induced by SA; \$\$ $p < 0.01$, \$\$\$ $p < 0.001$ and \$\$\$\$ $p < 0.0001$ significantly lower than the inflammatory effect induced by Isoptoflucon*.

prophylaxis is greater than in the acute treatment, because the drug is longer in contact with the eyeball, in turn, the residence time is increased when the formulation is in a state of gel. PG2 and PG5 would be suitable for the prevention of inflammation without the need for repetitive administrations of the formulation to obtain a significant therapeutic effect.

3.3.9. Ocular bioavailability

The remaining amount of FMT (determined by RP-HPLC) in the different ocular tissues of PG2, PG5, PG8, FMT-PLGA-NPs and Isoptoflucon* are visualized in Fig. S.5 Supplementary Material. At the corneal level, the formulation FMT-PLGA-NPs and Isoptoflucon* presented similar values without significant differences and other formulations were not detectable at this level. In Fig. S.5 Supplementary Material it is possible to visualize that the FMT-PLGA-NPs ($p < 0.0001$) and PG8 ($p < 0.01$) showed a concentration obviously higher than the commercial drug in the sclera. PG5 and PG were those formulations that presented an accumulation at the aqueous humour level of 2 and 3 times more than Isoptoflucon*, respectively. At the level of the crystalline, it is possible to show that only the FMT-PLGA-NPs and PG5

obtained a significant difference against to the commercial drug ($p < 0.0001$), this because the gel has an intermediate viscosity that allows it to release the drug slowly and remain a longer residence time in the precorneal area. In turn, NPs due to their ability to protect the drug from ocular metabolism and increase the solubility of the drug to be encapsulated in the lipophilic matrix of PLGA are the potential reasons for the accumulation of these two formulations in the crystalline [6,43]. Finally, at the vitreous humour level, it is not possible to show significant differences in the accumulation of the drug among all the formulations analyzed. According to the release information, the anti-inflammatory efficacy and the bioavailability, PG5 presents the characteristics that best suit a formulation with anti-inflammatory activity and with the slow and prolonged release of the drug, which allows it to reach deep ocular tissues.

4. Conclusions

Using a multifactorial design, it was possible to select three formulations of gels loaded FMT-PLGA-NPs (PG2, PG5 and PG8), which have in common the same amount of P407 (20% w/v) and with a

variable MC concentration (0–1% w/v). The optimized gels presented suitable rheometric characteristics for use as an ophthalmological suspension of *in-situ* gelation, such as fluidity at room temperature, a gelling capacity in SFL, a viscosity and $T_{sol-gel}$ that allow it to be in a gel state at corneal temperature with an optimal viscosity to increase the residence time in the cornea than other commercial eye drops. In turn, with the analysis of TEM images corroborated that the NPs in the gels maintained their spherical shape and their Zav, without evidence of agglomerates. The gelling system gave the formulations a proven stability of 60 days and with the recommendation of a gentle agitation before its administration, due to the behaviour of suspension at room temperature. In the *in vivo* studies of efficacy and inflammatory prophylaxis, the optimized gels obtained a greater capacity in decreasing the OII in contrast to the Isoptoflucon® and without effects of ocular irritation (studies in HET-CAM® and Draize test). According to the release information, the anti-inflammatory efficacy and the bioavailability, PG5 is the one that presents the characteristics that best suit a formulation with anti-inflammatory activity and with the slow and prolonged release of the drug, which allows it to reach deep ocular tissues such as aqueous humour and crystalline. Finally, the formulation of PG5 would be useful for the treatment of inflammatory eye diseases, avoiding the repetitive administration of eye drops, which would improve the patient's adherence to treatment.

Conflict of interest

No conflicting relationship exists for any author.

Acknowledgments

Appendix A. Supplementary data

Supplementary material related to this article can be found, in the online version, at https://doi.org/10.1016/j.colsurfb.2018.11.065.

References

[1] P.-Q. Chen, X.M. Han, Y.N. Zhu, J. Xu, Comparison of the anti-inflammatory effects of fluorometholone 0.1% combined with levofloxacin 0.5% and tobramycin/dexamethasone eye drops after cataract surgery, Int. J. Ophthalmol. 9 (2016) 1619–1623, https://doi.org/10.18240/ijo.2016.11.13.

[2] S. Shokoohi-Rad, R. Daneshvar, M. Jafarian-Shahri, P. Rajaee, Comparison between Betamethasone, Fluorometholone and Loteprednol Etabonate on intraocular pressure in patients after keratorefractive surgery, J. Curr. Ophthalmol. 30 (2018) 130–135, https://doi.org/10.1016/j.joco.2017.11.008.

[3] M.A. Awan, P.K. Agarwal, D.G. Watson, C.N.J. McGhee, G.N. Dutton, Penetration of topical and subconjunctival corticosteroids into human aqueous humour and its therapeutic significance, Br. J. Ophthalmol. 93 (2009) 708–713, https://doi.org/10.1136/bjo.2008.154906.

[4] J. Araújo, E. Gonzalez, M.A. Egea, M.L. Garcia, E.B. Souto, Nanomedicines for ocular NSAIDs: safety on drug delivery, Nanomedicine 5 (2009) 394–401, https://doi.org/10.1016/j.nano.2009.02.003.

[5] D.N. Kapoor, A. Bhatia, R. Kaur, R. Sharma, G. Kaur, S. Dhawan, PLGA: a unique polymer for drug delivery, Ther. Deliv. 6 (2015) 41–58, https://doi.org/10.4155/tde.14.91.

[6] F.P. Guengerich, Intersection of the roles of cytochrome P450 enzymes with xenobiotic and endogenous substrates: relevance to toxicity and drug interactions, Chem. Res. Toxicol. 30 (2017) 2–12, https://doi.org/10.1021/acs.chemrestox.6b00226.

[7] R. Gonzalez-Pizarro, M. Silva-Abreu, A.C. Calpena, M.A. Egea, M. Espina, M.L. García, Development of fluorometholone-loaded PLGA nanoparticles for treatment of inflammatory disorders of anterior and posterior segments of the eye, Int. J. Pharm. 547 (2018) 338–346, https://doi.org/10.1016/J.IJPHARM.2018.05.050.

[8] B. Balzus, F.F. Sahle, S. Hönzke, C. Gerecke, F. Schumacher, S. Hedtrich, B. Kleuser, R. Bodmeier, Formulation and ex vivo evaluation of polymeric nanoparticles for

[9] K. Tahara, K. Karasawa, R. Onodera, H. Takeuchi, Feasibility of drug delivery to the eye's posterior segment by topical instillation of PLGA nanoparticles, Asian J. Pharm. Sci. 12 (2017) 394–399, https://doi.org/10.1016/J.AJPS.2017.03.002.

[10] B. Srividya, R.M. Cardoza, P. Amin, Sustained ophthalmic delivery of ofloxacin from a pH triggered in situ gelling system, J. Control. Release 73 (2001) 205–211, https://doi.org/10.1016/S0168-3659(01)00279-6.

[11] A. Rozier, C. Mazuel, J. Grove, B. Plazonnet, Gelrite®: A novel, ion-activated, in-situ gelling polymer for ophthalmic vehicles, Effect Bioavailab. Timolol. Int. J. Pharm. 57 (1989) 163–168, https://doi.org/10.1016/0378-5173(89)90305-0.

[12] T. Ishibashi, N. Yokoi, A.J. Bron, J.M. Tiffany, A. Komuro, S. Kinoshita, Retention of reversibly thermo-gelling timolol on the human ocular surface studied by video meniscometry, Curr. Eye Res. 27 (2003) 117–122, https://doi.org/10.1076/ceyr.27.2.117.15948.

[13] K.Y. Lee, C.W. Cho, Y.B. Lee, S.-C. Shin, I.J. Oh, Rheological behavior of poloxamer 407 solution and effect of poly(ethylene glycol) on the gelling, J. Korean Pharm. Sci. 33 (2003) 15–19, https://doi.org/10.4333/KPS.2003.33.1.015.

[14] L. Kessel, L. Johnson, H. Arvidsson, M. Larsen, The relationship between body and ambient temperature and corneal temperature, Investig. Opthalmol. Vis. Sci. 51 (2010) 6593–6597, https://doi.org/10.1167/iovs.10-5659.

[15] N. Morsi, D. Ghorab, H. Refai, H. Teba, Ketorolac tromethamine loaded nanodispersion incorporated into thermosensitive in situ gel for prolonged ocular delivery, Int. J. Pharm. 506 (2016) 57–67, https://doi.org/10.1016/J.IJPHARM.2016.04.021.

[16] D. Kumar, N. Jain, N. Gulati, U. Nagaich, Nanoparticles laden in situ gelling system for ocular drug targeting, J. Adv. Pharm. Technol. Res. 4 (2013) 9–17, https://doi.org/10.4103/2231-4040.107495.

[17] V. Nekkanti, A. Marwah, R. Pillai, Media milling process optimization for manufacture of drug nanoparticles using design of experiments (DOE), Drug Dev. Ind. Pharm. 41 (2015) 124–130, https://doi.org/10.3109/03639045.2013.850709.

[18] K. Konieczka, A. Schoetzau, S. Koch, D. Hauenstein, J. Flammer, Cornea thermography: optimal evaluation of the outcome and the resulting reproducibility, Transl. Vis. Sci. Technol. 7 (2018) 14, https://doi.org/10.1167/tvst.7.3.14.

[19] W. Lihong, C. Xin, G. Yongxue, B. Yiying, C. Gang, Thermoresponsive ophthalmic poloxamer/tween/carbopol in situ gels of a poorly water-soluble drug fluconazole: preparation and in vitro – in vivo evaluation, Drug Dev. Ind. Pharm. 40 (2014) 1402–1410, https://doi.org/10.3109/03639045.2013.828221.

[20] G. Dumortier, J.L. Grossiord, F. Agnely, J.C. Chaumeil, A review of poloxamer 407 pharmaceutical and pharmacological characteristics, Pharm. Res. 23 (2006) 2709–2728, https://doi.org/10.1007/s11095-006-9104-4.

[21] D. Klose, C. Delplace, J. Siepmann, Unintended potential impact of perfect sink conditions on PLGA degradation in microparticles, Int. J. Pharm. 404 (2011) 75–82, https://doi.org/10.1016/J.IJPHARM.2010.10.054.

[22] K. Yamaoka, T. Nakagawa, T. Uno, Application of Akaike's information criterion (AIC) in the evaluation of linear pharmacokinetic equations, J. Pharmacokinet. Biopharm. 6 (1978) 165–175, https://doi.org/10.1007/BF01117450.

[23] ICCVAM, ICCVAM-recommended Test Method Protocol: Hen's Egg Test – Chorioallantoic Membrane (HET-CAM) Test Method, NIH Publ. N° 10-7553, (2010), pp. B29–B38 (Accessed January 27, 2018), http://iccvam.niehs.nih.gov/methods/ocutox/MildMod-TMER.htm.

[24] D. Jírová, K. Kejlová, S. Janoušek, H. Bendová, M. Malý, H. Kolářová, M. Dvořáková, Eye irritation hazard of chemicals and formulations assessed by methods in vitro, Neuro Endocrinol. Lett. 35 (Suppl. 2) (2014) 133–140 (Accessed August 3, 2018), http://www.ncbi.nlm.nih.gov/pubmed/25638377.

[25] N.P. Luepke, F.H. Kemper, The HET-CAM test: An alternative to the draize eye test, Food Chem. Toxicol. 24 (1986) 495–496, https://doi.org/10.1016/0278-6915(86)90099-2.

[26] E. Sánchez-López, M.A. Egea, A. Cano, M. Espina, A.C. Calpena, M. Ettcheto, A. Camins, E.B. Souto, A.M. Silva, M.L. García, PEGylated PLGA nanospheres optimized by design of experiments for ocular administration of dexibuprofen —in vitro, ex vivo and in vivo characterization, Colloids Surf. B Biointerfaces 145 (2016) 241–250, https://doi.org/10.1016/j.colsurfb.2016.04.054.

[27] Y. Ali, K. Lehmussaari, Industrial perspective in ocular drug delivery, Adv. Drug Deliv. Rev. 58 (2006) 1258–1268, https://doi.org/10.1016/J.ADDR.2006.07.022.

[28] S. Stolnik, M. Garnett, M. Davies, L. Illum, M. Bousta, M. Vert, S. Davis, The colloidal properties of surfactant-free biodegradable nanospheres from poly(β-malic acid-co-benzyl malate)s and poly(lactic acid-co-glycolide), Colloids Surf. A Physicochem. Eng. Asp. 97 (1995) 235–245, https://doi.org/10.1016/0927-7757(95)03081-N.

[29] Z.M.A. Fathalla, A. Vangala, M. Longman, K.A. Khaled, A.K. Hussein, O.H. El-Garhy, R.G. Alany, Poloxamer-based thermoresponsive ketorolac tromethamine in situ gel preparations: Design, characterisation, toxicity and transcorneal permeation studies, Eur. J. Pharm. Biopharm. 114 (2017) 119–134, https://doi.org/10.1016/J.EJPB.2017.01.008.

[30] G. Abrego, H. Alvarado, E.B. Souto, B. Guevara, L.H. Bellowa, A. Parra, A. Calpena, M.L. Garcia, Biopharmaceutical profile of pranoprofen-loaded PLGA nanoparticles containing hydrogels for ocular administration, Eur. J. Pharm. Biopharm. 95 (2015) 261–270, https://doi.org/10.1016/j.ejpb.2015.01.026.

[31] H. Almeida, M.H. Amaral, P. Lobão, J.M. Sousa Lobo, Applications of poloxamers in ophthalmic pharmaceutical formulations: an overview, Expert Opin. Drug Deliv. 10 (2013) 1223–1237, https://doi.org/10.1517/17425247.2013.796360.

[32] M. Mansour, S. Mansour, N.D. Mortada, S.S. Abd ElHady, Ocular poloxamer-based ciprofloxacin hydrochloride in situ forming gels, Drug Dev. Ind. Pharm. 34 (2008) 744–752, https://doi.org/10.1080/03639040801926030.

[33] J.Y. Chang, Y.K. Oh, H. Choi, Y.B. Kim, C.K. Kim, Rheological evaluation of

thermosensitive and mucoadhesive vaginal gels in physiological conditions, Int. J. Pharm. 241 (2002) 155–163, https://doi.org/10.1016/S0378-5173(02)00232-6.

[34] A. Cano, M. Ettcheto, M. Espina, C. Auladell, A.C. Calpena, J. Folch, M. Barenys, E. Sánchez-López, A. Camins, M.L. García, Epigallocatechin-3-gallate loaded PEGylated-PLGA nanoparticles: a new anti-seizure strategy for temporal lobe epilepsy, Nanomed. Nanotechnol. Biol. Med. 14 (2018) 1073–1085, https://doi.org/10.1016/J.NANO.2018.01.019.

[35] E. Sánchez-López, M. Ettcheto, M.A. Egea, M. Espina, A.C. Calpena, J. Folch, A. Camins, M.L. García, New potential strategies for Alzheimer's disease prevention: pegylated biodegradable dexibuprofen nanospheres administration to APPswe/PS1dE9, Nanomedicine 13 (2017) 1171–1182, https://doi.org/10.1016/j.nano.2016.12.003.

[36] E. Bilensoy, M. Abdur Rouf, I. Vural, M. Šen, A. Atilla Hincal, Mucoadhesive, thermosensitive, prolonged-release vaginal gel for clotrimazole: β-cyclodextrin complex, AAPS PharmSciTech 7 (2006) E54–E60, https://doi.org/10.1208/pt070238.

[37] X. Huang, C.S. Brazel, On the importance and mechanisms of burst release in matrix-controlled drug delivery systems, J. Control. Release 73 (2001) 121–136, https://doi.org/10.1016/S0168-3659(01)00248-6.

[38] M. Gou, X. Li, M. Dai, C. Gong, X. Wang, Y. Xie, H. Deng, L. Chen, X. Zhao, Z. Qian, Y. Wei, A novel injectable local hydrophobic drug delivery system: biodegradable nanoparticles in thermo-sensitive hydrogel, Int. J. Pharm. 359 (2008) 228–233, https://doi.org/10.1016/J.IJPHARM.2008.03.023.

[39] A.C.M. dos Santos, A.C.S. Akkari, I.R.S. Ferreira, C.R. Maruyama, M. Pascoli, V.A. Guilherme, E. de Paula, L.F. Fraceto, R. de Lima, P. da S. Melo, D.R. de Araujo, Poloxamer-based binary hydrogels for delivering tramadol hydrochloride: sol-gel transition studies, dissolution-release kinetics, in vitro toxicity, and pharmacological evaluation, Int. J. Nanomed. 10 (2015) 2391–2401, https://doi.org/10.2147/IJN.S72337.

[40] H. Almeida, P. Lobão, C. Frigerio, J. Fonseca, R. Silva, J.M. Sousa Lobo, M.H. Amaral, Preparation, characterization and biocompatibility studies of thermoresponsive eyedrops based on the combination of nanostructured lipid carriers (NLC) and the polymer Pluronic F-127 for controlled delivery of ibuprofen, Pharm. Dev. Technol. 22 (2017) 336–349, https://doi.org/10.3109/10837450.2015.1125922.

[41] M. Mallandrich, F. Fernández-Campos, B. Clares, L. Halbaut, C. Alonso, L. Coderch, M.L. Garduño-Ramírez, B. Andrade, A. del Pozo, M.E. Lane, A.C. Calpena, Developing transdermal applications of ketorolac tromethamine entrapped in stimuli sensitive block copolymer hydrogels, Pharm. Res. 34 (2017) 1728–1740, https://doi.org/10.1007/s11095-017-2181-8.

[42] M.A. Grimaudo, S. Pescina, C. Padula, P. Santi, A. Concheiro, C. Alvarez-Lorenzo, S. Nicoli, Poloxamer 407/TPGS mixed micelles as promising carriers for cyclosporine ocular delivery, Mol. Pharm. 15 (2018) 571–584, https://doi.org/10.1021/acs.molpharmaceut.7b00939.

[43] M. Narvekar, H.Y. Xue, J.Y. Eoh, H.L. Wong, Nanocarrier for poorly water-soluble anticancer drugs—barriers of translation and S solutions, AAPS PharmSciTech 15 (2014) 822–833, https://doi.org/10.1208/s12249-014-0107-x.
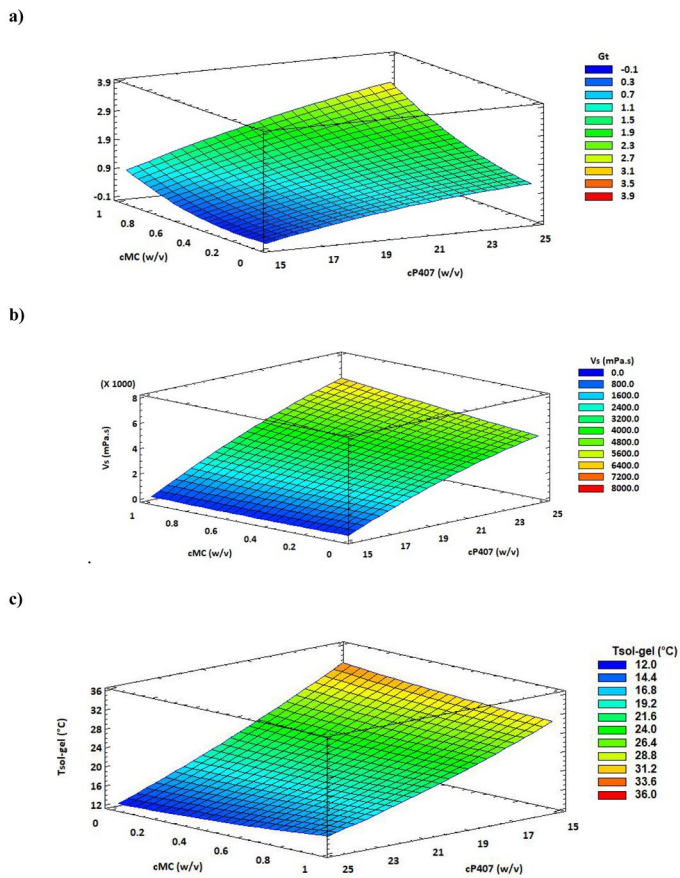
Supplementary Material

a)

b)

c)

Fig. S.1. Surface response. a) Gt, b) Vs, c) $T_{sol-gel}$.

Fig. S.2. Photos of the formulations optimized in the gelling capacity test. a) PG2, b) PG5, c) PG8.
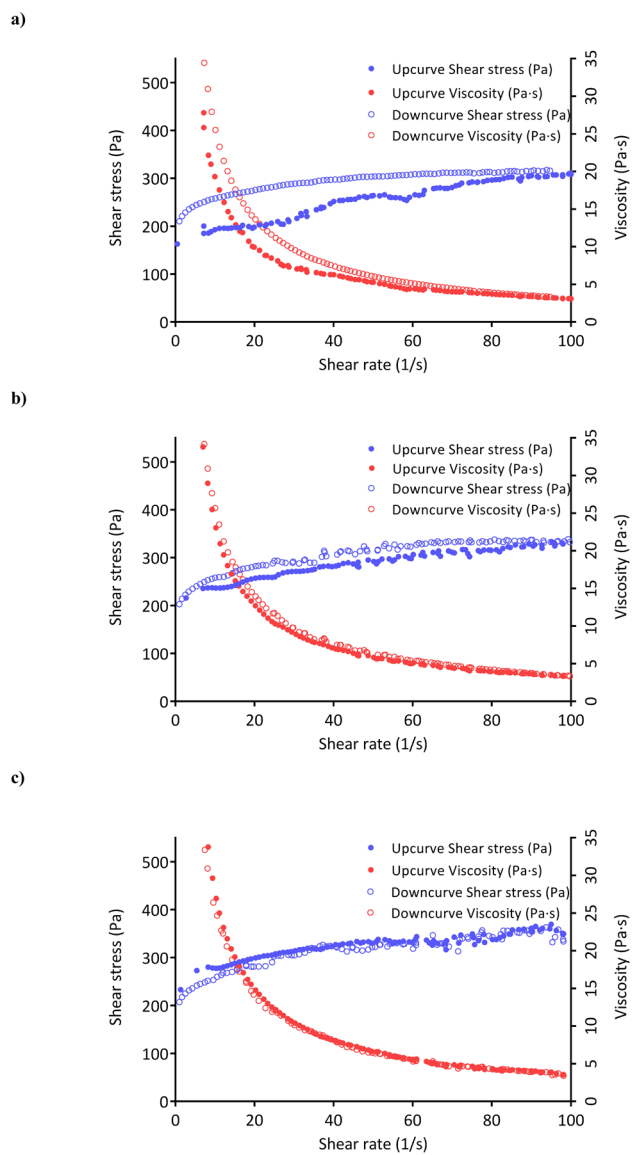
Fig. S.3. Flow and viscosity of the optimized gels. a) PG2, b) PG5, c) PG8.

Table S.1
Independents variables and codes used in the experimental design.

Independents variables (w/v)	Levels		
	-1	0	+1
cP407	15.0	20.0	25.0
cMC	0.0	0.5	1.0

Table S.2
Flow ability of optimized gels.

Formulation	Flow ability at different temperatures (°C)		
	5 ± 0.5	25 ± 0.5	35 ± 0.5
PG1	+++	+++	+++
PG2	+++	++	-
PG3	+++	-	-
PG4	+++	+++	+++
PG5	++	++	-
PG6	++	-	-
PG7	++	++	++
PG8	+	+	-
PG9	+	-	-

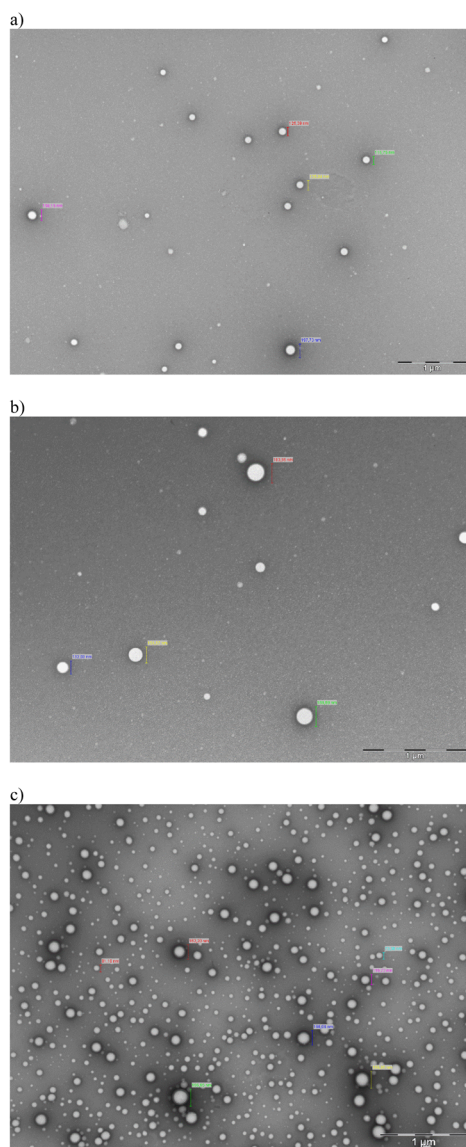+++ = freely flow, ++ = regular flows, + = flow with difficulty, - not flow.

Fig. S.4. Transmission electron microscopy analysis of gels. a) PG2, b) PG5, c) PG8.
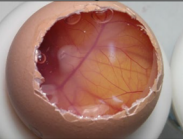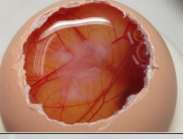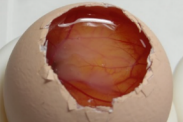
Table S.3
Ocular tolerance by HET-CAM® test.
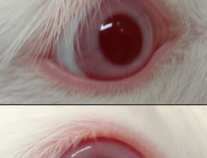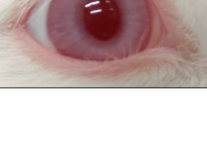
Formulation	Medium Score	Classification	Image after 5 min
PG2	0.61 ± 0.20	Nonirritating	
PG5	0.40 ± 0.20	Nonirritating	
PG8	0.41 ± 0.07	Nonirritating	

Table S.4
Ocular tolerance by Draize test.

Formulation	Medium Score	Classification	Image at endpoint
PG2	0.00 ± 0.00	Nonirritating	
PG5	0.00 ± 0.00	Nonirritating	
PG8	0.00 ± 0.00	Nonirritating	
FMT-PLGA-NPs	0.00 ± 0.00	Nonirritating	
Isoptoflucon®	0.00 ± 0.00	Nonirritating	

Fig. S.5. Bioavailability of PG2, PG5, PG8, FMT-PLGA-NPs and Isoptoflucon® in the different ocular structures. Values are expressed as mean ± SD; ** $p < 0.01$, ***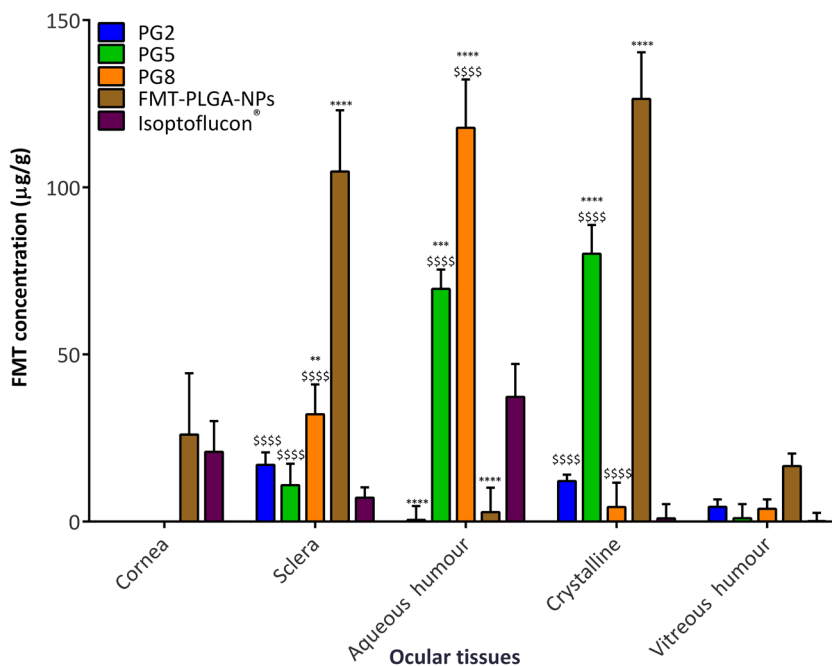 $p < 0.001$ and **** $p < 0.0001$ significance with respect to the concentration of FMT from Isoptoflucon®; \$\$ $p < 0.01$, \$\$\$ $p < 0.001$ and \$\$\$\$ $p < 0.0001$ significance with respect to the concentration of FMT from FMT-PLGA-NPs.

3.3. Ocular penetration of fluorometholone-loaded PEG-PLGA nanoparticles functionalized with cell-penetrating peptides

Roberto González-Pizarro[a,e], Graziella Parrotta[c], Rodrigo Vera[b,f,g], Elena Sánchez-López[a,d,e], Ruth Galindo[a], Frank Kjeldsen[c], Josefa Badia[b,f,g], Laura Baldoma[b,f,g], Marta Espina[a,e], María Luisa García[a,d,e]

[a]Department of Pharmacy, Pharmaceutical Technology and Physical Chemistry, Faculty of Pharmacy and Food Sciences, University of Barcelona, 08028 Barcelona, Spain.
[b]Department of Biochemistry and Physiology, Faculty of Pharmacy and Food Sciences, University of Barcelona, 08028 Barcelona, Spain.
[c]Department of Biochemistry and Molecular Biology, Faculty of Science, University of Southern Denmark, 5230 Odense, Denmark.
[d]Biomedical Research Networking Center in Neurodegenerative Diseases (CIBERNED), Madrid, Spain
[e]Institute of Nanoscience and Nanotechnology (IN2UB), University of Barcelona, Barcelona, Spain.
[f]Institute of Biomedicine, University of Barcelona (IBUB), Barcelona, Spain.
[g]Institut de Recerca Sant Joan de Déu (IRSJD), Barcelona, Spain.

Ocular penetration of fluorometholone-loaded PEG-PLGA nanoparticles functionalized with cell-penetrating peptides

Roberto González-Pizarro[a,e], Graziella Parrotta[c], Rodrigo Vera[b,f,g], Elena Sánchez-López[a,d,e], Ruth Galindo[a], Frank Kjeldsen[c], Josefa Badia[b,f,g], Laura Baldoma[b,f,g], Marta Espina[a,e], María Luisa García[a,d,e].

[a]Department of Pharmacy, Pharmaceutical Technology and Physical Chemistry, Faculty of Pharmacy and Food Sciences, University of Barcelona, 08028 Barcelona, Spain.
[b]Department of Biochemistry and Physiology, Faculty of Pharmacy and Food Sciences, University of Barcelona, 08028 Barcelona, Spain.
[c]Department of Biochemistry and Molecular Biology, Faculty of Science, University of Southern Denmark, 5230 Odense, Denmark.
[d]Biomedical Research Networking Center in Neurodegenerative Diseases (CIBERNED), Madrid, Spain
[e]Institute of Nanoscience and Nanotechnology (IN2UB), University of Barcelona, Barcelona, Spain.
[f]Institute of Biomedicine, University of Barcelona (IBUB), Barcelona, Spain.
[g]Institut de Recerca Sant Joan de Déu (IRSJD), Barcelona, Spain.

Abstract

Aim: Development of Fluorometholone-loaded PEG-PLGA nanoparticles (NPs) functionalized with cell-penetrating peptides for the treatment of ocular inflammatory disorders. **Materials and methods:** Synthesized polymers and peptides were used for elaboration of functionalized NPs, which were characterized physicochemically. Cytotoxicity and ability to modulate the expression of proinflammatory cytokines were evaluated *in vitro* using human corneal epithelial cells (HCE-2). NPs uptake was assayed in both *in vitro* and *in vivo* models. **Results:** NPs showed physicochemical characteristics

suitable for ocular administration without evidence of cytotoxicity. TAT-NPs and G2-NPs were internalized and displayed anti-inflammatory activity in both HCE-2 cells and mouse eye. **Conclusion:** TAT-NPs and G2-NPs could be considered a novel strategy for the treatment of ocular inflammatory diseases of the anterior and posterior segment.

Key words

Fluorometholone, Ocular anti-inflammatory, Polymeric NPs, Cell-penetrating peptides, drug delivery.

Introduction

Uveitis is one of the most common intraocular inflammatory diseases affecting the anterior and posterior segments of the eye. Corticosteroid eye drops such as Fluorometholone (FMT) are used in the clinic for the treatment of anterior uveitis, such as iritis, cyclitis or iridocyclitis. The main disadvantage of eye drops dosage forms is the dilution and elimination by the tear turnover, which decreases their precorneal residence time. Consequently, the anti-inflammatory effect is limited in the anterior segment of the eye [1–3]. Regarding posterior uveitis such as diffuse choroiditis and vitritis, systemic corticosteroids, intravitreal injections or implants are used to achieve an effective pharmacological effect nevertheless, these methods entail a recurrence of unwanted side effects [4]. Furthermore, most topical administration ophthalmic suspensions contain benzalkonium chloride as a preservative, which induces ocular irritation [5,6]. Although most ocular corticosteroids induce glaucoma by increasing intraocular pressure (IOP) in prolonged treatment, FMT has a significantly lower risk of causing this disease [7–9]. Nowadays, new strategies such as the encapsulation of corticosteroids in polymeric

nanoparticles (NPs) of average size smaller than 300 nm and nanostructured gels have shown their capacity to increase the precorneal residence time and reach tissues of the posterior segment of the eye [10–14]. Moreover, the objective in ocular pharmacotherapy is to prevent drug inactivation by cytochrome P450, and its elimination by efflux transports and multidrug resistance proteins [15,16]. Therefore, the new nanostructured systems should protect the drug and allow internalization in ocular cells avoiding its elimination by both molecular (metabolizing enzymes) and anatomical (tear turnover and dilution) mechanisms. With regard to the previous approach, cell-penetrating peptides (CPPs) constitute a molecular strategy that would allow the internalization of macromolecules such as NPs. CPPs are sequences of less than 30 amino acids, rich in arginine (Arg) residues and positively charged. Internalization mechanisms range from direct translocation to receptor-mediated endocytosis. CPPs such Penetratin (pAntp$_{43-58}$) and the transcriptional activator peptide sequence (TAT$_{49-57}$) of human immunodeficiency virus 1 (HIV-1) have been shown to be effective for the cellular internalization of polypeptides and the transfection of nucleic acids. Besides, many of the CPPs share characteristics with antimicrobial peptides (AMPs), such as cationic sequences with multiple Arg residues [17–19]. Several CPPs such as TAT$_{49-57}$ and pAntp$_{43-58}$ have demonstrated antiviral and antibacterial activity [20,21]. On the other hand, the peptide called G2, considered within the group of AMPs, has shown antiviral activity in herpes simplex I. Two studies have shown that G2 has CPP and antiviral activity against herpes simplex virus types I and II [22,23].

In the current study, FMT-loaded maleimide-PEG-PLGA NPs (FMT-m-PEG-PLGA-NPs) functionalized with CPPs (TAT$_{49-57}$, pAntp$_{43-58}$ and G2) have been developed with the

aim of increase the anti-inflammatory therapeutic effectiveness of FMT with the capacity to reach the anterior as posterior segment of the eye. The maleimide-PEG-PLGA (m-PEG-PLGA) polymer was synthesized and characterized by nuclear magnetic resonance (H-NMR), X-ray diffraction spectroscopy (XRD) and Fourier transform infrared spectroscopy (FTIR). On the other hand, the synthesized peptides, TAT_{49-57}, $pAntp_{43-58}$ and G2, were analysed by mass spectrometry. The physicochemical properties and the degree of conjugation of FMT-m-PEG-PLGA-NPs with each CPP were studied. Cytotoxicity, inhibition of proinflammatory cytokines, uptake assays (*in vitro* and *in vivo*) were carried out to provide evidence of the innocuousness and effectiveness of functionalized NPs as a new strategy in the treatment of ocular inflammatory conditions.

Materials and methods

Materials

FMT and PLGA RG 503H were purchased from Capot Chemical (Hangzhou, China) and Evonik Corporation (Birmingham, USA), respectively. Maleimide-PEG-NH$_2$ (m-PEG) (5 KDa) was obtained from Nanosoft Polymers (Nanosoft Biotechnology LLC, USA). Ethyl-3-(3-dimethylaminopropyl) carbodiimide hydrochloride (EDC), N-hydroxysuccinimide (NHS), N-diisopropylethylamine (DIEA), Rhodamine 110 (Rho) chloride, poly (vinyl alcohol) (PVA), insulin, hydrocortisone, trypsin-EDTA (1X), lipopolysaccharide (LPS) and tetrazolium bromide (MTT) were purchased from Sigma Aldrich (St. Louis, USA). Keratinocyte serum-free medium (SFM), human recombinant epidermal growth factor (EFG), bovine pituitary extract, penicillin, streptomycin, fetal bovine serum (FBS), IL-1β, IL-6, IL-8 and TNFα Human ELISA Kit were acquired from

Thermo Fisher Scientific (Life Technologies, USA). Human corneal epithelial cell line immortalized with adenovirus 12-SV40 hybrid virus (HCE-2, ATCC® CRL-11135) was purchased from LGC Standards (Barcelona, Spain). Amino acids and NovaSyn TGR resin were obtained from Novabiochem (Hohenbrunn, Germany). Water through Millipore® MilliQ system was used for all the experiments and all the other reagents were of analytical grade.

Synthesis of the polymers Rho-PLGA and m-PEG-PLGA

33.3 µmol of PLGA RG 503H (1,0 g) were dissolved in 3 mL of chloroform, then allowed to react with 234.6 µmol of NHS (27 mg) and EDC (45 mg) overnight under continuous stirring in a sealed glass vial. Subsequently, PLGA RG 503 H (NHS-PLGA) was activated, precipitated with 10 mL of cold diethyl ether and centrifuged at 4,000 rpm for 10 min at 20 °C. The supernatant was removed, the recovered polymer was dissolved in 3 mL of chloroform and precipitated with cold diethyl ether. This washing/precipitation cycle was carried out 3 times. The NHS-PLGA obtained was dried using nitrogen gas (N_2) and then lyophilized and stored at -20 °C.

33.2 µmol of NHS-PLGA (1,000 mg), 35 µmol of m-PEG (167 mg) or Rho (12.78 mg) were dissolved in 3 mL of chloroform with 234.3 µmol of DIEA and left to react overnight under continuous stirring. The obtained polymer was subjected to three washing/precipitation cycles using an 80/20 mixture of diethyl ether/cold methanol. Finally, the polymer was lyophilized and stored at -20 °C. The yield obtained from polymers (m-PEG-PLGA and Rho-PLGA) was calculated by the following equation:

$$\text{Yield (\%)} = \frac{\text{weight of (m} - \text{PEG} - \text{PLGA)}}{\text{weight of (NHS} - \text{PLGA} + \text{m} - \text{PEG)}} \cdot 100$$

$$(1)$$

To follow the synthesis of the polymer and changes in its molecular structure, it was analysed by H-NMR. PLGA RG 503H, NHS-PLGA, m-PEG, m-PEG-PLGA and Rho-PLGA were dissolved in deuterated dimethyl sulfoxide (DMSO-d_6). The spectrum was recorded at 298 K on a Varian VNMRS 400 MHZ spectrometer (Agilent Technologies, USA). To calculate the PEGylation efficiency and percentage of mass relative (MR) of the m-PEG bound to the NHS-PLGA polymer, the following equations were used [24,25]:

$$\text{PEGylation efficiency (\%)} = \frac{\text{IP}_{\text{PEG}}(\delta = 3.31)/n}{\sum \text{IP}_{\text{PLGA}}(\delta = 5.21; 4.90; 3.31)/n} \cdot 100$$

$$(2)$$

$$\text{MR (\%)} = \frac{\text{MW}_{\text{PEG}} \left[\text{IP}_{\text{PEG}}/n\right]}{\text{MW}_{\text{PLGA}} \left[\text{IP}_{\text{PLA},\delta=5.21}/n\right]} \cdot 100$$

$$(3)$$

MW: molecular weight. PEG = 42.04 g·mol^{-1}, PLGA = 130.10 g·mol^{-1}.

IP: Peak integration.

n: number of protons PLGA = 6 $^+$H [PLA (δ = 5.21) = 1 $^+$H; PGA (δ = 4.90) = 2 $^+$H; PLA (δ = 1.47) = 3 $^+$H] and PEG (δ = 3.31) = 4 $^+$H.

Structural studies of polymers

The molecular changes of the synthesized polymer and its crystalline or amorphous state were evaluated by FTIR and XRD. FTIR spectra of polymers separately were obtained using a Thermo Scientific Nicolet iZ10 with an ATR diamond and DTGS detector. The scanning range was 525–4000 cm^{-1} [26]. The amorphous or crystalline state of NHS-PLGA, m-PEG and m-PEG-PLGA were determined by XRD measurements using Siemens D500 system (Karlsruher, GER). X-ray powder diffractograms were recorded using a Cu K"

radiation (45 kV, 40 mA, λ = 1.544 Å) in the range (2θ) from 2° to 60° with a step size of 0.026° and measuring time of 195.8 s per step [26].

Preparation and characterization of FMT-m-PEG-PLGA-NPs

FMT-m-PEG-PLGA-NPs were prepared by the solvent displacement method [26]. Briefly, the m-PEG-PLGA (10.0 mg·mL^{-1}) and FMT (0.5 mg·mL^{-1}) were dissolved in 5 mL of acetone. The organic phase was added slowly dropwise, under stirring, into 10 mL of an aqueous solution of PVA (15 mg·mL^{-1}) adjusted to pH 4.0. Subsequently, the organic solvent was evaporated under reduced pressure. Finally, the PVA was eliminated by ultracentrifugation (30,000 rpm for 30 min) and resuspended in 10 mL of phosphate buffered saline (PBS). For the synthesis of the fluorescent NPs (^{Rho}NPs), 20 mg of the polymer Rho-PLGA and 80 mg of m-PEG-PLGA were used.

Morphometry [average particle size (Zav), polydispersity index (PI)] and zeta potential (ZP) of NPs were determined in a Zetasizer NanoZS (Malvern Instruments, Malvern, UK) by dynamic light scattering (DLS) and electrophoretic mobility, respectively. Samples were diluted in MilliQ water (1:10) and experiments were performed with disposable capillary cells DTS1070 (Malvern Instruments) at 25 °C. The reported values correspond to the mean ± SD.

The entrapment efficiency (EE) of FMT in the NPs was quantified indirectly by measuring the non-entrapped drug in the dispersion medium. The free FMT was separated by a filtration/centrifugation technique (1:10 dilution) at 25 °C and 5,000 rpm for 10 min. The EE was calculated according to the following equation:

$$EE\ (\%) = \frac{cFMT_0 - cFMT_1}{cFMT_0} \cdot 100$$

(4)

where $cFMT_0$ and $cFMT_1$ are the total amount of FMT and free FMT in the filtrated, respectively. Samples were evaluated by HPLC, according to the method described previously [26]. Data were processed using Empower 3® Software.

Synthesis of CPPs

The peptide sequences, TAT_{49-57} (CGGGRKKRRQRRR), $pAntp_{43-58}$ (CGGGRQIKIWFQNRRMKWKK) and G2 (CGGGMPRRRRIRRRQK) were synthesized by automated solid-phase parallel peptide synthesizer (ResPep, Intavis AG, Germany) using NovaSyn TGR resin (0.25 mmol·g^{-1}) and 9-fluorenylmethoxycarbonyl (Fmoc) strategy. Couplings were carried out with benzotriazol-1-yl-oxytripyrrolidinophosphonium hexafluorophosphate (PyBOP)/N-methylmorpholine (NMM) as activator and a 5-fold molar excess of Fmoc-amino acids. In order to reduce the formation of side products, a capping step was used to permanently block any unreacted amino group after the coupling reaction or to acetylate the N-terminus of a completed peptide. Capping solution used was based on a ratio of 1:1:3 of acetic anhydride (Ac$_2$O), DIEA and DMF (N, N dimethylformamide). The Fmoc-deprotection step was performed twice with 20% piperidine in DMF for 30 min. Synthesized peptides were exposed for 3 h to a solution composed of 94% TFA: 1% triisopropylsylane (TIS): 2.5% dithiothreitol (DTT): 2.5% MilliQ water for the deprotection of the side chain and the cleavage from the resin. Peptides were isolated by precipitation with ice cold diethyl ether with subsequent centrifugation (3,000 rpm for 4 min at 4 °C). Each peptide dissolved in 30% acetic acid in water were

concentrated and dried using speed-vac system (Eppendorf Concentrator). Peptides were purified using a Jupiter® 3μ C18 300A column (150 x 4.6 mm, Phenomenex®) coupled to a 1260 semipreparative RP-HPLC (Agilent Technologies, USA). The method used was a gradient of 90% water (0.1% TFA)/90% acetonitrile (0.1% TFA). Crude peptides were purified to a yield of 90% by RP-HPLC at 220 nm. Desalted peptides were analysed by matrix-assisted laser desorption ionization source/tandem time-of-flight (MALDI-TOF/TOF) mass spectrometer (Ultraflextreme, Bruker Daltonik GmbH, Germany) using a α-cyano-4-hydroxycinnamic acid matrix.

Conjugation of CPPs with FMT-m-PEG-PLGA-NPs

1.45 μmol of FMT-m-PEG-PLGA-NPs (5 mL of NPs) were reacted with 1.45 μmol of CPP (2.34 mg of TAT_{49-57}, 3.65 mg of $pAntp_{43-58}$ and 2.87 mg of G2) overnight under magnetic stirring. Next, ultracentrifugation of the NPs was performed (28,000 rmp for 30 min at 4 °C) to remove the peptide unconjugated and the pellet containing NPs was resuspended in PBS. In order to confirm the conjugation with the CPPs, derivatized NPs were lyophilized and analysed by H-NMR (previously dissolved DMSO-d_6). MR was used for the calculation of each CPP bound to FMT-m-PEG-PLGA-NPs according to the following equation [24]:

$$MR\ (\%) = \frac{MW_{CPP}\left[IP_{CPP}/n\right]}{MW_{PLGA}\left[IP_{PLA}/n\right]} \cdot 100$$

(5)

MW: molecular weight. TAT_{49-57} = 1612.94 g·mol^{-1}, $pAntp_{43-58}$ = 2519.36 g·mol^{-1}, G2 = 1982.12 g·mol^{-1}, PLGA = 130.10 g·mol^{-1}.

n: number of protons: TAT_{49-57} (δ = 7.0-8.2 ppm):46 $^+$H, $pAntp_{43-58}$ (δ = 6.8-8.2): 64 $^+$H, G2 (δ = 7.0-8.2): 50 $^+$H and PLA (δ = 5.21): 1 $^+$H.

***In vitro* biological studies**

Cell culture

The culture medium for HCE-2 cells was SFM supplemented with bovine pituitary extract 0.05 mg·mL^{-1} and EFG 5 ng·mL^{-1} containing insulin 0.005 mg·mL^{-1}, FBS 10%, hydrocortisone 500 ng·mL^{-1} and penicillin 100 U·mL^{-1} plus streptomycin 100 mg·mL^{-1}. Cells were grown on 25 cm^2 culture flask to confluency (80%) in a humidified 10% CO_2 atmosphere at 37 °C. The culture medium was changed every 3 days.

Cytotoxicity study

The effect on cell viability of NPs conjugated with each CPP was evaluated *in vitro* using the MTT assay. For this, 1 x 10^5 HCE-2 cells in 0.1 mL were seeded in 96-well plates and incubated for 24 h at 37 ºC. Then, cells were exposed to different concentrations of TAT-NPs, pAntp-NPs, G2-NPs and Isoptoflucon® (ophthalmic commercial drug). After 24 or 48 h of incubation, cells were washed with PBS and incubated with 0.25 % MTT in fresh medium for 2 h at 37ºC in dark. Subsequently, medium was removed, and cells were lysed by the addition of 99% DMSO. Finally, the absorbance was measured at λ = 560 nm using an automatic Modulus™ Microplate Photometer (Turner BioSystems). The data were analysed by calculating the percentage of MTT reduction compared to the control (untreated cells, 100% viability).

Determination of proinflammatory cytokines

To evaluate the anti-inflammatory activity of the derivatized NPs (TAT-NPs, pAntp-NPs and G2-NPs) and the commercial drug (Isoptoflucon®), HCE-2 cells were seeded (1 x 10^5 cell·mL^{-1}) in 12-well plates and grown until 90% confluency. The different NPs were added to the culture medium at 50 μg·mL^{-1} and inflammation was induced with LPS (1 μg·mL^{-1}). Cells stimulated only with LPS were considered the positive control and untreated cells as the negative control. After 48 h incubation, the supernatants were collected and centrifuged (10,000 rpm for 5 min) at 4 ºC and stored at 80 ºC until use. Secreted levels of the pro-inflammatory cytokines IL-1β, IL-6, IL-8 and TNFα were quantified by enzyme-linked immunosorbent assay (ELISA) sets (BD Biosciences) according to manufacturer's instructions. The results were expressed as pg·mL^{-1}.

Cellular uptake study

To assess internalization of NPs in HCE-2 cells, 1 x 10^5 cell·mL^{-1} HCE-2 were grown in 8-well chamber slider (ibidi®) until approximately 80% confluence and then incubated with 50 μg·mL^{-1} ^{Rho}NPs (^{Rho}TAT-NPs, ^{Rho}pAntp-NPs, ^{Rho}G2-NPs and ^{Rho}FMT-m-PEG-PLGA-NPs) at 37 ºC for 48 h. Non-internalized ^{Rho}NPs were then removed by three PBS washes and cells were fixed with 3% paraformaldehyde for 30 min at 25 °C. Afterwards, cells were washed 3 times with PBS and the nuclei were stained with DAPI for 15 min at 25 °C. Finally, cells were washed 3 times and mounting solution (PBS) was added for microscopic analysis. Images were acquired using a Leica TCS SP5 confocal laser scanning microscopy (Leica Microsystems, Germany) with 63x oil immersion objective lens.

In vivo study: ocular uptake

C57BL/6J wild type (WT) male mice of 3 months of age were used. Animals were under controlled temperature, humidity and light conditions with ad lib access to food and water. Mice were treated in accordance to ethical guidelines of the European Community Council Directive 86/609/EEC and the procedures established by the Department of Agriculture, Branch and Fisheries of the Generalitat de Catalunya (approved by the ethics committee of the University of Barcelona).

Fluorescent formulations (50 µL) were administered in the right eye and the contralateral eye was used as a control. After 48 h treatment, all the animals were sacrificed. The eyes were enucleated and fixed in 4% paraformaldehyde for 24 h at 4 °C. Then, the samples were embedded in Optimal Cutting Temperature Compound and stored at -40 °C. Horizontal sections of 20 mm were collected using a Leica CM3050s cryostat (Leica Microsystems, Germany). The bright and fluorescent fields of the sections were taken by a fluorescent inverted microscope (Leica DMI4000 B).

Statistical analysis

Multiple comparisons were developed using two-way ANOVA with Tukey post hoc test with a significance of $p < 0.05$ after having confirmed the normality and equality of variances by Bartlett in the groups. All analysed data were presented as mean ± SD. GraphPad Prism® 6.01 software and ImageJ was used to analyze the data and images, respectively.

Results

Synthesis of Rho-PLGA and m-PEG-PLGA

The yield of the synthesis of the polymers Rho-PLGA and m-PEG-PLGA after lyophilization was 85.7-92.1% and 81.4-90.1%, respectively. The H-NMR analysis identified the characteristic peaks of each polymer synthesized. Particularly, in the PLGA RG 503H the peaks are visualized at 5.21 ppm for CH proton of lactide, 4.90 ppm for CH_2 proton of glycolide and 1.47 ppm for CH_3 proton of lactide (Figure S.1a Supplementary Material). In the case of the NHS-PLGA, the same previous peaks are revealed plus a peak at 2.7 ppm corresponding to the CH_2 proton of the NHS (Figure S.1b Supplementary Material). The polymer synthesized m-PEG-PLGA (Figure 1), showed the same peaks as the PLGA RG 503H with the presence of the characteristics of m-PEG (Figure S.1c Supplementary Material) at 7.00 ppm for CH proton of the maleimide and 3.31 ppm for CH_2 of ethylene glycol proton. In addition, the binding of m-PEG and Rho (Figure S.1d Supplementary Material) to the NHS-PLGA polymer is confirmed by the absence of the CH_2 proton NHS peak at 2.70 ppm. The PEGylation efficiency of the NHS-PLGA polymer was between 26.9% to 30.1% (MR between 7.62- 9.02%).

Structural studies of polymers

To investigate the degree of crystallization after the conjugation between the polymers NHS-PLGA and m-PEG, a study was carried out in XRD. In Figure 2a it is possible to show that the polymers PLGA RG 503H, NHS-PLGA and m-PEG-PLGA showed similar diffractograms of amorphous characteristics. In the case of m-PEG, it exhibits 2 peaks indicative of crystallinity at 19.15° and 23.41° (2Θ).
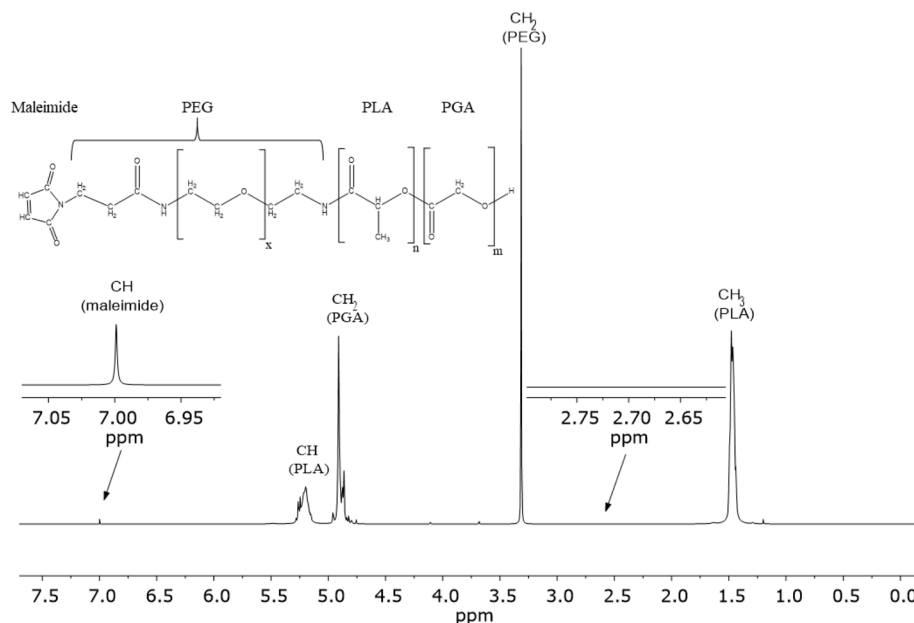
Figure 1. H-NMR spectrum of m-PEG-PLGA.

FTIR spectra of PLGA polymers RG 503H, NHS-PLGA, m-PEG and m-PEG-PLGA are shown in Figure 2b. The m-PEG spectrum exhibits a characteristic peak at 2877 cm^{-1} corresponding to the stretching vibration of CH$_2$. The repeating CH$_2$-CH$_2$-O unit of m-PEG is visualized at 1280 (stretching of C-C-O) and 1099 cm^{-1} (stretching of C-O-C). The bands at 1466 and 1342 cm^{-1} represent CH bending of the m-PEG. Finally, the peak at 1707 cm^{-1} is attributed to the C=O of the maleimide. PLGA RG 503H, NHS-PLGA and m-PEG-PLGA are shown to present similar spectra with characteristic stretching vibration peaks at 2862-3025 (CH$_3$, CH$_2$ and CH), 1749 (C=O), 1162 (C-O) and 1087 cm^{-1} (C-C-O). In addition, the NHS-PLGA has a wide band at 3321 cm^{-1} corresponding to the C-O-N of the NHS. The carbonyl groups (C=O) of the NHS are represented at peaks 1653 and 1560 cm^{-1}.

a)

b)

Figure 2. Structural studies of polymers. a) XRD diffractograms, b) FTIR spectra.
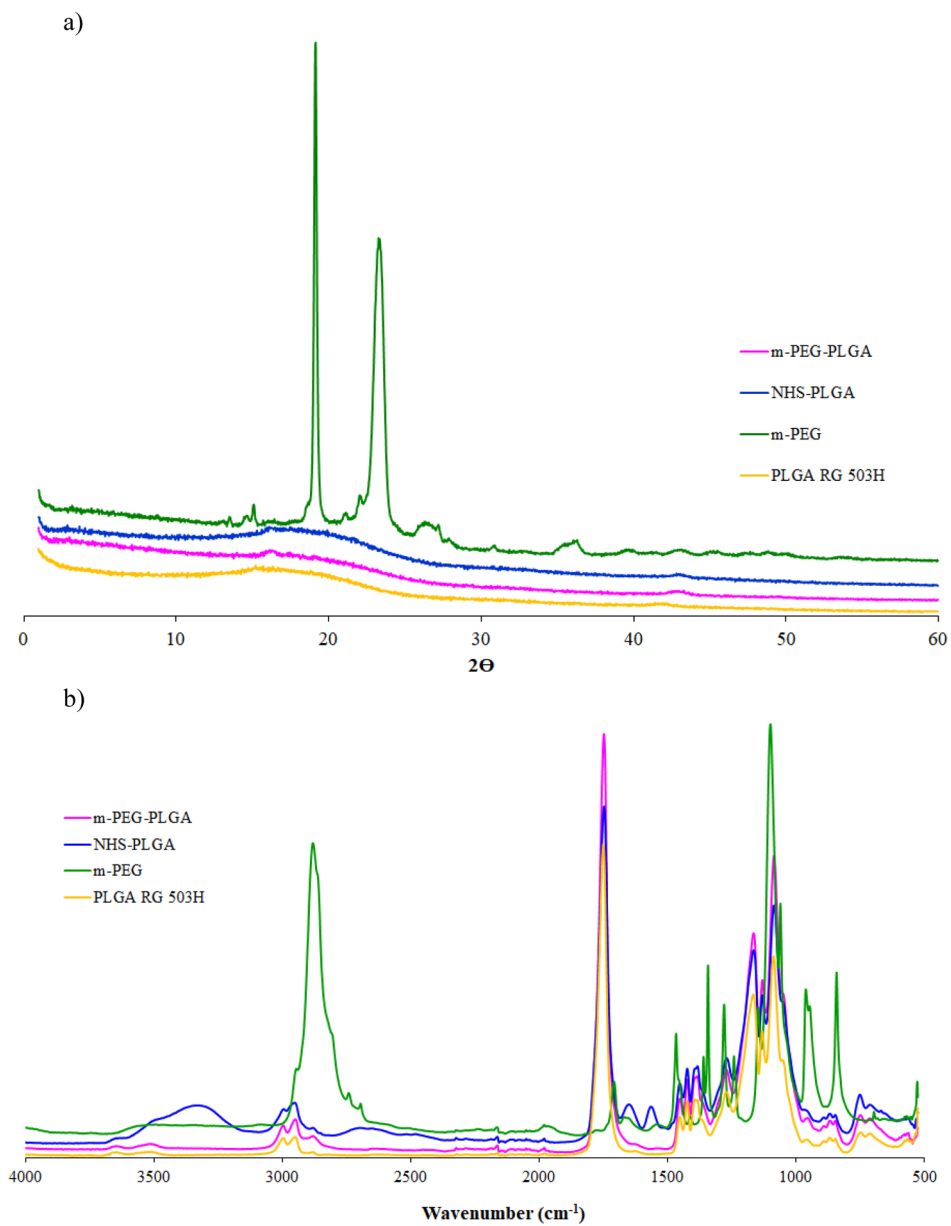
Characterization of FMT-m-PEG-PLGA-NPs

Once the FMT-m-PEG-PLGA-NPs were synthesized and resuspended in PBS, Zav, PI and ZP were 150.3 ± 1.2 nm, 0.112 ± 0.007 and -8.32 ± 0.65 mV, respectively. The ^{Rho}NPs with 20% Rho-PLGA, Zav obtained was 170.9 nm ± 1.3 nm with a PI of 0.139 ± 0.038 and ZP of -13.30 ± 0.49 mV. The EE of both the FMT-m-PEG-PLGA-NPs and ^{Rho}NPs was $99.3 \pm 0.19\%$ and $98.6 \pm 0.17\%$, respectively.

Synthesis of CPPs

Amylated CPPs that possess in their sequence 4 glycine as a spacer and a cysteine in the N-terminus to be linked with the maleimide were synthesized by the solid phase method with an automatic synthesizer. The molecular weight of the CPPs with a purity of 90% were analysed by MALDI-TOF/TOF (Figure S.2 Supplementary Material).

Conjugation of CPPs with FMT-m-PEG-PLGA-NPs

After lyophilizing the NPs conjugated with the CPPs, these were analysed by H-NMR (Figure S.3 Supplementary Material) in order to calculate MR (%) in the polymer. Functionalization was calculated by integrating the aromatic and amide/amine regions of the peptides in contrast to the CH integration of the PLA ($\delta = 5.21$). The TAT$_{49-57}$ were integrated amide/amine regions ($\delta = 7.0\text{-}8.2$ ppm) with 46 protons corresponding to amides, amines and the guanidinium side chains. The pAntp$_{43-58}$ with 64 protons, the regions of the aromatic groups (tryptophan and phenylalanine) and amide/amine were integrated ($\delta = 7.0\text{-}8.2$). Finally, the G2 with 57 protons, the corresponding amide/amine regions were integrated ($\delta = 7.0\text{-}8.2$). According to the previous analysis, the functionalization grades of

TAT$_{49\text{-}57}$, pAntp$_{43\text{-}58}$ and G2 were 2.0%, 4.6% and 0.6%, respectively. The Zav, the PI and

the ZP of the TAT-NPs, pAntp-NPs and G2-NPs are visualized in Table 1.

**Table 1.** Characterization of NPs conjugated with CPPs.

	Zav ± SD (nm)	PI ± SD	ZP ± SD (mV)
TAT-NPs	164.0 ± 0.7	0.077 ± 0.030	-0.29 ± 0.06
pAntp-NPs	167.2 ± 2.6	0.074 ± 0.008	0.15 ± 0.06
G2-NPs	169.7 ± 2.1	0.078 ± 0.180	-1.06 ± 0.27

Cytotoxicity study

Toxicity of NPs on the HCE-2 cell line was evaluated at two different concentrations

using the MTT viability assay. Cell viability was analysed at 24 and 48 h (Figure 3). Results

showed that at 24 h none of the NPs conjugated with CPPs was cytotoxic as cell viability

was kept close to 100% when assayed both at low (5 µg·mL^{-1}) and high (50 µg·mL^{-1})

concentration. At 48 h, cell viability was reduced to about 80-90 % with TAT-NPs and

pAntp-NPs at 5 µg·mL^{-1} and close to 70% at 50 µg·mL^{-1}. In contrast, no toxicity was

observed for G2-NPs. In this case, the increased MTT activity compared to untreated cells

could be attributed to a proliferative effect of this NP. Cytotoxicity of Isoptoflucon$^{®}$ eye

drops (containing FMT as the active drug) was also analysed in parallel at the same

concentrations, and cell viability was of around 82% (at 5 µg·mL^{-1}) and 38% (at 50 µg·mL^{-1}

concentration) at 24 h, and 72% and 28%, respectively, when cells were incubated for 48

h. These results indicate that encapsulation of FMT in NPs reduces drug cytotoxicity.
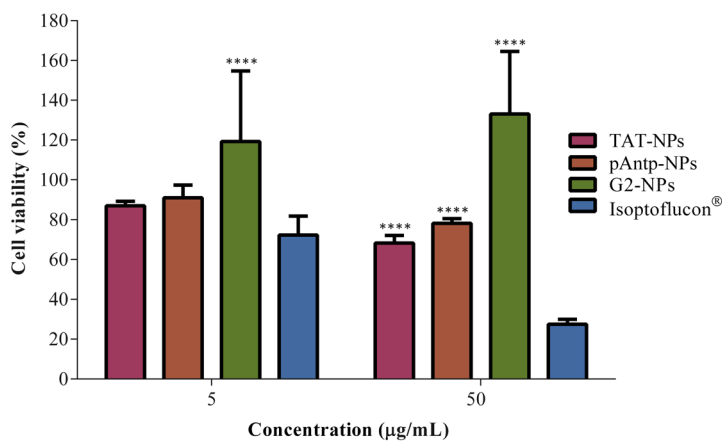
a)
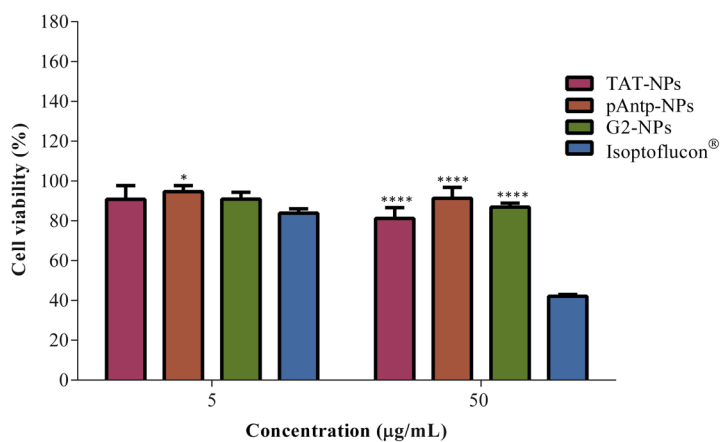
b)

Figure 3. Effect of NPs on viability of HCE-2 cells: a) at 24 h, and b) 48 h. MTT reduction values of untreated control cells were set as 100% cell viability. Data are expressed as mean ± SD; *$p < 0.05$, **$p < 0.01$, ***$p < 0.001$ and ****$p < 0.0001$ significant difference compared to Isoptoflucon® at the same concentration.

Evaluation of the anti-inflammatory activity of NPs

Since LPS induces inflammation via TLR4 receptors, we sought to evaluate the capability of NPs conjugated with CPPs to inhibit the inflammatory response by analysing secreted IL-1β, IL-6 and IL-8 cytokines in LPS-stimulated HTC-2 cells. Results are shown in Figure 4. In the absence of NPs (positive control) LPS induced a significant increase in all cytokines analysed. The TAT-NPs, pAntp-NPs and G2-NPs significantly decreased the expression of IL-1β similarly to Isoptoflucon® ($p< 0.001$) (Figure 4a). Concerning, IL-6, IL-8 and TNFα, secreted levels were reduced by TAT-NPs and G2-NPs, whereas pAntp-NPs only reduced IL-8 although to a lesser extent than the other NPs (Figure 4b-d). In the case of TNFα (Figure 4d), the formulation pAntp-NPs showed a greater cytokine expression than the positive control (LPS-treated cells). Overall, these results indicated that the best anti-inflammatory effect was achieved with G2-NPs. In this case the reduction of LPs-induced cytokine levels was close to that observed for Isoptoflucon®, except for IL-8.

Cellular uptake of [Rho]NPs

Cellular uptake of [Rho]NPs (50 μg·mL[1]) was analysed in the HCE-2 cell line. After 24 h incubation, the NP-associated green fluorescence was visualized by confocal fluorescence microscopy in all cells challenged with NPs but not in the untreated control cells. The nucleus was visualized with DAPI. In the merged images the [Rho]NPs were visualized in the cytoplasm. The formulations [Rho]TAT-NPs and [Rho]G2-NPs yielded the stronger fluorescence signal. The analysis with Interactive 3D Surface Plot of ImageJ confirmed this fact and allowed to discern that cells treated with [Rho]TAT-NPs displayed higher intensity than cells incubated with the [Rho]G2-NPs formulation. Intensity of fluorescence emitted by the other

internalized formulations (^{Rho}pAntp-NPs and ^{Rho}FMT-m-PEG-PLGA-NPs) was lower, without apparent accumulation within of HCE-2 cells.
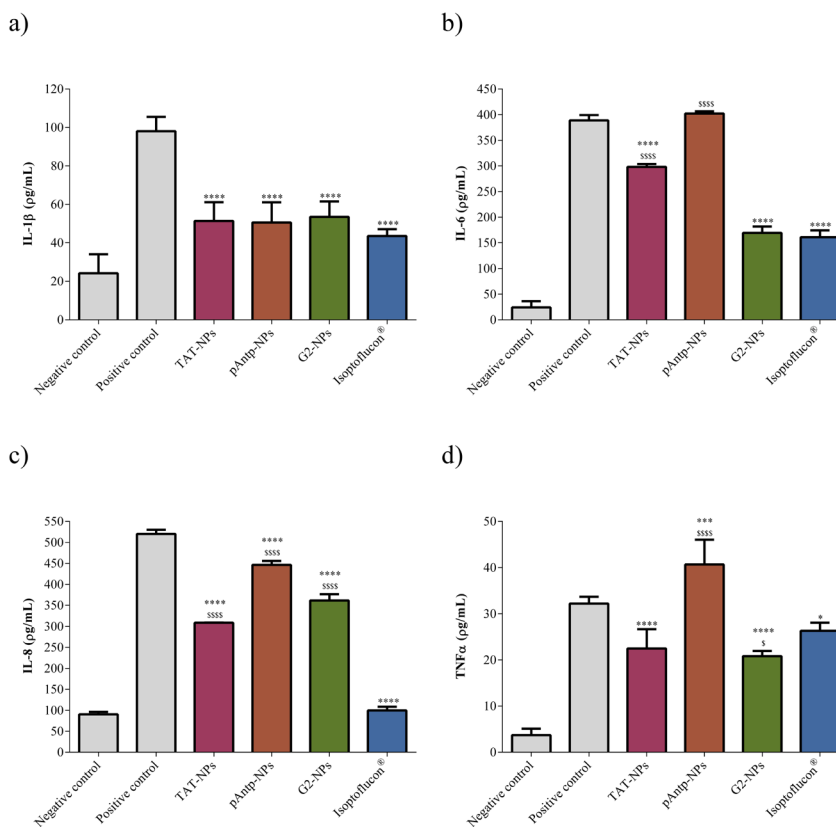
a)

b)

c)

d)

Figure 4. Quantification of secreted proinflammatory cytokines in LPS-stimulated HCE-2 cells incubated in the absence and presence of the indicated NPs (50 µg·mL^{-1}) for 24 h. a) IL-1β, b) IL-6, c) IL-8, d) TNFα. Negative control: untreated control cells. Values are expressed as mean ± SD; *$p<$ 0.05, **$p<$ 0.01, ***$p<$ 0.001 and ****$p<$ 0.0001 significantly different compared to positive control (LPS-stimulated cells). $^{\$}p<$ 0.05, $^{\$\$}p<$ 0.01, $^{\$\$\$}p<$ 0.001 and $^{\$\$\$\$}p<$ 0.0001 significantly different compared to Isoptoflucon$^{®}$.
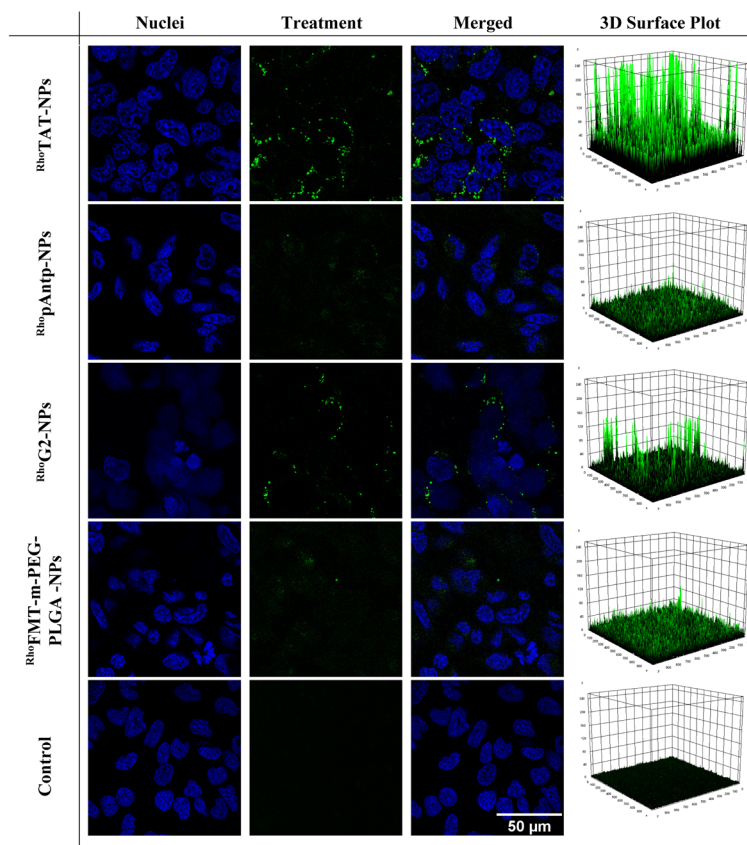
Figure 5. Cellular uptake of NPs conjugated with CPPs. HCE-2 cells were incubated with the indicated fluorescent-labelled NPs (50 μg·mL^{-1}) for 24 h and analysed using laser scanning confocal spectral microscope. Images are representative of three independent biological experiments. Quantification of the green signal corresponding to internalized NPs is shown by 3D surface plots.

Ocular uptake of ^{Rho}NPs

After ocular treatment of C57BL/6J WT mice for 48 h with ^{Rho}TAT-NPs, ^{Rho}G2-NPs, ^{Rho}pAntp-NPs and ^{Rho}FMT-m-PEG-PLGA-NPs, the sectioned eyes were analysed by fluorescence microscopy (Figure 6). Again, greater fluorescence was observed in both the

91

anterior and posterior segment in samples treated with the formulations [Rho]TAT-NPs and [Rho]G2-NPs. The formulations [Rho]pAntp-NP and [Rho]FMT-m-PEG-PLGA-NPs were distributed in greater proportion in the posterior than in the anterior segment.
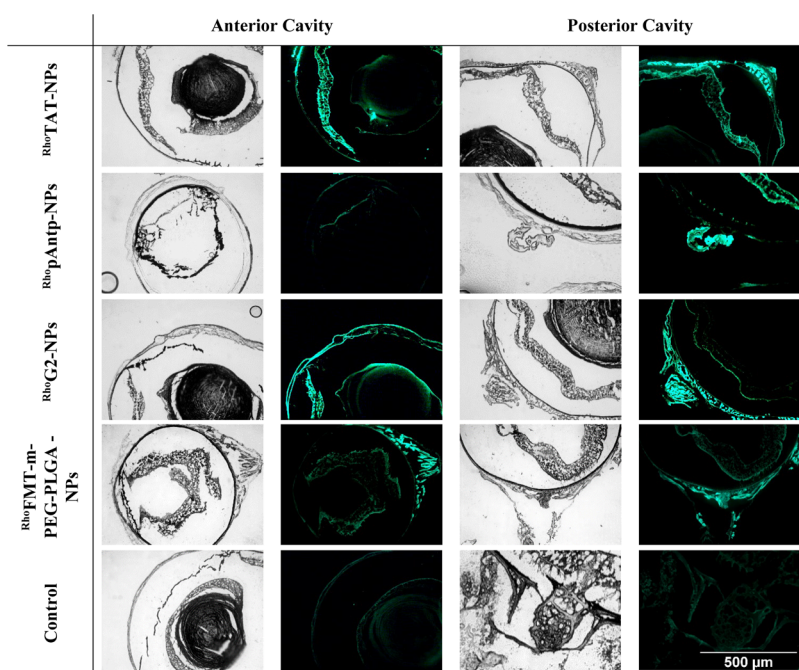

Figure 6. Ocular uptake of NPs conjugated with CPPs. C57BL/6J WT male mice were treated with the indicated fluorescent-labelled NPs ($50 \ \mu g \cdot mL^{-1}$) for 48 h and analysed using fluorescent inverted microscope.

Discussion

In the present study, the polymers Rho-PLGA and m-PEG-PLGA were successfully synthesized with high performance using the carbodiimide pathway as a conjugation strategy [27,28]. The conjugation of both Rho and m-PEG to NHS-PLGA was confirmed by the removal of the CH_2 group from the NHS in the H-NMR spectrum (Figure 1 and

Figure S.1d Supplementary Material). Furthermore, the m-PEG moiety was identified in the PLGA due to the appearance of ethylene glycol and maleimide peaks (Figure 1), with a pegylation degree close to 30% (MR~ 9% m/m) [29,30]. The XRD and FTIR profiles confirmed the information obtained by H-NMR regarding the synthesis of the m-PEG-PLGA polymer. The diffractogram of the m-PEG-PLGA (Figure 2a) showed a profile of amorphous characteristics without the presence of crystalline peaks of PEG, agreeing with other authors that the presence of less than 10% (m/m) of PEG in the polymer its peaks are not visualized in the XRD or in the FTIR spectrum [31–33]. Despite this fact, the structural change of the NHS-PLGA to the m-PEG-PLGA was evidenced in the FTIR and H-NMR analysis by the elimination of C=O and C-O-N peaks of the NHS, confirming the union m-PEG to the polymer (Figure 2b). The developed FMT-m-PEG-PLGA-NPs displayed a Zav less than 150 nm with a monodisperse population distribution, a negative surface charge and EE close to 99% (0.5 mg·mL^{-1}). It has been described that particles with sizes greater than 10 μm could cause ocular irritation. Hence, the NPs elaborated in this study would circumvent such an effect. Moreover, the agglomeration and/or precipitation of NPs would be avoided with their negative ZP [34,35].

The CPPs TAT$_{49-57}$, pAntp$_{43-58}$ and G2 characterized by MALDI-TOF/TOF presented an *m/z* value of 1613.296, 2520.192, 1983.102, respectively (Figure S.2 Supplementary Material). These CPPs, properly purified and characterized, were conjugated with the FMT-m-PEG-PLGA-NPs. The monodisperses system was maintained in the final NPs and the Zav increased by an average of 17 nm more. Furthermore, the conjugation of the CPPs to the NPs was evidenced both by the change of the Zav and by the change of the ZP to a less

negative value by the cationic characteristics of the CPPs (Table 1) [24]. Through H-NMR analysis, it was possible to calculate the MR of the functionalized CPPs in the NPs. The pAntp$_{43-58}$ (MR = 4.6%) was the CPP that was conjugated to a greater degree in mass followed by TAT$_{49-57}$ (MR = 2.0%) and G2 (MR = 0.6%). These data indicate that the maleimide-cysteine conjugation pathway is a thermodynamically favourable reaction that allows the conjugation of small amounts of peptides to polymeric NPs [36–38].

Functionalized NPs with CPPs did not show cytotoxicity at both low and high concentration (5 and 50 µg·mL^{-1}) at 24 h (Figure 3). At the same incubation time, the commercial drug tested at the low concentration reduced cell viability close to 84%, a value that was significantly different ($p < 0.05$) to the formulation pAntp-NPs. At a higher concentration, Isoptoflucon® increased its cytotoxicity. This may be due to the composition of the commercial drug, which contains excipients such as benzalkonium chloride and polysorbate 80 that decrease cell viability [39–41]. After 48 h treatment, cells incubated with 5 µg·mL^{-1} of the formulations TAT-NPs, pAntp-NPs and Isoptoflucon® displayed viability rates close to 80%. At 50 µg·mL^{-1} the cytotoxicity of the commercial drug (Figure 3b) was more evident than that of the formulations TAT-NPs, pAntp-NPs and G2-NPs ($p < 0.0001$). The G2-NPs formulation had no cytotoxic effects as cell viability was kept around 100% at both low and high concentrations. At 48 h viability values were even higher that 100%, which can particularly be due to the non-conjugated sites of the maleimide with G2. The low percentage of MR of G2 in the polymer m-PEG-PLGA in comparison to the other CPPs indicate that the accessible sites of unreacted maleimide may cause an increase in the cellular metabolism and therefore a greater MTT response [42]. Figure S. Supplementary

Material shows that the formulation without conjugated CPP (FMT-m-PEG-PLGA-NPs) with all the sites of unconjugated maleimide had greater MTT values than G2 ($p < 0.01$) and the other formulations ($p < 0.0001$) when assayed in HCE-2 cells at a concentration of 50 µg·mL^{-1} for 48 h.

Functionalized NPs (TAT-NPs, pAntp-NPs and G2-NPs) and the commercial drug (Isoptoflucon®) showed anti-inflammatory similar effect ($p > 0.05$) in the reduction of IL-1β production in cells stimulated with LPS (Figure 4a) ($p < 0.0001$). However, concerning IL-6 (Figure 4b), only G2-NPs triggered comparable effects to the commercial drug ($p < 0.0001$), whereas pAntp-NPs were unable to diminish the high IL-6 expression induced by LPs. All the conjugated NPs significantly decreased the expression of IL-8 (Figure 3c), but none of them managed to reduce it as did Isoptoflucon®. Remarkably, the G2-NPs formulation showed a higher effect in the reduction of TNFα expression than the commercial drug ($p < 0.05$) while TAT-NPs reduced TNFα levels to the same proportion as Isoptoflucon® ($p > 0.05$) (Figure 3d). In contrast, pAntp-NPs promoted greater TNFα secretion than positive control (LPS-stimulated cells). This effect could probably be related with the mechanism used for cellular internalization of pAntp$_{43-58}$. Particularly, the most accepted cellular internalization mechanism for the pAntp$_{43-58}$ is translocation, which would generate excessive destabilization of the cell membrane in HCE-2 cells, activating the inflammatory cascade that lead to increased secretion of certain cytokines. The most prominent effect was evidenced for TNFα [43].

Overall, this study shows that G2-NPs is the formulation that has a greater effect in the reduction of the proinflammatory cytokines tested, followed by TAT-NPs. The G2

peptide, although not described as a canonical CPP, has been characterized as an antiviral peptide and contain the conserved features of a CPP, such as a 5-30 amino acid sequence rich in Arg residues and positively charged (cationic) [21,44]. This study provides evidence that the G2 peptide increases the anti-inflammatory effect of FMT by creating membrane pores that allow the internalization of drug containing NPs in HCE-2 cells. In fact, *in vitro/in vivo* uptake studies confirmed that ^{Rho}TAT-NPs and ^{Rho}G2-NPs were the formulations that displayed higher internalization scores. *In vitro* studies in HCE-2 cells revealed that the highest density of internalized NPs, represented by the intensity of emitted fluorescence, was achieved with ^{Rho}TAT-NPs (Figure 5). The other formulations were internalized but with a lower extent, without fluorescence accumulation as in the case of ^{Rho}TAT-NPs and ^{Rho}G2-NPs. At the *in vivo* level (Figure 6), fluorescence intensity of ^{Rho}G2-NPs increased with respect to the *in vitro* study. This effect could be mainly due to unreacted maleimide (without G2) which can be conjugated with the sulfhydryl groups of mucin present in the lacrimal film [45]. This would increase the residence time in the cornea, helping internalization of the NPs in the ocular internal tissues. Analysis of the non-functionalized NPs (^{Rho}FMT-m-PEG-PLGA-NPs) also reflects an increase in the internalized NPs signal, that could also be attributed to their interaction with mucin. Finally, a certain number of pAntp-NPs manages to reach the posterior segment of the eye (optic nerve) without being retained at the cornea level.

Conclusion

NPs functionalized with the peptides TAT_{49-57}, $pAntp_{43-58}$ and G2 had physicochemical characteristics suitable for ocular topical administration. TAT-NPs and

G2-NPs were shown to be the most effective both *in vitro* and *in vivo* studies, mainly reducing proinflammatory cytokines. This work demonstrated that in the CPP conjugated NPs, free unconjugated maleimide interacts with the mucin present in the tear film, increasing the residence time of the nanostructured system. According to the above reasons, TAT-NPs and G2-NPs could constitute a new non-invasive system for ocular treatment of conditions affecting both the anterior and posterior tissues.

Conflict of interest

No conflicting relationship exists for any author.

Acknowledgments

References

1. Harthan J, Fromstein S, Morettin C, Opitz D. Diagnosis and treatment of anterior uveitis: optometric management. *Clin. Optom.* 8, 23–35 (2016).

2. Samudre SS, Lattanzio FA, Williams PB, Sheppard JD. Comparison of topical steroids for acute anterior uveitis. *J. Ocul. Pharmacol. Ther.* 20(6), 533–547 (2004).

3. Ali J, Fazil M, Qumbar M, Khan N, Ali A, Ali A. Colloidal drug delivery system: amplify the ocular delivery. *Drug Deliv.* 23(3), 700–716 (2016).

4. Yasin MN, Svirskis D, Seyfoddin A, Rupenthal ID. Implants for drug delivery to the posterior segment of the eye: a focus on stimuli-responsive and tunable release systems. *J. Control. Release*. 196, 208–221 (2014).

5. Kim Y-H, Jung J-C, Jung S-Y, Yu S, Lee KW, Park YJ. Comparison of the efficacy of fluorometholone with and without benzalkonium chloride in ocular surface disease. *Cornea*. 35(2), 234–242 (2016).

6. Jee D, Park SH, Kim MS, Kim EC. Antioxidant and inflammatory cytokine in tears of patients with dry eye syndrome treated with preservative-free versus preserved eye drops. *Investig. Opthalmolog. Vis. Sci.* 55(8), 5081–5089 (2014).

7. Bielory BP, Perez VL, Bielory L. Treatment of seasonal allergic conjunctivitis with ophthalmic corticosteroids: in search of the perfect ocular corticosteroids in the treatment of allergic conjunctivitis. *Curr. Opin. Allergy Clin. Immunol.* 10(5), 469–477 (2010).

8. Shokoohi-Rad S, Daneshvar R, Jafarian-Shahri M, Rajaee P. Comparison between betamethasone, fluorometholone and loteprednol etabonate on intraocular pressure in patients after keratorefractive surgery. *J. Curr. Ophthalmol.* 30(2), 130–135 (2018).

9. Pinto-Fraga J, López-Miguel A, González-García MJ, *et al.* Topical fluorometholone protects the ocular surface of dry eye patients from desiccating stress: a randomized controlled clinical trial. *Ophthalmology*. 123(1), 141–153 (2016).

10. Silva-Abreu M, Calpena AC, Espina M, *et al.* Optimization, biopharmaceutical profile and therapeutic efficacy of pioglitazone-loaded PLGA-PEG nanospheres as a novel strategy for ocular inflammatory disorders. *Pharm. Res.* 35(1), 11 (2018).

11. Mandal A, Bisht R, Rupenthal ID, Mitra AK. Polymeric micelles for ocular drug delivery: from structural frameworks to recent preclinical studies. *J. Control. Release*. 248, 96–116

(2017).

12. Kalam MA. The potential application of hyaluronic acid coated chitosan nanoparticles in ocular delivery of dexamethasone. *Int. J. Biol. Macromol.* 89, 559–568 (2016).

13. Reimondez-Troitiño S, Csaba N, Alonso MJ, de la Fuente M. Nanotherapies for the treatment of ocular diseases. *Eur. J. Pharm. Biopharm.* 95, 279–293 (2015).

14. Gonzalez-Pizarro R, Carvajal-Vidal P, Halbault Bellowa L, Calpena AC, Espina M, García ML. *In-situ* forming gels containing fluorometholone-loaded polymeric nanoparticles for ocular inflammatory conditions. *Colloids Surfaces B Biointerfaces*. 175, 365–374 (2019).

15. Guengerich FP. Intersection of the roles of cytochrome P450 enzymes with xenobiotic and endogenous substrates: relevance to toxicity and drug interactions. *Chem. Res. Toxicol.* 30(1), 2–12 (2017).

16. Aukunuru J V, Sunkara G, Bandi N, Thoreson WB, Kompella UB. Expression of multidrug resistance-associated protein (MRP) in human retinal pigment epithelial cells and its interaction with BAPSG, a novel aldose reductase inhibitor. *Pharm. Res.* 18(5), 565–572 (2001).

17. Melikov K, Chernomordik L V. Arginine-rich cell penetrating peptides: from endosomal uptake to nuclear delivery. *Cell. Mol. Life Sci.* 62(23), 2739–2749 (2005).

18. Pescina S, Ostacolo C, Gomez-Monterrey IM, *et al.* Cell penetrating peptides in ocular drug delivery: state of the art. *J. Control. Release*. 284, 84–102 (2018).

19. Guidotti G, Brambilla L, Rossi D. Cell-penetrating peptides: from basic research to clinics. *Trends Pharmacol. Sci.* 38(4), 406–424 (2017).

20. Bahnsen JS, Franzyk H, Sandberg-Schaal A, Nielsen HM. Antimicrobial and cell-

penetrating properties of penetratin analogs: effect of sequence and secondary structure. *Biochim. Biophys. Acta - Biomembr.* 1828(2), 223–232 (2013).

21. Delcroix M, Riley LW, Delcroix M, Riley LW. Cell-penetrating peptides for antiviral drug development. *Pharmaceuticals*. 3(3), 448–470 (2010).

22. Tiwari V, Liu J, Valyi-Nagy T, Shukla D. Anti-heparan sulfate peptides that block herpes simplex virus infection *in vivo. J. Biol. Chem.* 286(28), 25406–25415 (2011).

23. Ali MM, Karasneh GA, Jarding MJ, Tiwari V, Shukla D. A 3-O-sulfated heparan sulfate binding peptide preferentially targets herpes simplex virus 2-infected cells. *J. Virol.* 86(12), 6434–6443 (2012).

24. Vasconcelos A, Vega E, Pérez Y, Gómara MJ, García ML, Haro I. Conjugation of cell-penetrating peptides with poly(lactic-co-glycolic acid)-polyethylene glycol nanoparticles improves ocular drug delivery. *Int. J. Nanomedicine*. 10, 609–631 (2015).

25. Lin WJ, Liu WJ. Polymeric nanoparticles conjugate a novel heptapeptide as an epidermal growth factor receptor-active targeting ligand for doxorubicin. *Int. J. Nanomedicine*. 7, 4749 (2012).

26. Gonzalez-Pizarro R, Silva-Abreu M, Calpena AC, Egea MA, Espina M, García ML. Development of fluorometholone-loaded PLGA nanoparticles for treatment of inflammatory disorders of anterior and posterior segments of the eye. *Int. J. Pharm.* 547(1–2), 338–346 (2018).

27. Valeur E, Bradley M. Amide bond formation: beyond the myth of coupling reagents. *Chem. Soc. Rev.* 38(2), 606–631 (2009).

28. Hermanson G. The chemistry of reactive groups. In: *Bioconjugate Techniques (Second Edition)*. Hermanson G (Ed.), Academic Press, London, 169–212 (2008).

29. Li Y-P, Pei Y-Y, Zhang X-Y, *et al.* PEGylated PLGA nanoparticles as protein carriers: synthesis, preparation and biodistribution in rats. *J. Control. Release*. 71(2), 203–211 (2001).

30. Zhang Q, Zhu J, Song L, *et al.* Engineering magnetic-molecular sequential targeting nanoparticles for anti-cancer therapy. *J. Mater. Chem. B*. 1(46), 6402–6410 (2013).

31. Pereira ED, Cerruti R, Fernandes E, *et al.* Influence of PLGA and PLGA-PEG on the dissolution profile of oxaliplatin. *Polímeros*. 26(2), 137–143 (2016).

32. Sánchez-López E, Ettcheto M, Egea MA, *et al.* Memantine loaded PLGA PEGylated nanoparticles for Alzheimer's disease: *in vitro* and *in vivo* characterization. *J. Nanobiotechnology*. 16(1), 32 (2018).

33. Cano A, Ettcheto M, Espina M, *et al.* Epigallocatechin-3-gallate loaded PEGylated-PLGA nanoparticles: a new anti-seizure strategy for temporal lobe epilepsy. *Nanomedicine Nanotechnology, Biol. Med.* 14(4), 1073–1085 (2018).

34. Ali Y, Lehmussaari K. Industrial perspective in ocular drug delivery. *Adv. Drug Deliv. Rev.* 58(11), 1258–1268 (2006).

35. Stolnik S, Garnett M, Davies M, *et al.* The colloidal properties of surfactant-free biodegradable nanospheres from poly(β-malic acid-co-benzyl malate)s and poly(lactic acid-co-glycolide). *Colloids Surfaces A Physicochem. Eng. Asp.* 97(3), 235–245 (1995).

36. Ravi S, Krishnamurthy VR, Caves JM, Haller CA, Chaikof EL. Maleimide-thiol coupling of a bioactive peptide to an elastin-like protein polymer. *Acta Biomater.* 8(2), 627–35 (2012).

37. Northrop BH, Frayne SH, Choudhary U. Thiol–maleimide "click" chemistry: evaluating the influence of solvent, initiator, and thiol on the reaction mechanism, kinetics, and

selectivity. *Polym. Chem.* 6(18), 3415–3430 (2015).

38. Sazano G, Torchilin W. Intracellular delivery of nanoparticles with cell penetrating peptides. In: *Cell-penetrating peptides: methods and protocols*. Langel Ü (Ed.), Humana Press, Totowa, NJ, 357–386 (2015).

39. Czajkowska-Kośnik A, Wolska E, Chorążewicz J, Sznitowska M. Comparison of cytotoxicity *in vitro* and irritation *in vivo* for aqueous and oily solutions of surfactants. *Drug Dev. Ind. Pharm.* 41(8), 1232–1236 (2015).

40. Liu Z, Li J, Nie S, Liu H, Ding P, Pan W. Study of an alginate/HPMC-based *in situ* gelling ophthalmic delivery system for gatifloxacin. *Int. J. Pharm.* 315(1), 12–17 (2006).

41. Khoh-Reiter S, Jessen BA. Evaluation of the cytotoxic effects of ophthalmic solutions containing benzalkonium chloride on corneal epithelium using an organotypic 3-D model. *BMC Ophthalmol.* 9, 5 (2009).

42. Ali B, Kanda Kupa LD, Heluany CS, *et al.* Cytotoxic effects of a novel maleimide derivative on epithelial and tumor cells. *Bioorg. Chem.* 72, 199–207 (2017).

43. Drin G, Déméné H, Temsamani J, Brasseur R. Translocation of the pAntp peptide and its amphipathic analogue AP-2AL. *Biochemistry*. 40, 1824–1834 (2001).

44. Splith K, Neundorf I. Antimicrobial peptides with cell-penetrating peptide properties and vice versa. *Eur. Biophys. J.* 40(4), 387–397 (2011).

45. Tonglairoum P, Brannigan RP, Opanasopit P, Khutoryanskiy V V. Maleimide-bearing nanogels as novel mucoadhesive materials for drug delivery. *J. Mater. Chem. B*. 4(40), 6581–6587 (2016).

Supplementary Material

a)

b)

c)

d)
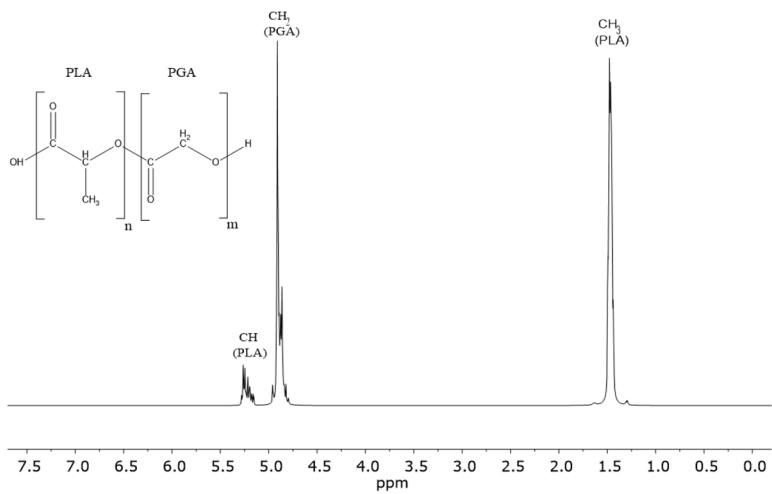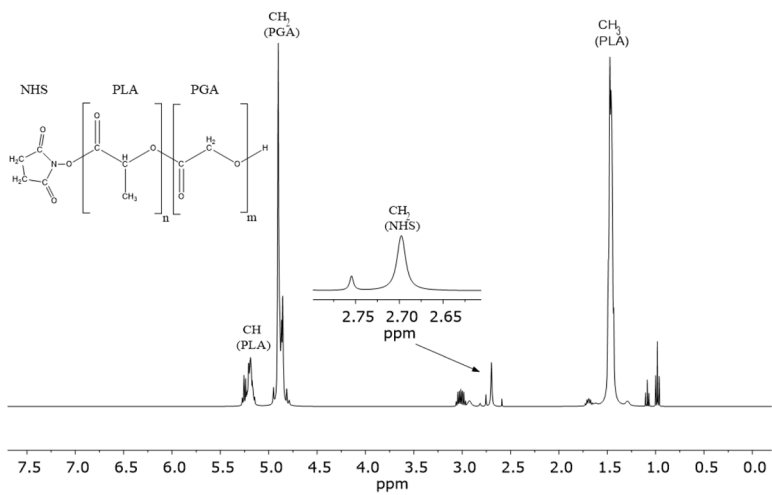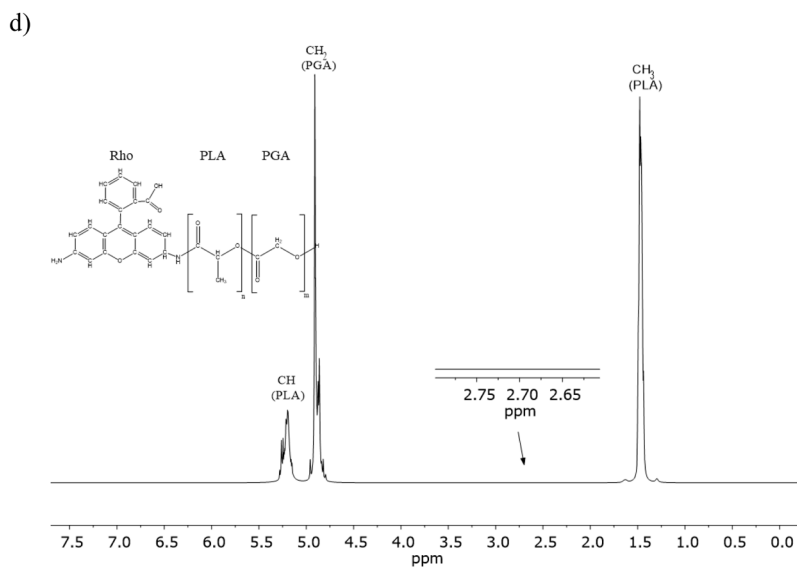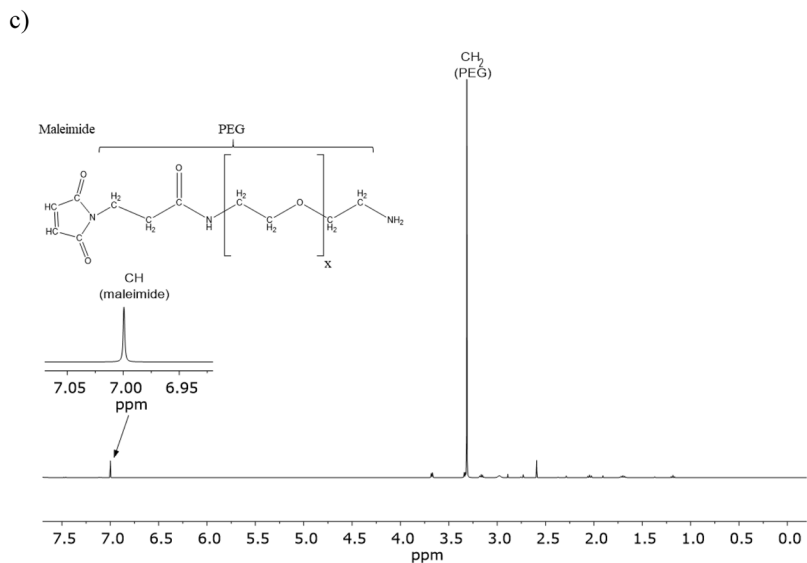
Fig. S.1. H-NMR spectra of polymers synthesized. a) PLGA RG 503H, b) NHS-PLGA
c) m-PEG and d) Rho-PLGA.

a)

b)
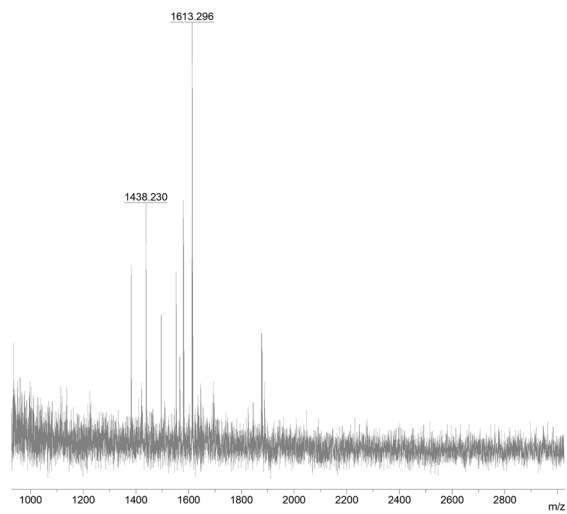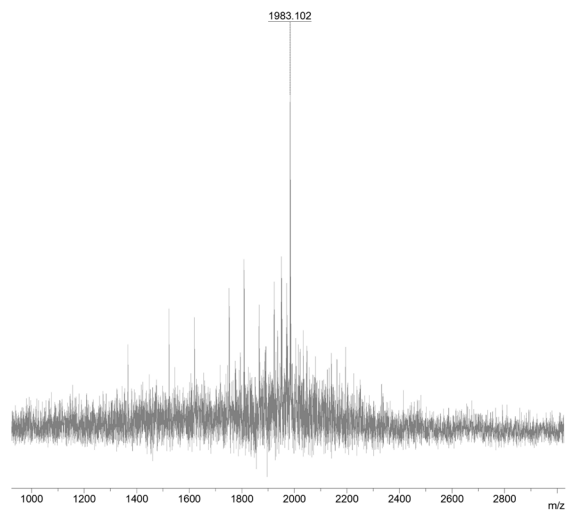
c)
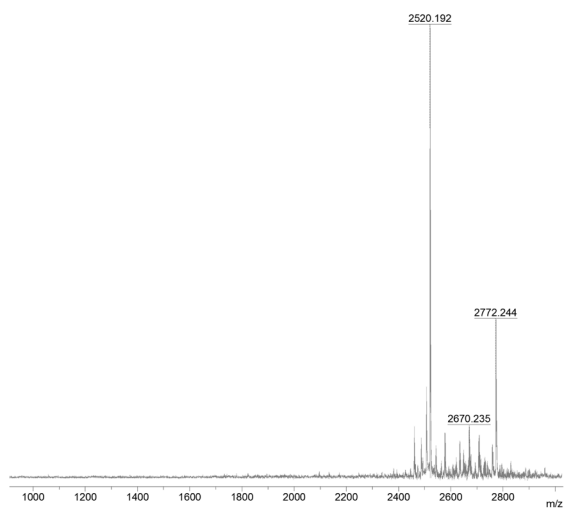
Fig. S.2. MALDI-TOF/TOF spectra. a) TAT$_{49-57}$ (*m/z* 1613.296), b) G2 (*m/z* 1983.102), c) pAntp$_{43-58}$ (*m/z* 2520.192).

a)

b)

c)
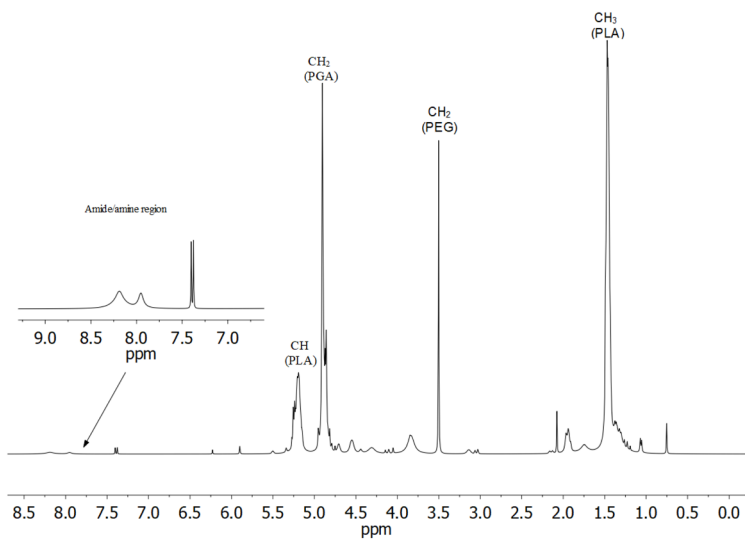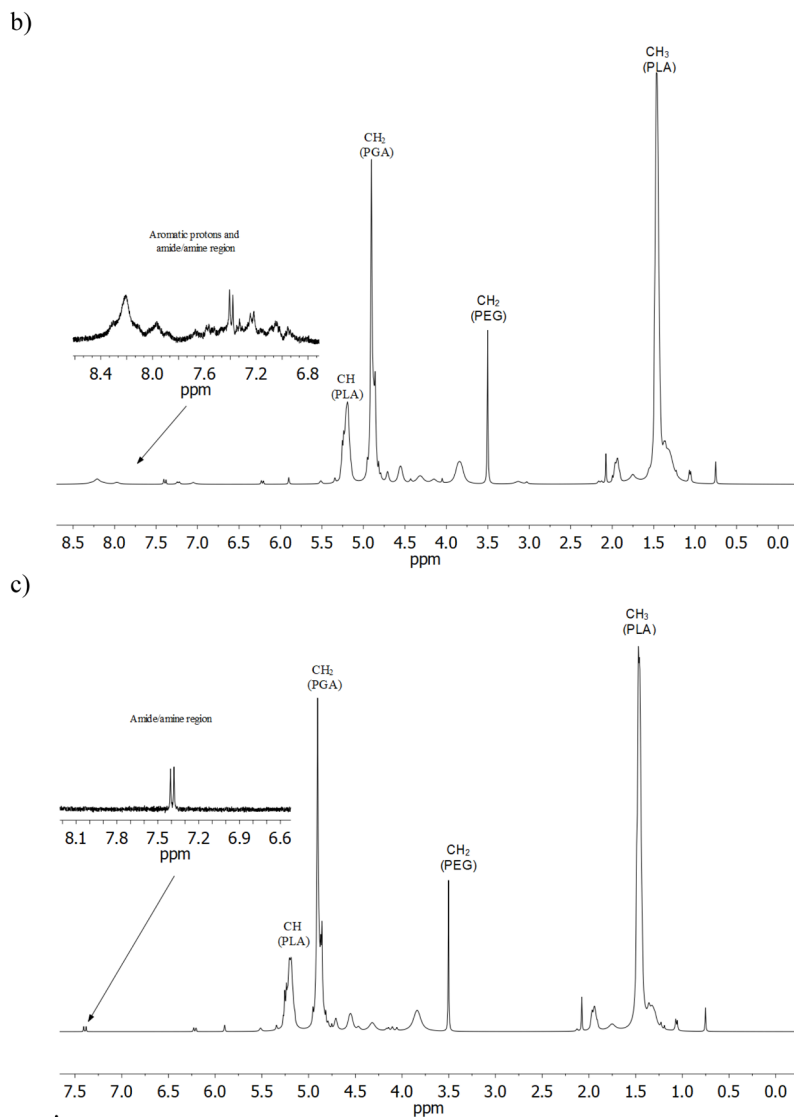
Fig. S.3. H-NMR spectra of the conjugation of CPPs with m-PEG-PLGA NPs. a) TAT-NPs, b) pAntp-NPs, c) G2-NPs.
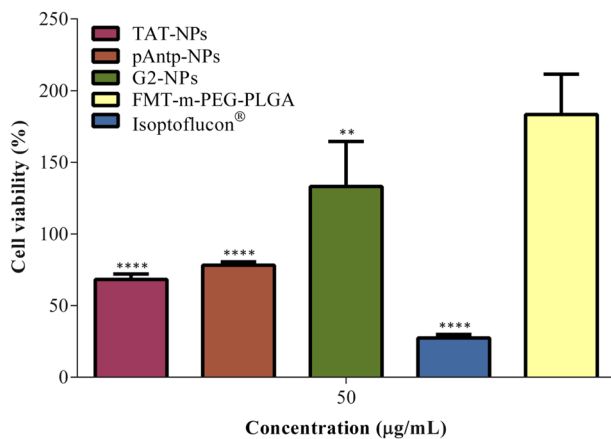
Fig. S.4. Effect of maleimide on cytotoxicity in the HCE-2. Values are expressed as mean ± SD; $*p < 0.05$, $**p < 0.01$, $***p < 0.001$ and $****p < 0.0001$ significantly difference compared to FMT-m-PEG-PLGA at the same concentration.

4. DISCUSIÓN

El objetivo del presente estudio fue el diseño de sistemas nanoestructurados con la capacidad de alcanzar estructuras tanto del segmento anterior como posterior del ojo para su aplicación en enfermedades inflamatorias oculares. Para ello se desarrollaron tres sistemas diferentes que contienen FMT: NPs de PLGA (FMT-PLGA-NPs), geles de formación *in-situ* con FMT-PLGA-NPs y NPs de maleímido-PEG-PLGA conjugadas con CPPs (TAT-NPs, pAntp-NPs y G2-NPs). A las formulaciones diseñadas se les evaluaron sus características fisicoquímicas, su tolerancia ocular *in vitro* y/o *in vivo,* su internalización ocular y su eficacia contra la inflamación ocular.

Las NPs se elaboraron a través de la técnica de desplazamiento de solvente, la cual está dirigida a fármacos hidrófobos tales como la FMT. Este fármaco se considera prácticamente insoluble en agua ($30 \text{ mg} \cdot \text{L}^{-1}$) por lo que esta técnica es ideal para su encapsulación en polímeros biodegradables como el PLGA y el maleímido-PEG-PLGA (Kapoor *et al.* 2015). Por otra parte, los geles de formación *in-situ* se realizaron con la técnica de dispersión/reposo utilizando el equipo Unguator® para la incorporación de las FMT-PLGA-NPs.

DISCUSIÓN

4.1. FMT-PLGA-NPs y geles de formación *in-situ*

En primer lugar se desarrollaron y optimizaron las FMT-PLGA-NPs a través del diseño de experimentos (DoE), en el que se estudiaron los factores que afectan la síntesis de las NPs. Estos factores fueron las concentraciones de FMT, de PLGA y de poloxámero 188 (P188). De lo anterior, se evidenció que la concentración de FMT y la de PLGA afectan proporcionalmente al tamaño promedio (Zav) y la eficiencia de encapsulación (EE) de las NPs, respectivamente. Lo contrario sucede con el P188, que afecta inversamente a la respuesta de Zav. A través del estudio DoE, se seleccionó una formulación con las mejores características fisicoquímicas, formulada con una concentración de 7,0 mg·mL^{-1} de PLGA, 15,0 mg·mL^{-1} de P188 y 1,5 mg·mL^{-1} de FMT. Las NPs obtuvieron un Zav de 149,1 nm, una polidispersión (PI) de 0,079, un potencial zeta (ZP) de -34,3 mV y una EE de 99,8%. Estas características hacen que las FMT-PLGA-NPs sean un sistema adecuado para la administración ocular, debido a que la población de NPs es monodispersa y menor de 10 µm, y un ZP alto y negativo, lo cual evitaría la irritación ocular por tamaño de partículas o por la precipitación de ellas (Stolnik *et al.* 1995; Ali and Lehmussaari 2006). Paralelamente, se confirmó a través de microscopia electrónica de trasmisión (TEM) que las NPs son esféricas sin evidencia de agregación y con un tamaño similar a lo observado por la técnica de dispersión dinámica de la luz (DLS).

Los estudios de interacción entre los componentes de las NPs optimizadas (FMT-PLGA-NPs) fueron llevado a cabo con las técnicas de difracción de rayos X (XRD), espectroscopia de infrarrojo con transformada

de Fourier (FTIR) y calorimetría diferencial de barrido (DSC). El estudio por XRD evidenció el estado semicristalino y cristalino del P188 y la FMT, respectivamente. El difractograma de las NPs permitió identificar que el fármaco estaba en un estado de dispersión molecular en la matriz polimérica (Panyam *et al.* 2004). Por otro lado, los espectros FTIR mostraron que no existen nuevos enlaces covalentes entre los componentes de las NPs que podrían desactivar la actividad farmacológica de la FMT (Sánchez-López *et al.* 2016). Finalmente, los termogramas de DSC demostraron que existe una interacción fármaco-polímero en las NPs, efecto atribuido a la encapsulación de un fármaco insoluble en agua en una matriz polimérica, provocando una disminución de la temperatura de transición vítrea del componente mayoritario del sistema, el PLGA (Abrego *et al.* 2014; Sánchez-López *et al.* 2017).

Los estudios biofarmacéuticos demostraron que el fármaco contenido en las NPs es liberado de manera más sostenida que el fármaco libre y que el fármaco comercial (Isoptoflucon®). Lo anterior se debe a la cinética tipo hipérbola de las NPs, donde, a las primeras horas existe una liberación rápida del fármaco unido lábilmente a la matriz polimérica (efecto de estallido), seguida de una liberación sostenida y creciente de la FMT (Anderson and Shive 2012; Allahyari and Mohit 2016). A través de los estudios de permeación *ex vivo* en córnea y esclera, se evidenció que las FMT-PLGA-NPs presentan mayor afinidad en atravesar la córnea que la esclera ($p < 0,001$), concordando con los resultados obtenidos por otros autores, en que las moléculas o sistemas hidrofóbicos como las NPs de PLGA permean más la córnea que la esclera (Lakhani, Patil and Majumdar

2018). A su vez, la FMT contenida en las NPs poseen una capacidad dos veces mayor en atravesar la córnea que el Isoptoflucon®.

A través de la utilización de la técnica de dispersión múltiple de la luz estática (S-MLS), se evidenciaron los fenómenos de inestabilización de las NPs, tales como la precipitación o floculación, que son imperceptibles al ojo humano. A partir de la señal de radiación retrodispersada por la muestra, se evidenció que las NPs son consideradas estables tanto a una temperatura de almacenamiento de 25 °C como a 4 °C, debido a que no hay una diferencia entre mediciones superior a un 20%. Sin embargo, se observó un inicio de inestabilidad en la formulación almacenada a 25 °C, debido al incremento de la solubilidad del P188 inducido por la temperatura. Lo anterior conllevaría que el P188 adherido a la superficie de las NPs se libere, causando una disminución en el ZP e iniciando los fenómenos de precipitación y/o floculación por formación de agregados (Storm *et al.* 1995; Fredenberg *et al.* 2011; Patel and Agrawal 2011). Consecuentemente, la temperatura ideal de almacenamiento de las FMT-PLGA-NPs de acuerdo a lo analizado, fue a los 4 °C, donde prácticamente la formulación se mantuvo sin cambios en su estabilidad, en el período estudiado.

La evaluación de la tolerancia ocular de las FMT-PLGA-NPs en estudios *in vitro* (HET-CAM®) e *in vivo* (Test de Draize) puso de relieve su inocuidad en el tratamiento inflamatorio ocular. Ambos estudios catalogaron a las NPs como no-irritantes, asegurando que la administración de este sistema nanoestructurado no provocará irritación ocular tal como lo demuestran otros estudios con NPs de PLGA (Alvarado *et al.* 2015; Parra *et al.* 2016).

El estudio de eficacia antiinflamatoria previa inducción de la inflamación con araquidonato de sodio (SA), demostró que las FMT-PLGA-NPs son significativamente más eficaces que el fármaco comercial en el tratamiento de la inflamación ocular aguda ($p< 0,01$). Además, el estudio de biodisponibilidad ocular comprobó que el fármaco de las NPs logra atravesar la córnea acumulándose en mayor proporción en el humor acuoso ($p< 0,0001$), el cual actuaría como un repositorio para luego distribuirse por los demás tejidos, haciéndolo útil para el tratamiento de ciertas uveítis posteriores (Warsi *et al.* 2014; Kalam and Alshamsan 2017; Bisht *et al.* 2018). Estos resultados están en concordancia con la información obtenida del estudio de permeación *ex vivo,* en el que las NPs logran atravesar la córnea. Para el caso del Isoptoflucon®, no fue posible detectar cantidades de FMT en ningún de los tejidos oculares estudiados a través de la técnica de cuantificación utilizada (HPLC), demostrando que las NPs desarrolladas son capaces de tratar enfermedades inflamatorias tanto del segmento anterior como posterior del ojo en comparación con el fármaco comercial.

En segundo lugar las FMT-PLGA-NPs, ya caracterizadas y evaluada su eficacia antiinflamatoria fueron incorporadas en geles termosensibles. Para ello se realizó un DoE, donde se evaluó como las concentraciones de metilcelulosa (MC) y poloxamer 407 (P407) afectaban la prueba de capacidad de gelificación (Gt), la temperatura de transición sol-gel ($T_{sol-gel}$) y la viscosidad (Vs) de los geles. Se evidenció que las concentraciones de MC y P407 son directamente influyentes en las respuestas del Gt y Vs ($p< 0,01$). Para el caso $T_{sol-gel}$, solo P407 tiene un efecto significativo inversamente proporcional ($p< 0,001$), es decir, a medida que la concentración de P407 aumenta, la $T_{sol-gel}$ disminuye (dos Santos *et al.* 2015;

DISCUSIÓN

M.A. Fathalla *et al.* 2017). De acuerdo al DoE, se seleccionaron tres formulaciones (PG2, PG5 y PG8), teniendo como principal criterio la formación del gel y su estabilidad a la temperatura corneal.

Los geles PG2 y PG5 presentaron una capacidad gelificante similar "gelificación lenta y disolución rápida", valor otorgado cuando una muestra del gel se mantiene suspendida al menos 30 minutos en una solución simulada de lágrimas a 34 °C. En el caso de la formulación PG8, su forma de gel se mantuvo al menos durante 2 horas. Estas diferencias entre formulaciones son debido a la concentración creciente de MC (0-1% p/v), lo cual aporta mayor rigidez al gel para que se mantenga un mayor tiempo constituido. Por otro lado, los reogramas de los geles confirmaron un perfil pseudoplástico a temperatura corneal con una viscosidad aparente de alrededor de 3000 mPa·s, valor relativamente alto que podría causar irritación ocular según la literatura (Abrego *et al.* 2015; Morsi *et al.* 2017). A pesar de lo anterior, la elevada tasa de cizalla ocular que va desde 0,03 s^{-1} entre parpadeos hasta 4000-28500 s^{-1} en el parpadeo y con un sistema de liberación pseudoplástico, interferiría menos con la película lagrimal que tiene el mismo perfil reométrico (perfil pseudoplástico), evitando de esta forma la irritación ocular. Conjuntamente, la alta viscosidad de los geles y la baja cizalla ocular permitiría aumentar el tiempo de residencia precorneal, incrementando la biodisponibilidad ocular del fármaco. En cambio, la alta cizalla inducida por el parpadeo rompería las interacciones entre las cadenas poliméricas del P407, permitiendo que fluya y se distribuya uniformemente a una viscosidad constante sobre la superficie ocular (Mansour *et al.* 2008; Almeida *et al.* 2013; M.A. Fathalla *et al.* 2017; Morsi *et al.* 2017).

Los geles optimizados demostraron tener una $T_{sol-gel}$ promedio de 21 °C, donde las formulaciones inician el incremento de su viscosidad y el componente elástico, ambos propio de un gel, hasta estabilizarse a una temperatura cercana a los 34 °C (Chang *et al.* 2002). Asimismo, la prueba habilidad de fluidez comprobó que los geles no fluyen como un líquido newtoniano a los 34 °C. Desde un punto de vista molecular, a temperaturas inferiores a la $T_{sol-gel}$ existe un comportamiento newtoniano, donde las cadenas poliméricas de P407 se encuentran desordenadas, no obstante, a partir de los 21 °C estas cadenas se ordenan en forma de micelas encapsulando en su interior las FMT-PLGA-NPs, hasta estabilizarse a la temperatura corneal (Djekic *et al.* 2015; Shelke *et al.* 2016). Este comportamiento de gelificación facilitaría la administración de este tipo de sistema pudiéndose dosificar en gotas oftálmicas, pero con los beneficios propios de un gel al entrar contacto con el ojo, evitando las rutas de eliminación anatómicas del ojo como la renovación lagrimal.

El sistema gelificante desarrollado fue examinado a través de TEM para corroborar que las FMT-PLGA-NPs se mantenían integras al incorporarse en los geles PG2, PG5 y PG8. Las imágenes del TEM evidenciaron que las NPs se distribuían uniformemente en el gel sin aglomeraciones, manteniendo su forma esférica y su tamaño promedio.

En el estudio de diálisis en celdas de Franz se caracterizó el perfil cinético de liberación de la FMT desde los geles. En los perfiles biofarmacéuticos se observó que los geles evitan el efecto de liberación rápida de la FMT desde las NPs como sucedió en el primer artículo. Los geles presentaron un perfil de primer orden con una liberación lenta y

sostenida de la FMT. A pesar de ello, el PG2 presentó una baja rigidez, debido a la ausencia de MC, por lo que la cantidad liberada de FMT a las 24 horas fue similar a las NPs. El caso contrario sucede con la formulación PG8, cuya liberación es muy lenta debido a la presencia de 1% de MC. Este estudio biofarmacéutico evidenció que la formulación PG5 (0,5% de MC) es la que posee características adecuadas, permitiendo la liberación lenta y sostenida desde la matriz gelificante (Huang and Brazel 2001; Bilensoy *et al.* 2006; Gou *et al.* 2008; dos Santos *et al.* 2015).

Se estudió la estabilidad de los geles que incorporan las NPs optimizadas en las mismas condiciones ideales que el primer artículo (4 °C) durante dos meses de almacenamiento. Los perfiles de retrodispersión evidenciaron que los geles no mostraron una diferencia mayor del 20% entre las mediciones, considerándose estables. El PG2 es la formulación que muestra indicios de precipitación por la ausencia de MC en su composición y no se observaron, en cambio, modificaciones del perfil de luz retrodispersada en PG5 y PG8, atribuido a la MC. Cabe destacar que las formulaciones a la temperatura del ensayo se encuentran en estado de suspensión, por lo cual se incrementaría la inestabilidad de los geles (Almeida *et al.* 2017; Mallandrich *et al.* 2017). Debido a lo anterior, se recomienda antes de su uso, realizar una agitación suave para asegurar la homogeneidad de la suspensión que se instilará en el ojo.

Se comprobó la inocuidad de los geles a través de las pruebas de HET-CAM® y Draize, que pusieron de relieve una óptima tolerancia ocular. Esto permitió demostrar que el perfil reométrico tipo pseudoplástico evita la

irritación ocular a pesar de poseer una viscosidad aparente elevada (Patel *et al.* 2016; Alkhatib *et al.* 2017; M.A. Fathalla *et al.* 2017).

Se comprobó la eficacia terapéutica de los geles termosensibles se comprobó a través de estudios de prevención y tratamiento de la inflamación ocular aguda inducida por SA. En ambos estudios, las formulaciones PG2 y PG5 fueron las que evidenciaron un efecto antiinflamatorio significativo en comparación al fármaco comercial ($p < 0,05$). Al mismo tiempo, el estudio de biodisponibilidad ocular demostró que la formulación PG5 es la que posee mayor capacidad para alcanzar los tejidos profundos del ojo tales como el cristalino y el humor acuoso (Kumar *et al.* 2013; Parmar *et al.* 2018; Shelley *et al.* 2018; Wen *et al.* 2018).

Los anteriores estudios demostraron que tanto las FMT-PLGA-NPs como el gel termosensible PG5 son efectivos en el tratamiento de la inflamación ocular que involucran las zonas posteriores de la córnea. Desde un punto de vista clínico, la formulación de NPs resultaría útil al inicio de un tratamiento antiinflamatorio diurno, debido a su liberación rápida en las primeras horas y su posterior liberación sostenida. Durante la noche, el gel termosensible permitiría el mantenimiento de la terapia antiinflamatoria ocular y además, como la formulación instilada es de características viscoelásticas su administración nocturna evitaría la incomodidad en el paciente (Nguyen *et al.* 2018).

4.2. NPs de maleímido-PEG-PLGA conjugadas con CPPs

Previamente a la conjugación de los CPPs a las NPs, se sintetizaron los polímeros Rodamina-PLGA (Rho-PLGA) y maleímido-PEG-PLGA (m-PEG-PLGA con la técnica de la vía de la carbodiimida (Hermanson 2008; Valeur and Bradley 2009). La estructura de estos polímeros fue comprobada a través de las técnicas de resonancia magnética nuclear (RMN-H), FTIR y XRD. En primer lugar, los espectros de RMN-H y FTIR confirmaron la unión entre el polímero NHS-PLGA y m-PEG, debido a la eliminación de los picos provenientes del grupo NHS que no están presentes en el espectro m-PEG-PLGA. Conjuntamente, el espectro de RMN-H del polímero m-PEG-PLGA evidenció la presencia de los grupos etilenglicol y maleímido del m-PEG, confirmándose su unión al NHS-PLGA. La utilización de los espectros RMN-H permitió calcular el grado de pegilación y la masa relativa (MR) del PEG en el polímero, siendo éste de un 30% y 9%, respectivamente. En segundo lugar, los difractogramas del m-PEG-PLGA mostraron un perfil amorfo, en concordancia con otros autores, que afirman que los picos cristalinos del PEG no son visualizados cuando su presencia es inferior al 10% en masa en el polímero (Pereira *et al.* 2016; Cano *et al.* 2018; Sánchez-López *et al.* 2018).

El polímero m-PEG-PLGA sintetizado fue utilizado para la elaboración de las NPs, las cuales presentaron un Zav cercano a 150 nm con un ZP negativo, una distribución monodispersa (PI< 0,2) y una EE de 99% (0,5 mg·mL^{-1}). Las anteriores características evitarían la irritación ocular y la precipitación temprana de las NPs (Stolnik *et al.* 1995; Ali and Lehmussaari 2006). Paralelamente, los pesos moleculares de los CPPs

(TAT$_{49\text{-}57}$, pAntp$_{43\text{-}58}$ y G2), sintetizados en fase sólida, fueron confirmados por espectroscopia de masas (MALDI-TOF/TOF). Consiguientemente, se realizó la conjugación entre el maleímido del polímero y el grupo tiol de la cisteína de los CPPs con las NPs en suspensión. De lo anterior, se obtuvieron NPs funcionalizadas con un aumento en el Zav de 17 nm y un ZP menos negativo con respecto a las NPs iniciales. Estos cambios en las características fisicoquímicas son consecuencia de la conjugación de los CPPs, que aumentan el tamaño de las NPs y por sus características catiónicas que modifican la carga superficial, variando el ZP hacia un valor más positivo (Vasconcelos *et al.* 2015). La técnica utilizada para la conjugación entre el maleímido y el residuo de cisteína de los CPPs resultó exitosa, obteniéndose un grado de conjugación (MR) del TAT$_{49\text{-}57}$, pAntp$_{43\text{-}58}$ y G2 en masa en el polímero m-PEG-PLGA de 2,0, 4,6 y 0,6 %, respectivamente (Ravi *et al.* 2012; Northrop, Frayne and Choudhary 2015; Sazano and Torchilin 2015).

Los estudios de citotoxicidad en HCE-2 realizados tanto a baja como alta concentración durante 24 horas (5 y 50 µg·mL^{-1}), evidenciaron que las NPs conjugadas poseen una viabilidad celular comparable al control negativo (células sin tratar). El fármaco comercial mostró indicios de citotoxicidad tanto a baja como a alta concentración a las 24 y 48 horas de tratamiento, debido a la presencia cloruro de benzalconio y polisorbato 80 en su composición (Liu *et al.* 2006; Khoh-Reiter and Jessen 2009; Czajkowska-Kośnik *et al.* 2015). A las 48 horas, la formulación G2 mostró una viabilidad celular aumentada con respecto al control negativo. De acuerdo a los resultados de RMN-H, se demostró que la conjugación del G2 al polímero fue baja en comparación a los demás CPPs. Adicionalmente se

ha evidenciado en otros estudios que el maleímido libre puede incrementar el metabolismo celular y por lo tanto, aumentar la respuesta del MTT (Ali *et al.* 2017). Lo anterior se corroboró a través del estudio de la viabilidad celular de NPs sin conjugar con CPP a una concentración 50 µg·mL^{-1} durante 48 horas, evidenciándose que los sitios sin conjugar del maleímido aumentan significativamente la respuesta del MTT ($p<$ 0,01) en comparación con las formulaciones con CPPs.

La disminución de la expresión de citoquinas proinflamatorias por parte de las NPs conjugadas se evidenció en la mayoría de los casos. Las formulaciones G2-NPs y TAT-NPs mostraron un efecto igual o mayor que el Isoptoflucon® en reducir la concentración de IL-1β, IL-6 y TNFα. Particularmente, la reducción de TNFα fue mayor por parte de G2-NPs ($p<$ 0,05), que en las otras citoquinas dejando claro que un AMPs puede tener actividad CPP (Delcroix *et al.* 2010; Splith and Neundorf 2011). La formulación pAntp-NPs incrementó la expresión de IL-8, probablemente debido a su mecanismo de internalización de celular, traslocación, que provocó una desestabilización excesiva de la membrana celular, teniendo como consecuencia la iniciación de la cascada inflamatoria mediada por citoquinas. De acuerdo a lo anterior, la administración de pAntp-NPs en células HCE-2 no resultaría útil debido a su efecto en la membrana celular, en cambio, en las formulaciones TAT-NPs y G2-NPs sus mecanismos de internalización permitieron incrementar la eficacia de la FMT en comparación al fármaco comercial (Drin *et al.* 2001).

Los estudios de captación de NPs tanto *in vivo* como *in vitro* demostraron que las TAT-NPs y G2-NPs son las formulaciones que más se

internalizaron. En el estudio *in vivo* es posible evidenciar que las G2-NPs poseen una internalización superior al estudio *in vitro*, debido a los sitios sin reaccionar del maleímido que se conjugan con los grupos tioles de la mucina ocular (Tonglairoum *et al.* 2016). Lo anterior conllevaría un aumento del tiempo residencia precorneal y, por ende, una mayor internalización en los tejidos oculares.

5. CONCLUSIONES

In this doctoral thesis, three controlled release polymeric nanostructured systems containing FMT were developed for the treatment of inflammatory conditions of the anterior and posterior segment of the eye.

- PLGA NPs (FMT-PLGA-NPs) and the *in-situ* forming gel (PG5) containing FMT that were optimized by DoE, obtained physicochemical characteristics suitable for ocular administration as eye drops.

- The use of the carbodiimide pathway as a synthesis strategy for the polymers Rho-PLGA and m-PEG-PLGA was appropriate, confirming its structure by H-NMR, FTIR and XRD techniques.

- CPPs were successfully synthesized by the automated solid-phase parallel peptides synthesis technique confirming their molecular weight by mass spectroscopy (MALDI-TOF/TOF).

- The conjugation of the peptide sequences with the NPs was confirmed by H-NMR, where the percentage amount (MR) conjugated to the polymer was higher with $pAntp_{43-58}$ followed by TAT_{49-57} and G2.

- The biopharmaceutical behaviour showed that the FMT-PLGA-NPs had a hyperbola release profile with an initial burst release effect followed by an increasing and sustained release of FMT. In addition, it was evidenced that NPs have greater affinity in crossing the cornea than the sclera.

- The incorporation of the FMT-PLGA-NPs to the thermosensitive gel (PG5) avoided the burst release in the first hours adjusting to a first order profile.

CONCLUSIONES

- Developed formulations (FMT-PLGA-NPs, PG5, TAT-NPs, pAntp-NPs and G2-NPs) showed an optimal tolerance in both *in vitro* (HET-CAM® and MTT) and/or *in vivo* (Draize test) assays.

- FMT-PLGA-NPs as the thermosensitive gel (PG5) tested in pigs and rabbits, respectively, demonstrated to be more effective in the treatment and prevention of ocular inflammatory conditions that the commercial drug.

- NPs conjugated with TAT_{49-57} and G2 decreased the expression of proinflammatory cytokines and improved internalization in both the HCE-2 cells and in the mouse eye. Particularly, G2-NPs showed an internalization *in vivo* greater than *in vitro* due to the free maleimide that bound to the thiol groups of the ocular surface mucin, increasing their precorneal residence time.

- Nanostructured systems with FMT developed could be a new strategy for the treatment of ocular inflammatory disorders. Particularly, the NPs would be useful in daytime treatment and the thermosensitive gel in the maintenance of nocturnal therapy.

6. REFERENCIAS

A

Abrego G, Alvarado H, Souto EB *et al.* Biopharmaceutical profile of pranoprofen-loaded PLGA nanoparticles containing hydrogels for ocular administration. *Eur J Pharm Biopharm* 2015;95:261–270.

Abrego G, Alvarado HL, Egea MA *et al.* Design of nanosuspensions and freeze-dried PLGA nanoparticles as a novel approach for ophthalmic delivery of pranoprofen. *J Pharm Sci* 2014;103:3153–3164.

Adibkia K, Omidi Y, Siahi MR *et al.* Inhibition of endotoxin-induced uveitis by methylprednisolone acetate nanosuspension in rabbits. *J Ocul Pharmacol Ther* 2007;23:421–432.

Agrahari V, Mandal A, Agrahari V *et al.* A comprehensive insight on ocular pharmacokinetics. *Drug Deliv Transl Res* 2016;6:735–754.

Akpek EK, Uy HS, Christen W *et al.* Severity of episcleritis and systemic disease association. *Ophthalmology* 1999;106:729–731.

Al-Kinani AA, Zidan G, Elsaid N *et al.* Ophthalmic gels: past, present and future. *Adv Drug Deliv Rev* 2018;126:113–126.

Ali B, Kanda Kupa LD, Heluany CS *et al.* Cytotoxic effects of a novel maleimide derivative on epithelial and tumor cells. *Bioorg Chem* 2017;72:199–207.

Ali MM, Karasneh GA, Jarding MJ *et al.* A 3-O-sulfated heparan sulfate binding peptide preferentially targets herpes simplex virus 2-infected

REFERENCIAS

cells. *J Virol* 2012;86:6434–6443.

Ali Y, Lehmussaari K. Industrial perspective in ocular drug delivery. *Adv Drug Deliv Rev* 2006;58:1258–1268.

Alkhatib Y, Dewaldt M, Moritz S *et al.* Controlled extended octenidine release from a bacterial nanocellulose/poloxamer hybrid system. *Eur J Pharm Biopharm* 2017;112:164–176.

Allahyari M, Mohit E. Peptide/protein vaccine delivery system based on PLGA particles. *Hum Vaccin Immunother* 2016;12:806–828.

Almeida H, Amaral MH, Lobão P *et al.* Applications of poloxamers in ophthalmic pharmaceutical formulations: an overview. *Expert Opin Drug Deliv* 2013;10:1223–1237.

Almeida H, Lobão P, Frigerio C *et al.* Preparation, characterization and biocompatibility studies of thermoresponsive eyedrops based on the combination of nanostructured lipid carriers (NLC) and the polymer pluronic F-127 for controlled delivery of ibuprofen. *Pharm Dev Technol* 2017;22:336–349.

Alvarado HL, Abrego G, Garduño-Ramirez ML *et al.* Development and validation of a high-performance liquid chromatography method for the quantification of ursolic/oleanic acids mixture isolated from Plumeria obtusa. *J Chromatogr B* 2015;983:111–116.

Anderson JM, Shive MS. Biodegradation and biocompatibility of PLA and PLGA microspheres. *Adv Drug Deliv Rev* 2012;64:72–82.

Angayarkanni N, Coral K, Bharathi Devi SR *et al.* The biochemistry of the eye. *Pharmacology of Ocular Therapeutics*. Cham: Springer International Publishing, 2016, 83–157.

Ansari MW, Nadeem A. *Atlas of Ocular Anatomy*. Cham: Springer International Publishing, 2016.

Araújo J, González E, Egea MA *et al.* Nanomedicines for ocular NSAIDs: safety on drug delivery. *Nanomedicine Nanotechnology, Biol Med* 2009;5:394–401.

Aukunuru J V, Sunkara G, Bandi N *et al.* Expression of multidrug resistance-associated protein (MRP) in human retinal pigment epithelial cells and its interaction with BAPSG, a novel aldose reductase inhibitor. *Pharm Res* 2001;18:565–572.

Awan MA, Agarwal PK, Watson DG *et al.* Penetration of topical and subconjunctival corticosteroids into human aqueous humour and its therapeutic significance. *Br J Ophthalmol* 2009;93:708–713.

B

Balzus B, Sahle FF, Hönzke S *et al.* Formulation and *ex vivo* evaluation of polymeric nanoparticles for controlled delivery of corticosteroids to the skin and the corneal epithelium. *Eur J Pharm Biopharm* 2017;115:122–130.

Barar J, Aghanejad A, Fathi M *et al.* Advanced drug delivery and targeting technologies for the ocular diseases. *Bioimpacts* 2016;6:49–67.

REFERENCIAS

Bilensoy E, Abdur Rouf M, Vural I *et al.* Mucoadhesive, thermosensitive, prolonged-release vaginal gel for clotrimazole: β-cyclodextrin complex. *AAPS PharmSciTech* 2006;7:E54–60.

Bisht R, Mandal A, Jaiswal JK *et al.* Nanocarrier mediated retinal drug delivery: overcoming ocular barriers to treat posterior eye diseases. *Wiley Interdiscip Rev Nanomedicine Nanobiotechnology* 2018;10:e1473.

Bolhassani A, Jafarzade BS, Mardani G. *In vitro* and *in vivo* delivery of therapeutic proteins using cell penetrating peptides. *Peptides* 2017;87:50–63.

C

Cano A, Ettcheto M, Espina M *et al.* Epigallocatechin-3-gallate loaded PEGylated-PLGA nanoparticles: a new anti-seizure strategy for temporal lobe epilepsy. *Nanomedicine Nanotechnology, Biol Med* 2018;14:1073–1085.

Chang JY, Oh Y-K, Choi H *et al.* Rheological evaluation of thermosensitive and mucoadhesive vaginal gels in physiological conditions. *Int J Pharm* 2002;241:155–163.

Chen P-Q, Han X-M, Zhu Y-N *et al.* Comparison of the anti-inflammatory effects of fluorometholone 0.1% combined with levofloxacin 0.5% and tobramycin/dexamethasone eye drops after cataract surgery. *Int J Ophthalmol* 2016;9:1619–1623.

Cheng Y-H, Tsai T-H, Jhan Y-Y *et al.* Thermosensitive chitosan-based hydrogel as a topical ocular drug delivery system of latanoprost for glaucoma treatment. *Carbohydr Polym* 2016;144:390–399.

Czajkowska-Kośnik A, Wolska E, Chorążewicz J *et al.* Comparison of cytotoxicity *in vitro* and irritation *in vivo* for aqueous and oily solutions of surfactants. *Drug Dev Ind Pharm* 2015;41:1232–1236.

D

Dalal MD, Nida Sen H, Nussenblatt RB. Ocular disease. *The Autoimmune Diseases*. Elsevier, 2014, 793–804.

Delcroix M, Riley LW, Delcroix M *et al.* Cell-penetrating peptides for antiviral drug development. *Pharmaceuticals* 2010;3:448–470.

Dennis EA, Norris PC. Eicosanoid storm in infection and inflammation. *Nat Rev Immunol* 2015;15:511–523.

Diebold Y, Calonge M. Applications of nanoparticles in ophthalmology. *Prog Retin Eye Res* 2010;29:596–609.

Djekic L, Krajisnik D, Martinovic M *et al.* Characterization of gelation process and drug release profile of thermosensitive liquid lecithin/poloxamer 407 based gels as carriers for percutaneous delivery of ibuprofen. *Int J Pharm* 2015;490:180–189.

Drin G, Déméné H, Temsamani J *et al.* Translocation of the pAntp peptide and its amphipathic analogue AP-2AL. *Biochemistry* 2001;40:1824–1834.

REFERENCIAS

Duan X, Li Y. Physicochemical characteristics of nanoparticles affect circulation, biodistribution, cellular internalization, and trafficking. *Small* 2013;9:1521–1532.

F

Farkhani SM, Valizadeh A, Karami H *et al.* Cell penetrating peptides: efficient vectors for delivery of nanoparticles, nanocarriers, therapeutic and diagnostic molecules. *Peptides* 2014;57:78–94.

Fredenberg S, Wahlgren M, Reslow M *et al.* The mechanisms of drug release in poly(lactic-co-glycolic acid)-based drug delivery systems—A review. *Int J Pharm* 2011;415:34–52.

G

Ghate D, Edelhauser HF. Ocular drug delivery. *Expert Opin Drug Deliv* 2006;3:275–287.

Gou M, Li X, Dai M *et al.* A novel injectable local hydrophobic drug delivery system: biodegradable nanoparticles in thermo-sensitive hydrogel. *Int J Pharm* 2008;359:228–233.

Guengerich FP. Intersection of the roles of cytochrome P450 enzymes with xenobiotic and endogenous substrates: relevance to toxicity and drug interactions. *Chem Res Toxicol* 2017;30:2–12.

Guidotti G, Brambilla L, Rossi D. Cell-penetrating peptides: from basic research to clinics. *Trends Pharmacol Sci* 2017;38:406–424.

Gulati S, Jain S. Ocular pharmacology of tear film, dry eye, and allergic conjunctivitis. *Pharmacologic Therapy of Ocular Disease*. 2016, 97–118.

Guly CM, Forrester J V. Investigation and management of uveitis. *BMJ (Clinical Res ed)* 2010;2:c4976.

H

Hämäläinen KM, Kanasen K, Auriola S *et al.* Characterization of paracellular and aqueous penetration routes in cornea, conjunctiva, and sclera. *Invest Ophthalmol Vis Sci* 1997;38:627–634.

Hazare S, Yang R, Chavan S *et al.* Aging disorders of the eye: challenges and approaches for their treatment. *Nano-Biomaterials For Ophthalmic Drug Delivery*. Cham: Springer International Publishing, 2016, 277–320.

Hermanson G. The chemistry of reactive groups. *Bioconjugate Techniques (Second Edition)*. London: Academic Press, 2008, 169–212.

Huang X, Brazel CS. On the importance and mechanisms of burst release in matrix-controlled drug delivery systems. *J Control Release* 2001;73:121–136.

Hughes PM, Olejnik O, Chang-Lin J-E *et al.* Topical and systemic drug delivery to the posterior segments. *Adv Drug Deliv Rev* 2005;57:2010–2032.

REFERENCIAS

I

Ibrahim HK, El-Leithy IS, Makky AA. Mucoadhesive nanoparticles as carrier systems for prolonged ocular delivery of gatifloxacin/prednisolone bitherapy. *Mol Pharm* 2010;7:576–585.

J

Jain D, Kumar V, S *et al.* Newer trends in *in situ* gelling systems for controlled ocular drug delivery. *J Anal Pharm Res* 2016;2:1–10.

Jain RA. The manufacturing techniques of various drug loaded biodegradable poly(lactide-co-glycolide) (PLGA) devices. *Biomaterials* 2000;21:2475–2490.

Jung Y seok, Park W, Park H *et al.* Thermo-sensitive injectable hydrogel based on the physical mixing of hyaluronic acid and pluronic F-127 for sustained NSAID delivery. *Carbohydr Polym* 2017;156:403–408.

K

Kalam MA. The potential application of hyaluronic acid coated chitosan nanoparticles in ocular delivery of dexamethasone. *Int J Biol Macromol* 2016;89:559–568.

Kalam MA, Alshamsan A. Poly (d, l-lactide-co-glycolide) nanoparticles for sustained release of tacrolimus in rabbit eyes. *Biomed Pharmacother* 2017;94:402–411.

Kapoor DN, Bhatia A, Kaur R *et al.* PLGA: a unique polymer for drug delivery. *Ther Deliv* 2015;6:41–58.

Kels BD, Grant-Kels JM. Human ocular anatomy. *Clin Dermatol* 2015;33:140–146.

Khoh-Reiter S, Jessen BA. Evaluation of the cytotoxic effects of ophthalmic solutions containing benzalkonium chloride on corneal epithelium using an organotypic 3-D model. *BMC Ophthalmol* 2009;9:5.

Kumar D, Jain N, Gulati N *et al.* Nanoparticles laden *in situ* gelling system for ocular drug targeting. *J Adv Pharm Technol Res* 2013;4:9–17.

Kumari A, Yadav SK, Yadav SC. Biodegradable polymeric nanoparticles based drug delivery systems. *Colloids Surf B Biointerfaces* 2010;75:1–18.

L

Lakhani P, Patil A, Majumdar S. Recent advances in topical nano drug-delivery systems for the anterior ocular segment. *Ther Deliv* 2018;9:137–153.

Lalu L, Tambe V, Pradhan D *et al.* Novel nanosystems for the treatment of ocular inflammation: current paradigms and future research directions. *J Control Release* 2017;268:19–39.

Li J, Mooney DJ. Designing hydrogels for controlled drug delivery. *Nat Rev Mater* 2016;1:16071.

REFERENCIAS

Lin T, Gong L. Topical fluorometholone treatment for ocular dryness in patients with Sjögren syndrome: a randomized clinical trial in China. *Medicine (Baltimore)* 2015;94:e551.

Liu Z, Li J, Nie S *et al.* Study of an alginate/HPMC-based *in situ* gelling ophthalmic delivery system for gatifloxacin. *Int J Pharm* 2006;315:12–17.

M

M.A. Fathalla Z, Vangala A, Longman M *et al.* Poloxamer-based thermoresponsive ketorolac tromethamine *in situ* gel preparations: design, characterisation, toxicity and transcorneal permeation studies. *Eur J Pharm Biopharm* 2017;114:119–134.

Macwan JS, Hirani A, Pathak Y. Challenges in ocular pharmacokinetics and drug delivery. *Nano-Biomaterials For Ophthalmic Drug Delivery*. Cham: Springer International Publishing, 2016, 593–611.

Makadia HK, Siegel SJ. Poly lactic-co-glycolic acid (PLGA) as biodegradable controlled drug delivery carrier. *Polymers (Basel)* 2011;3:1377–1397.

Malavade S. Overview of the ophthalmic system. *Nano-Biomaterials For Ophthalmic Drug Delivery*. Cham: Springer International Publishing, 2016, 9–36.

Mallandrich M, Fernández-Campos F, Clares B *et al.* Developing transdermal applications of ketorolac tromethamine entrapped in

stimuli sensitive block copolymer hydrogels. *Pharm Res* 2017;34:1728–1740.

Mansour M, Mansour S, Mortada ND *et al.* Ocular poloxamer-based ciprofloxacin hydrochloride *in situ* forming gels. *Drug Dev Ind Pharm* 2008;34:744–752.

McKenzie M, Betts D, Suh A *et al.* Hydrogel-based drug delivery systems for poorly water-soluble drugs. *Molecules* 2015;20:20397–20408.

Morgan CM, Schatz H, Vine AK *et al.* Ocular complications associated with retrobulbar injections. *Ophthalmology* 1988;95:660–665.

Morsi N, Ibrahim M, Refai H *et al.* Nanoemulsion-based electrolyte triggered *in situ* gel for ocular delivery of acetazolamide. *Eur J Pharm Sci* 2017;104:302–314.

N

National center for Biotechnology Information. PubChem compound database; CID=9878. *PubChem* 2019.

Nguyen H, Eng S, Ngo T *et al.* Delivery of therapeutics for deep-seated ocular conditions - status quo. *J Pharm Pharmacol* 2018;70:994–1001.

Northrop BH, Frayne SH, Choudhary U. Thiol–maleimide "click" chemistry: evaluating the influence of solvent, initiator, and thiol on the reaction mechanism, kinetics, and selectivity. *Polym Chem* 2015;6:3415–3430.

REFERENCIAS

P

Pan Q, Xu Q, Boylan NJ *et al.* Corticosteroid-loaded biodegradable nanoparticles for prevention of corneal allograft rejection in rats. *J Control Release* 2015;201:32–40.

Panyam J, William D, Dash A *et al.* Solid-state solubility influences encapsulation and release of hydrophobic drugs from PLGA/PLA nanoparticles. *J Pharm Sci* 2004;93:1804–1814.

Papaliodis GN. Introduction. *Uveitis*. Cham: Springer International Publishing, 2017, 3–7.

Parhi R. Cross-linked hydrogel for pharmaceutical applications: a review. *Adv Pharm Bull* 2017;7:515–530.

Parmar K, Patel JK, Bhatia D *et al.* Thermoresponsive gel drug delivery for retina and posterior segment disease. *Drug Delivery for the Retina and Posterior Segment Disease*. Cham: Springer International Publishing, 2018, 397–409.

Pärn K, Eriste E, Langel Ü. The antimicrobial and antiviral applications of cell-penetrating peptides. *Cell-Penetrating Peptides: Methods and Protocols*. Totowa, NJ: Humana Press, 2015, 223–245.

Parra A, Clares B, Rosselló A *et al. Ex vivo* permeation of carprofen from nanoparticles: a comprehensive study through human, porcine and bovine skin as anti-inflammatory agent. *Int J Pharm* 2016;501:10–17.

Patel N, Nakrani H, Raval M *et al.* Development of loteprednol etabonate-loaded cationic nanoemulsified *in-situ* ophthalmic gel for sustained delivery and enhanced ocular bioavailability. *Drug Deliv* 2016;23:3712–3723.

Patel VR, Agrawal YK. Nanosuspension: an approach to enhance solubility of drugs. *J Adv Pharm Technol Res* 2011;2:81–87.

Pereira ED, Cerruti R, Fernandes E *et al.* Influence of PLGA and PLGA-PEG on the dissolution profile of oxaliplatin. *Polímeros* 2016;26:137–143.

Pescina S, Ostacolo C, Gomez-Monterrey IM *et al.* Cell penetrating peptides in ocular drug delivery: state of the art. *J Control Release* 2018;284:84–102.

Pinto-Fraga J, López-Miguel A, González-García MJ *et al.* Topical fluorometholone protects the ocular surface of dry eye patients from desiccating stress: a randomized controlled clinical trial. *Ophthalmology* 2016;123:141–153.

R

Rafie F, Javadzadeh Y, Javadzadeh AR *et al. In vivo* evaluation of novel nanoparticles containing dexamethasone for ocular drug delivery on rabbit Eye. *Curr Eye Res* 2010;35:1081–1089.

Rao JP, Geckeler KE. Polymer nanoparticles: preparation techniques and size-control parameters. *Prog Polym Sci* 2011;36:887–913.

Ravi S, Krishnamurthy VR, Caves JM *et al.* Maleimide-thiol coupling of a bioactive peptide to an elastin-like protein polymer. *Acta Biomater* 2012;8:627–635.

Reim M, Schrage NF, Becker J. Interactions between ocular surface fluid and cornea related to contact lenses. *Eur J Ophthalmol* 2001;11:105–115.

Rhen T, Cidlowski JA. Antiinflammatory action of glucocorticoids — new mechanisms for old drugs. *N Engl J Med* 2005;353:1711–1723.

S

Sabzevari A, Adibkia K, Hashemi H *et al.* Polymeric triamcinolone acetonide nanoparticles as a new alternative in the treatment of uveitis: *In vitro* and *in vivo* studies. *Eur J Pharm Biopharm* 2013;84:63–71.

Sakai T, Kohno H, Ishihara T *et al.* Treatment of experimental autoimmune uveoretinitis with poly(lactic acid) nanoparticles encapsulating betamethasone phosphate. *Exp Eye Res* 2006;82:657–663.

Sánchez-López E, Egea MA, Cano A *et al.* PEGylated PLGA nanospheres optimized by design of experiments for ocular administration of dexibuprofen —*in vitro*, *ex vivo* and *in vivo* characterization. *Colloids Surfaces B Biointerfaces* 2016;145:241–250.

Sánchez-López E, Ettcheto M, Egea MA *et al.* New potential strategies for Alzheimer's disease prevention: pegylated biodegradable dexibuprofen nanospheres administration to APPswe/PS1dE9. *Nanomedicine*

Nanotechnology, Biol Med 2017;13:1171–1182.

Sánchez-López E, Ettcheto M, Egea MA *et al.* Memantine loaded PLGA PEGylated nanoparticles for Alzheimer's disease: *in vitro* and *in vivo* characterization. *J Nanobiotechnology* 2018;16:32.

dos Santos ACM, Akkari ACS, Ferreira IRS *et al.* Poloxamer-based binary hydrogels for delivering tramadol hydrochloride: sol-gel transition studies, dissolution-release kinetics, *in vitro* toxicity, and pharmacological evaluation. *Int J Nanomedicine* 2015;10:2391–2401.

Sazano G, Torchilin W. Intracellular delivery of nanoparticles with cell penetrating peptides. *Cell-Penetrating Peptides: Methods and Protocols*. Totowa, NJ: Humana Press, 2015, 357–386.

Shelke S, Shahi S, Jalalpure S *et al.* Poloxamer 407-based intranasal thermoreversible gel of zolmitriptan-loaded nanoethosomes: formulation, optimization, evaluation and permeation studies. *J Liposome Res* 2016;26:313–323.

Shelley H, Rodriguez-Galarza RM, Duran SH *et al. In situ* gel formulation for enhanced ocular delivery of nepafenac. *J Pharm Sci* 2018;107:3089–3097.

Shi N-Q, Qi X-R, Xiang B *et al.* A survey on "Trojan Horse" peptides: opportunities, issues and controlled entry to "Troy." *J Control Release* 2014;194:53–70.

REFERENCIAS

Shokoohi-Rad S, Daneshvar R, Jafarian-Shahri M *et al.* Comparison between betamethasone, fluorometholone and loteprednol etabonate on intraocular pressure in patients after keratorefractive surgery. *J Curr Ophthalmol* 2018;30:130–135.

Silva AC, Amaral MH, González-Mira E *et al.* Solid lipid nanoparticles (SLN) - based hydrogels as potential carriers for oral transmucosal delivery of risperidone: preparation and characterization studies. *Colloids Surfaces B Biointerfaces* 2012;93:241–248.

Splith K, Neundorf I. Antimicrobial peptides with cell-penetrating peptide properties and vice versa. *Eur Biophys J* 2011;40:387–397.

Stolnik S, Garnett MC, Davies MC *et al.* The colloidal properties of surfactant-free biodegradable nanospheres from poly(β-malic acid-co-benzyl malate)s and poly(lactic acid-co-glycolide). *Colloids Surfaces A Physicochem Eng Asp* 1995;97:235–245.

Storm G, Belliot SO, Daemen T *et al.* Surface modification of nanoparticles to oppose uptake by the mononuclear phagocyte system. *Adv Drug Deliv Rev* 1995;17:31–48.

T

The Standardization of Uveitis Nomenclature (SUN) Working Group. Standardization of uveitis nomenclature for reporting clinical data. results of the first international workshop. *Am J Ophthalmol* 2005;140:509–516.

Tiwari V, Liu J, Valyi-Nagy T *et al.* Anti-heparan sulfate peptides that block herpes simplex virus infection *in vivo*. *J Biol Chem* 2011;286:25406–25415.

Tonglairoum P, Brannigan RP, Opanasopit P *et al.* Maleimide-bearing nanogels as novel mucoadhesive materials for drug delivery. *J Mater Chem B* 2016;4:6581–6587.

Tripathi RC, Parapuram SK, Tripathi BJ *et al.* Corticosteroids and glaucoma risk. *Drugs Aging* 1999;15:439–450.

V

Valeur E, Bradley M. Amide bond formation: beyond the myth of coupling reagents. *Chem Soc Rev* 2009;38:606–631.

Vandervoort J, Ludwig A. Preparation and evaluation of drug-loaded gelatin nanoparticles for topical ophthalmic use. *Eur J Pharm Biopharm* 2004;57:251–261.

Vasconcelos A, Vega E, Pérez Y *et al.* Conjugation of cell-penetrating peptides with poly(lactic-co-glycolic acid)-polyethylene glycol nanoparticles improves ocular drug delivery. *Int J Nanomedicine* 2015;10:609–631.

Vega E, Egea MA, Garduño-Ramírez ML *et al.* Flurbiprofen PLGA-PEG nanospheres: role of hydroxy-β-cyclodextrin on *ex vivo* human skin permeation and *in vivo* topical anti-inflammatory efficacy. *Colloids Surf B Biointerfaces* 2013;110:339–346.

REFERENCIAS

W

Warsi MH, Anwar M, Garg V *et al.* Dorzolamide-loaded PLGA/vitamin E TPGS nanoparticles for glaucoma therapy: pharmacoscintigraphy study and evaluation of extended ocular hypotensive effect in rabbits. *Colloids Surfaces B Biointerfaces* 2014;122:423–431.

Wen Y, Ban J, Mo Z *et al.* A potential nanoparticle-loaded *in situ* gel for enhanced and sustained ophthalmic delivery of dexamethasone. *Nanotechnology* 2018;29:425101.

Wu Y, Liu Y, Li X *et al.* Research progress of *in-situ* gelling ophthalmic drug delivery system. *Asian J Pharm Sci* 2018;14:1–15.

Y

Yang X, Trinh HM, Agrahari V *et al.* Nanoparticle-based topical ophthalmic gel formulation for sustained release of hydrocortisone butyrate. *AAPS PharmSciTech* 2015;17:294–306.

Yasin MN, Svirskis D, Seyfoddin A *et al.* Implants for drug delivery to the posterior segment of the eye: a focus on stimuli-responsive and tunable release systems. *J Control Release* 2014;196:208–221.

Yu Y, Feng R, Yu S *et al.* Nanostructured lipid carrier-based pH and temperature dual-responsive hydrogel composed of carboxymethyl chitosan and poloxamer for drug delivery. *Int J Biol Macromol* 2018;114:462–469.